1-1-1983

Stability op blade flutter limit cycles in compressor blade cascades NASA research grant NAG 3-135 wake-oscillator models.

Bahhan Azizi

STABILITY OF BLADE FLUTTER LIMIT CYCLES IN COMPRESSOR BLADE CASCADES

NASA RESEARCH GRANT NAG 3-135
WAKE-OSCILLATOR MODELS

BY

BAHMAN AZIZI

A Thesis

Presented to the Graduate Committe

of Lehigh University

in Candidacy for the Degree of

Master of Science

in

Mechanical Engineering

Lehigh University

1983

This thesis is accepted and approved in partial fulfillment of the requirements for the degree of Master of Science in Mechanical Engineering.

11 MAY 1983
Date

Professor in Charge

Chairmen of Department

Acknowledgement

This project was sponsored in part by the National Aeronautics and Space Administration, Lewis Research Center, Cleveland, Ohio.

Table of Contents

List of Tables

List of Figures

Abstract

In this report a mathematical model of flutter in the cascades of blades in compressors and fans will be presented. The model predicts that a 10% variation in blade natural frequencies around the rotor can cause some blades to flutter while the transient oscillations of other blades die out. The type of sustained oscillation exhibited is that of nonlinear limit cycles.

There is considerable experimental evidence of limit-cycle flutter in mistuned blade-disc assemblies, a phenomenon that can be modeled only by nonlinear differential equations. The major difference between this work and previous models is the incorporation of nonlinear damping forces which permit limit cycles to develop.

Nomenclature

a	Aerodynamic Coupling Parameter, Nondimensionalized Parameter
b	Aerodynamic Coupling Parameter, Blade Semi-chord
c_1, c_2	Den Hartog Damping Parameters
c_l	Lift Coefficient
c_L	Wake Oscillator Motion
c_{LO}	Aerodynamic Damping Coefficient
c_m	Cofficient of Moment
d	Aerodynamic Coupling Parameter
f	Frequency
g	$\mathcal{L}^{-1}[G(s)]$
h	Lateral Motion, Height of the Blade
k	Reduced Frequency for Unsteady Motion
l	Length of the Blade
m	Mass of the Blade, Mass per Unit Span
n	Aerodynamic Coupling Parameter
q_r	Lagrangian Generalized Variables
s	Struhal Number
t	Time
w	Frequency of the System
w_n	Natural Frequency of the Mechanical System
w_s	Frequency Coefficient
w_R	Reduced Frequency
x	Mechanical Oscillator State Variable
A	Aerodynamic Coupling Parameter

A_i	Coefficients of Polynomial Approximation
B	Aerodynamic Damping Coefficient
D	Diameter, Damping Parameter
F	Dimensionless Coefficient
G	Aerodynamic Damping Coefficient, Transfer Function
H	Aerodynamic Coupling Parameter
I	Blade Number
I_α	Mass Moment of Inertia
K	Spring Constant
L	Lift
M	Moment
R_e	Reynolds Number
S	Blade Area
S_α	Static Mass Moment per Unit Span about the Elastic Axis
T	Kinetic Energy
U	Flow Speed
V	Potential Energy
X	Amplitude of the Oscillations
α	Pitch, Angular Deflection, Rotational Motion,
β	Damping Coefficient
ϵ	A Small Number
γ	Describing Function
λ	Eigenvalue
μ	Viscosity
ρ	Density

ξ Configuration Factor

τ Normalized Time

1. Introduction

Bladed cascades in turbines and compressors vibrate in a variety of ways that are not yet fully understood. Although each blade around the rotor is manufactured to the same specifications, they do not behave alike in operation. Each blade vibrates with a unique frequency. This may be atributed to the small discrepancies that are created in the blades during manufacture. Such a bladed rotor is called a mistuned rotor.

Numerous linear analytical methods have been developed for the prediction of the behavior of a mistuned system - see Ewins [8]. In these methods a mistuned fan assembly model is formulated by representing each blade as a linear torsional oscillator. The torsional inertias of these oscillators are considered uniform but their stiffnesses are allowed to vary according to the square of the natural frequency of each blade.

The character of the oscillations witnessed in the rotor blade torsional vibration data from NASA-LRC engine tests show strong evidence of a type of flutter classified as limit cycle oscillations - see Lubomski [14]. Linear equations are incapable of showing limit cycle oscillations, only a non-linear model can successfully exhibit this type of behavior. In the work that follows, we shall develop a mathematical model which will show some blades in the cascade can exhibit self-excited stable oscillations while the oscillations of other blades die

out. These blades will show different amplitudes and phase angles relative to each other. The model will also exhibit the stationarity found in the NASA-LRC flutter data. The equations require the user to enter the values of the aerodynamic damping terms and the stiffness of each blade around the rotor. In this work the problem is solved for 24 blades on the rotor, however, with the method outlined in section 10 any number of blades can be modeled. Using the data, the model will predict which of the blades flutter and which of them do not. The above is done in five parts:

1. The phenomenon of limit cycle oscillations is first explained and then the literature is cited.

2. The equations of motion are next written for the physical situation using Lagrange's equations. These equations are simulated using static lift and moment curves (for four different blades). It will be shown that the equations of motion are incapable of showing limit cycle oscillations with static lift and moment curves. An energy injection/extraction is necessary to produce these oscillations. It will also be shown that once this energy injection/extraction damping term exists, limit cycle oscillations are achieved no matter what kind of blade (with a certain lift and moment curve) is used. This indicates the importance of the damping term in an otherwise linear system and is essential to the susceptibility of the system to limit cycle. Linear models cannot portray self-sustaining oscillations.

3. A damping term is next introduced into the equations representing the energy injection/suction mentioned above. It will be shown that the nature of this hypothetical aerodynamic damping will determine the susceptibility of the system to limit cycle. In fact, the robustness of the limit cycle is not affected even if a blade with a linear moment relationship is used.

4. Since limit cycle oscillations are possible once the energy injection/extraction above is introduced, the equations must be tuned to determine which blades (having a range of natural frequencies) will or will not flutter. Two methods are described.

5. The model for the mistuned assembly will incorporate the effect of individual blade natural frequencies with common aerodynamic damping and aero-elastic and mechanical coupling between the blades. The method of tuning mentioned is used to determine which of the blades in a cascade will flutter and which of them do not.

2. Limit Cycle Oscillations

Consider the second order autonomous system

$$\dot{x}_1 = f_1 (x_1 (t) , x_2 (t)) \tag{2.1}$$

and

$$\dot{x}_2 = f_2 (x_1 (t) , x_2 (t)) \tag{2.2}$$

In the study of second order systems a plot of x_1 on the abscissa and x_2 on the ordinate is called the state plane plot. Now consider

$$\ddot{y} = f (\dot{y}(t) , y(t)) \tag{2.3}$$

then

$$x_1 = y \quad \therefore \quad \dot{x}_1 = \dot{y} \tag{2.4}$$

and

$$x_2 = \dot{y} \quad \therefore \quad \dot{x}_2 = \ddot{y} \tag{2.5}$$

that is we have

$$\dot{x}_1 = x_2 \tag{2.6}$$

$$\dot{x}_2 = f (x_1 (t) , x_2 (t)) \tag{2.7}$$

In this system one of the state variables is the derivative of the other. In this case the plot of x_1 versus x_2 is called a phase plane plot. It is with the help of the phase plane that we can explain self-excited oscillations. Phenomena of this kind were first studied by Poincaré who gave them the name of limit cycles.

A limit cycle of the system 2.1 and 2.2 is a closed, periodic and isolated curve of the type in Figures 2.1 and 2.2. The term isolated means that every solution, regardless of it's initial state, approaches

a single closed curve. The physical meaning of this type of oscillation is explained by the plot of the position versus time, in which the oscillations reach a steady amplitude after passing through the transient stage. The frequency of the self-excited vibration is the natural frequency of the system.

The limit cycle oscillations can be created by a type of positive -negative damping coefficient

$$\ddot{x} + f(\dot{x}) + x = 0. \tag{2.8}$$

An example of this is Van der Pol's equation

$$\ddot{\alpha} + (c_1 + c_2 \dot{\alpha}^2) \alpha + \alpha = 0. \qquad c_1 < 0 \text{ and } c_2 > 0 \tag{2.9}$$

This means that the damping force has a negative value for small $\dot{x}$. The negative damping causes the system energy to increase, causing the amplitude of x and $\dot{x}$ to increase. When $\dot{x}$ becomes large, the damping term is positive and therefore it dissipates energy causing the amplitude to decrease. After some transient time is expired, a periodic vibration is established. The initial state of the oscillator is unimportant in deciding the final value of the amplitude.

As Figures 2.1 and 2.2 show, the oscillations tend to a closed trajectory. Limit cycles however, are not very easily detectable. To check further, a plot of the angular position versus time is sketched. The angular position, after passing through a transient state, reaches the steady state amplitude indicative of limit cycle oscillations. In limit cycle oscillations, the energy that is injected into the system in one part of the cycle is taken out in another part. When the limit

cycle is established, therefore, the total energy of the system averaged over a cycle must approach a constant value. This is shown in Figure 2.3. The energy reaches a finite value asymtotically as the steady state is approached.

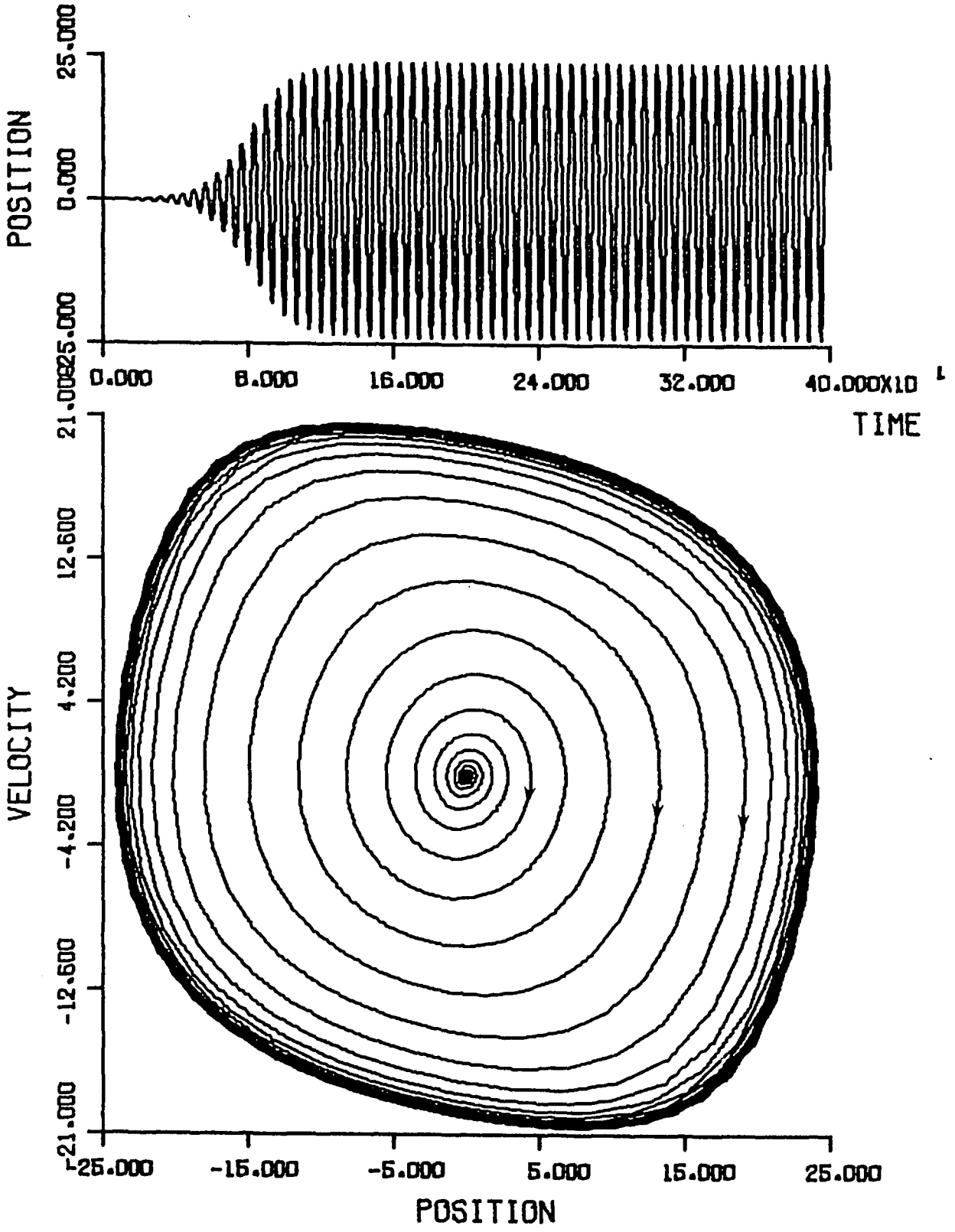

Figure 2-1. Limit Cycle Oscillations

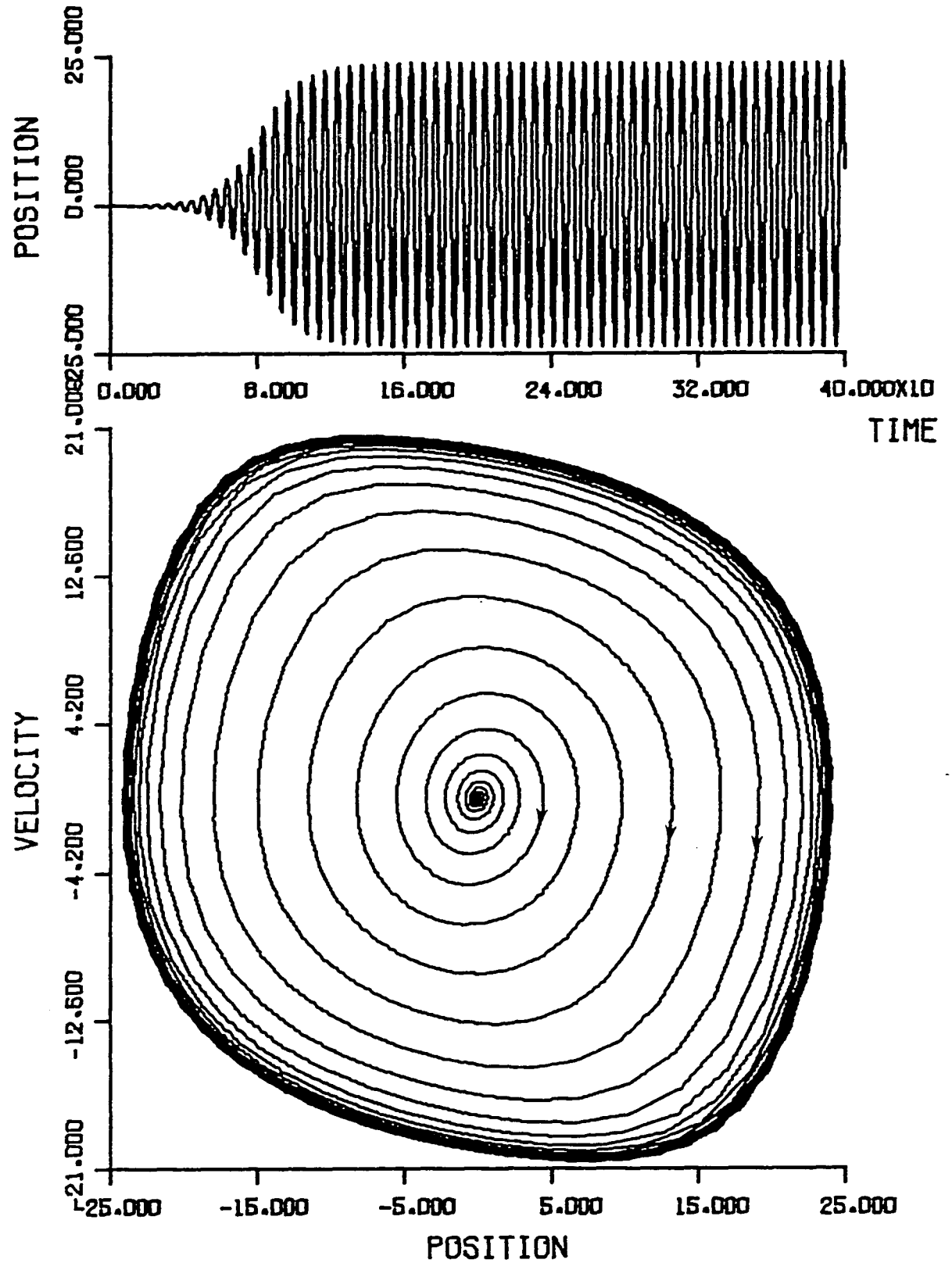

Figure 2-1. Limit Cycle Oscillations

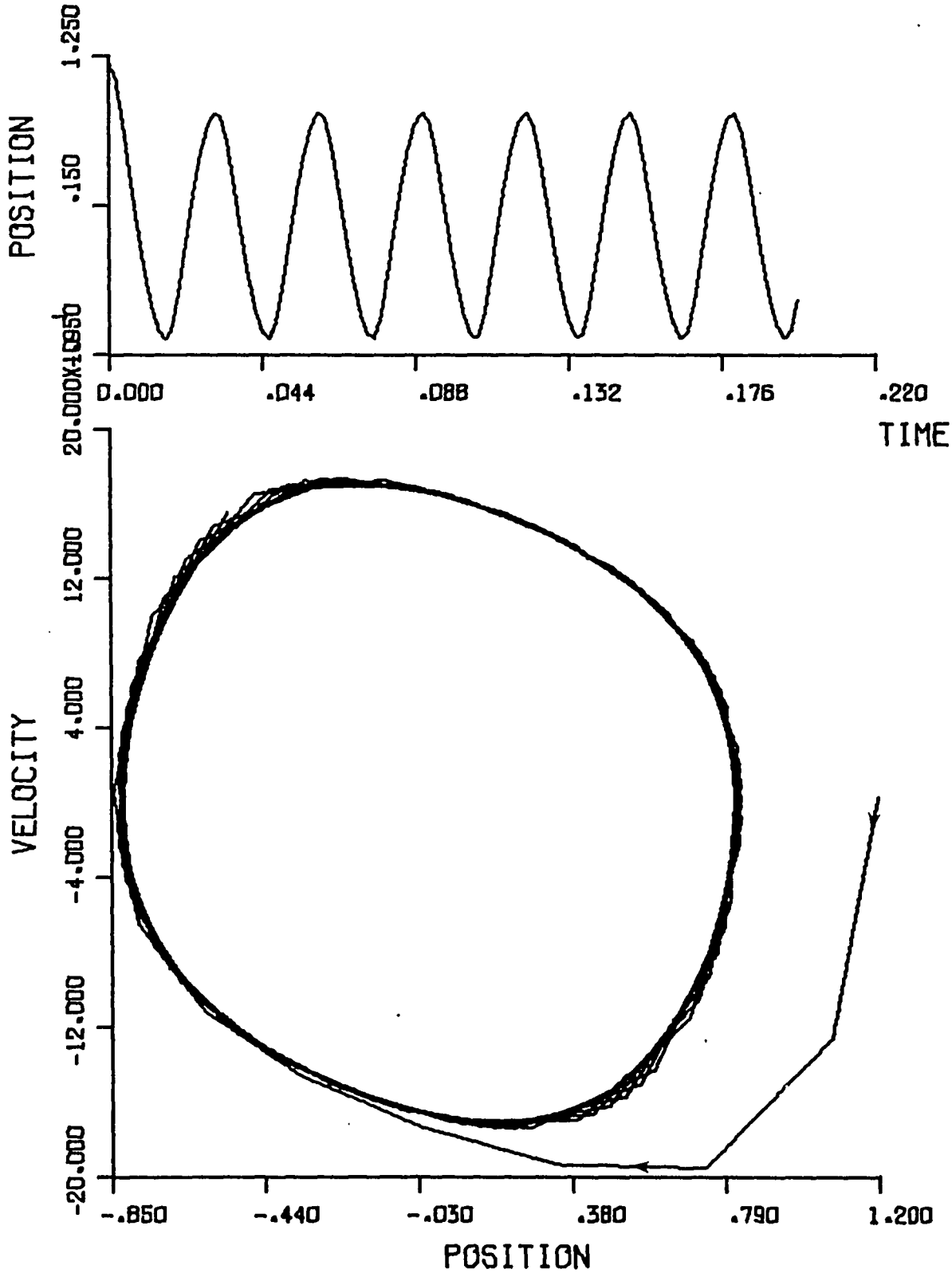

Figure 2-2. Limit Cycle Oscillations

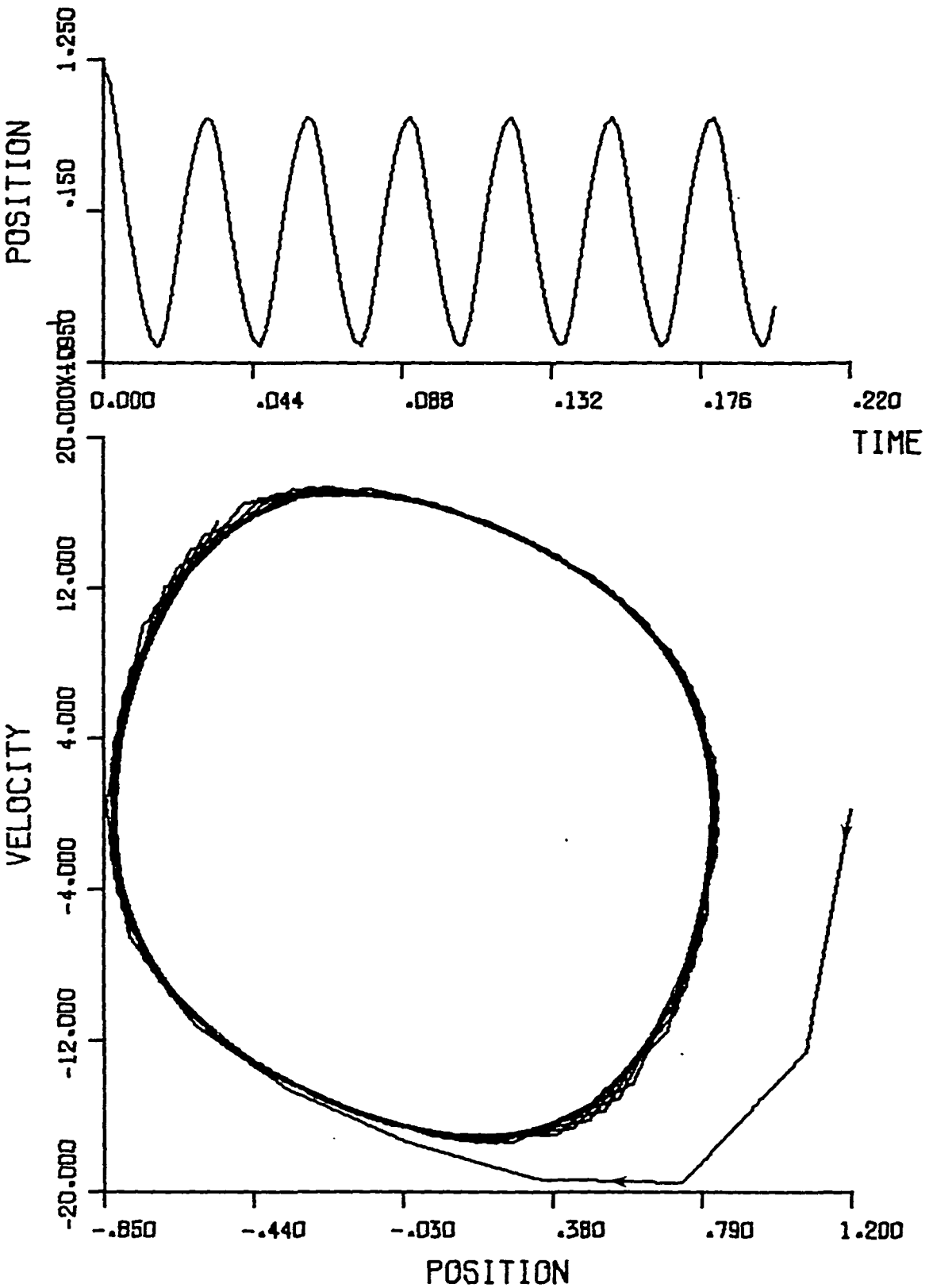

Figure 2-2. Limit Cycle Oscillations

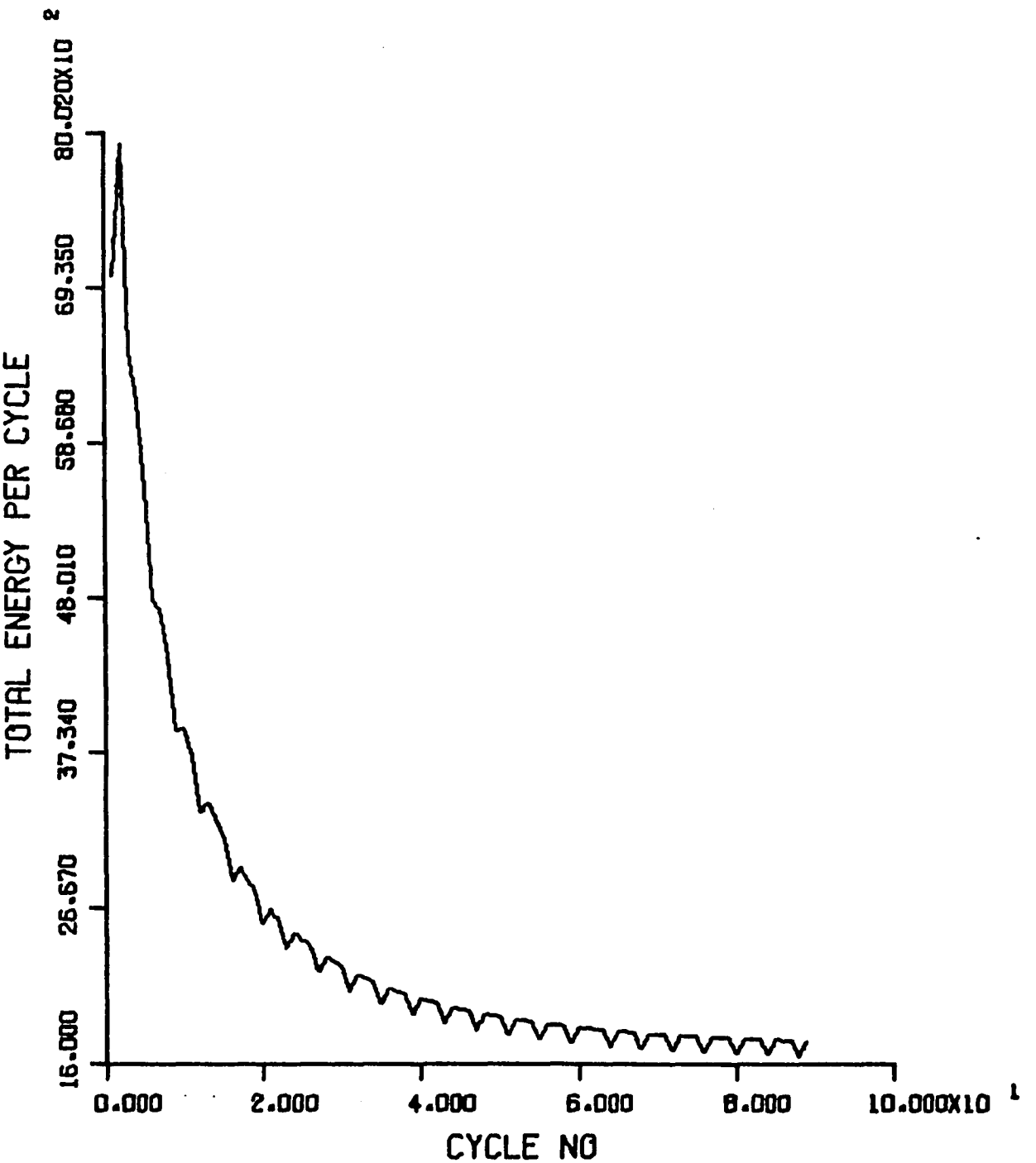

Figure 2-3. Energy Plot of Limit Cycle Oscillations

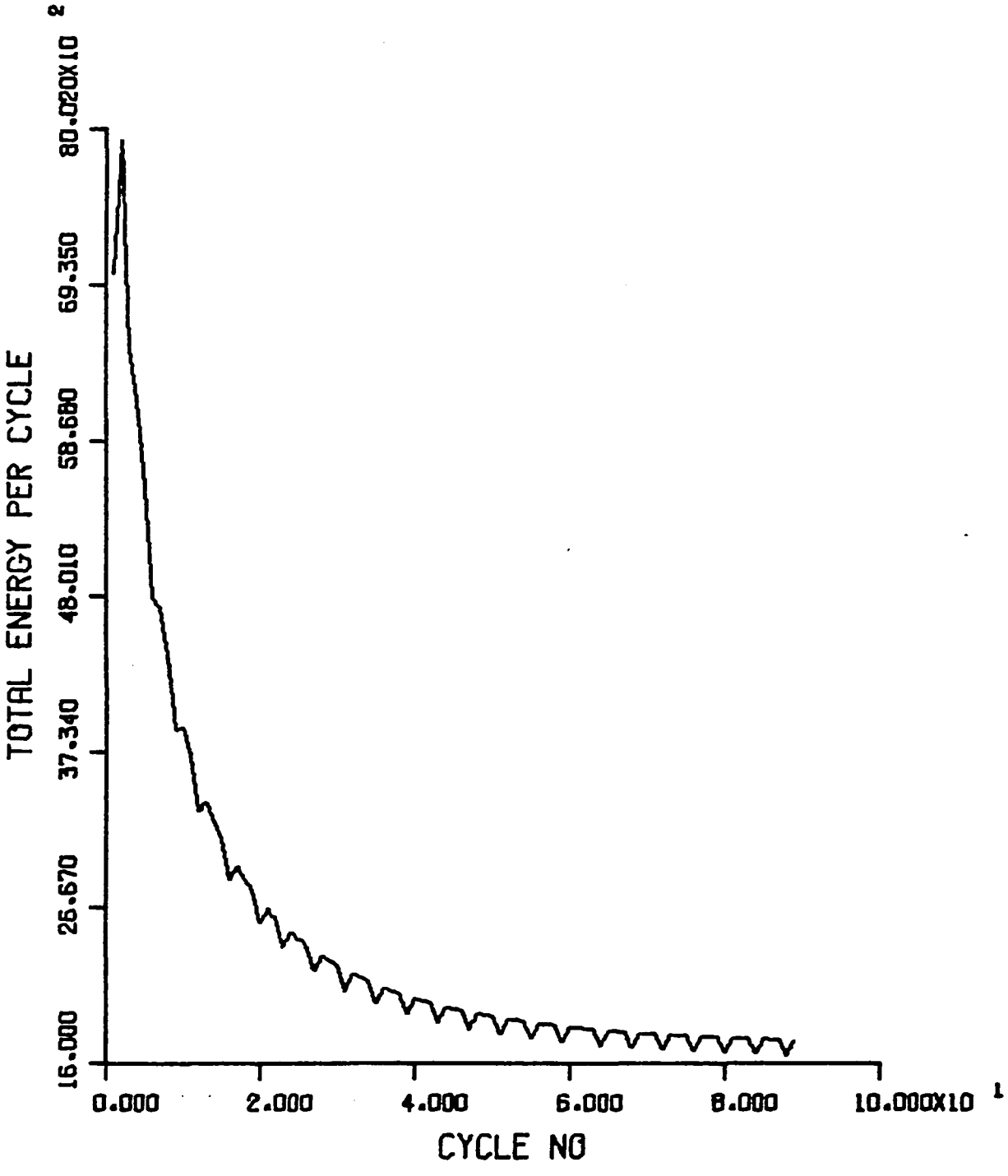

Figure 2-3. Energy Plot of Limit Cycle Oscillations

3. Literature Search

In this section, the mathematical representation of vortex-induced oscillations is introduced (equations 3-7 and 3-8). It will be shown that a variety of different authors have used some variation of these two coupled equations. Choosing any of these variations will produce the desired behavior.

A vibration system capable of exhibiting limit cycle oscillations possesses a mechanism which injects energy in one part of each cycle and extracts it in another part. Mathematically

$$m\ddot{\alpha} + \epsilon f(\dot{\alpha}) + K\alpha = 0. \qquad (3.1)$$

The pioneering work in the area of equations of type 3.1 with non-linear damping was done by Van der Pol [23]. Van der Pol's equation is

$$\ddot{\alpha} + (c_1 + c_2\dot{\alpha}^2)\dot{\alpha} + \alpha = 0. \qquad (3.2)$$

This is a special form of equation 3.1 which is the simplest possible relaxation oscillator and can exhibit a stable limit cycle.

Numerous papers have been written about the oscillation of bluff bodies perpendicular to uniform, steady flow. There is a definite lack of understanding of the aerodynamic events in this type of oscillation at high reduced frequency - see Equation 3.4. With the exception of a few, the models are variations of Equation 3.2 or the relaxation oscillator suggested by Den Hartog [7]

$$m\ddot{\alpha} + (c_1 + c_2\alpha^2)\dot{\alpha} + K\alpha = 0. \qquad (3.3)$$

Parkinson [16] has categorized the flow-induced vibration into two

sections: vortex induced resonance and galloping. Defining reduced frequency as

Reduced Frequency = $w_R = w_n\ s\ /\ U$ (3.4)

for the simpler case (galloping) we have $w_R << 1$. In this case the free stream velocity and the motion of the body are small. For this type of motion, the following second order non-linear equation presented by Parkinson and Smith [17] adequately describes the motion

$$\ddot{\alpha} + 2\ \beta\dot{\alpha} + \alpha = a\ [\ A_1(\dot{\alpha}/U) - A_2(\dot{\alpha}/U)^3 + A_3(\dot{\alpha}/U)^5 + A_4(\dot{\alpha}/U)^7\ ] \qquad (3.5)$$

where

$$\dot{x} = dx\ /\ d\tau \quad ;\quad \tau = w_n\ t \qquad (3.6)$$

where $\tan^{-1}(\dot{\alpha}/U)$ is the instantaneous angle of attack. In this case it is sufficient to find the coefficients A_1, A_2, A_3 and A_4 from a static lift versus α curve. This model successfully explains galloping. When the motion is faster than before and $w_R \sim 1$, the static curve will no longer suffice. This type of oscillation is called the vortex induced oscillation and the simplest model that can predict the behavior of this system requires two coupled second order ordinary differential equations. At least one of these equations (that of the wake oscillator) is non-linear

Linear mechanical oscillator:

$$\ddot{\alpha} + 2\ \beta\dot{\alpha} + \alpha = n\ c_L\ U^2 \qquad (3.7)$$

Nonlinear wake oscillator:

$$\ddot{c}_L - Aw_n\dot{c}_L + (B/w_n)\dot{c}_L^3 + w_n^2 c_L = d\ \dot{\alpha}\ . \qquad (3.8)$$

Equations 3.7 and 3.8 are capable of showing limit cycles and frequency entrainment.

Berger [3] has generalized the last two equations for the one- degree of freedom oscillator transverse to the flow by

$$\ddot{\alpha} + 2\beta\dot{\alpha} + \alpha = a\Omega^2 c_L \tag{3.9}$$

$$\ddot{c}_L + f^*(\dot{c}_L) + \Omega^2 c_L = b\dot{\alpha} \tag{3.10}$$

where

$$\dot{x} = dx / d\tau = dx / w_n\, dt\ . \tag{3.11}$$

In all these equations the damping and coupling parameters are unknown. They are generally obtained by experiments. In our case, we will try to find the parameters by numerical solution of the equations and analytical methods. Skop and Griffin [20] actually make appropriate choices of some physical quantities for the empirical equations and find good agreement with the experimental data

$$\ddot{\alpha}/D + 2\beta w_n(\dot{\alpha}/D) + w_n^2(\alpha/D) = (\rho U^2 L/2m)c_L \tag{3.12}$$

$$\ddot{c}_L - w_s G[c_{LO}^2 - 4/3(\dot{c}_L/w_s)^2]\dot{c}_L + w_s^2[1 - 4/3\ H\ c_L^2]\ c_L = w_s\ f(\dot{\alpha}/D)\ . \tag{3.13}$$

The frequency coefficient and the four dimensionless coefficients C, G, H and F have to be evaluated from experiments. The coupling and damping parameters in this model have physical interpretations.

The model proposed by Griffin, Skop and Koopman [9] is different from the others in that they have added a non-linearity to the spring term, as well as to the damping term, in the lift oscillator equation.

As one can easily notice, an endless variety of non-linearities in the wake oscillator can be thought of to produce the energy injection/suction mechanism which is characteristic of limit cycles. Hartlen and Currie [10] introduced the first of these models which was

followed by others. Their non-linearity is of the Van der Pol type

$$\ddot{\alpha} + 2\beta\dot{\alpha} + \alpha = n u^2 C_L \tag{3.14}$$

$$\ddot{c}_L - A w_n \dot{c}_L + (B/w_n)\dot{c}_L^3 + w_n^2 c_L = d\dot{\alpha}. \tag{3.15}$$

Currie, Hartlen and Martin [6] later added a non-linear spring term in the mechanical oscillator

$$\ddot{\alpha} + 2\beta\dot{\alpha} + (1-\epsilon\alpha^2)\alpha = a w_n^2 c_L \tag{3.16}$$

which is used with the Hartlen and Currie wake oscillator (equation 3.15). Finally Landl [13] chose to work with a linear mechanical oscillator coupled to a Den Hartog type relaxation oscillator

$$\ddot{\alpha} + \beta\dot{\alpha} + \alpha = a w_n^2 c_L \tag{3.17}$$

$$\ddot{c}_L + (A - Bc_L^2 + dc_L^4)\dot{c}_L + w_n^2 c_L = b\dot{\alpha} \tag{3.18}$$

Landl has shown that his model predicts much of the behavior of experiments done by Parkinson.

Although Hartlen and Currie present justification for their model, none of the models mentioned use any flow field theory to derive their equations. Iwan and Blevins [11] have used semi-impirical flow field theory to derive their non-linear oscillator equations. This is described in Blevin's book [4] which also has a discussion of frequency synchronization, entrainment and lock-in. The latter subjects are also discussed in the book by Minorski [15].

Iwan and Blevins, like Skop and Griffin, have found physically interpreted parameters. They also reduce the number of parameters that appear in the equations and explain new experiments which can quantify these parameters.

In short, all of the authors mentioned above have used some variation of two coupled second order equations for a mechanical oscillator and a wake oscillator

$$\ddot{\alpha} + 2\beta\dot{\alpha} + \alpha = a\, c_L \tag{3.19}$$

$$\ddot{c}_L + f(\dot{c}_L)\,\dot{c}_L + w_n^2\, c_L = b\dot{\alpha} \tag{3.20}$$

$$\dot{x} = dx / d\tau = dx / w_n dt\ . \tag{3.21}$$

Choosing any of the models presented here will yield similar results. Simplicity is more inherent in the model by Hartlen and Currie since they have chosen a Van der Pol type oscillator.

4. Equations of Motion

Lagrange's equations can be used to find the equations of motion of the blade shown in Figure 4-1. The blade shown in this figure has two degrees of freedom (i.e. rotational motion α and lateral motion h). This analysis will later be used for a blade in rotational flutter.

Lagrange's equation for a non-conservative system is

$$d/dt\ (\partial T/\partial \dot{q}_r) - \partial T/\partial q_r + \partial v/\partial q_r = F_r \tag{4.1}$$

where F_r are the generalized non-conservative forces, and

$$T = 1/2\ m\ \dot{h}^2 + 1/2\ I_\alpha \dot{\alpha}^2 + S_\alpha \dot{\alpha} \dot{h} \tag{4.2}$$

$$V = 1/2\ K_h\ h^2 + 1/2\ K_\alpha \alpha^2 \tag{4.3}$$

$$\partial T / \partial q_r = 0 \tag{4.4}$$

A- taking $q_r = h$

$$d/dt\ (\partial T/\partial \dot{h}) + \partial V/\partial h = F_r \tag{4.5}$$

$$d/dt(m\dot{h}+S_\alpha\dot{\alpha}) + K_h h = F_r = -L \tag{4.6}$$

$$m\ddot{h} + S_\alpha \ddot{\alpha} + K_h h = -L \tag{4.7}$$

B- taking $q_r = \alpha$

$$d/dt(\partial T/\partial \dot{\alpha}) + \partial V/\partial \alpha = F_r = \text{MOMENT} \tag{4.8}$$

then

$$I_\alpha \ddot{\alpha} + S_\alpha \ddot{h} + K_\alpha \alpha = M\ . \tag{4.9}$$

For a non-conservative system the Lagrangian can be written as L+R, where R is in the form of Rayleigh's dissipation term. Therefore, when damping is present the equations of motion become

$$m\ddot{h} + S_\alpha \ddot{\alpha} + K_h h = -L \tag{4.10}$$

$$I_\alpha \ddot{\alpha} + S_\alpha \ddot{h} + K_\alpha \alpha = M + \text{Damping Force}\ . \tag{4.11}$$

Equations 4.10 and 4.11 are the equations of motion for the blade shown in Figure 4.1 having two degrees of freedom in the rotational and lateral directions.

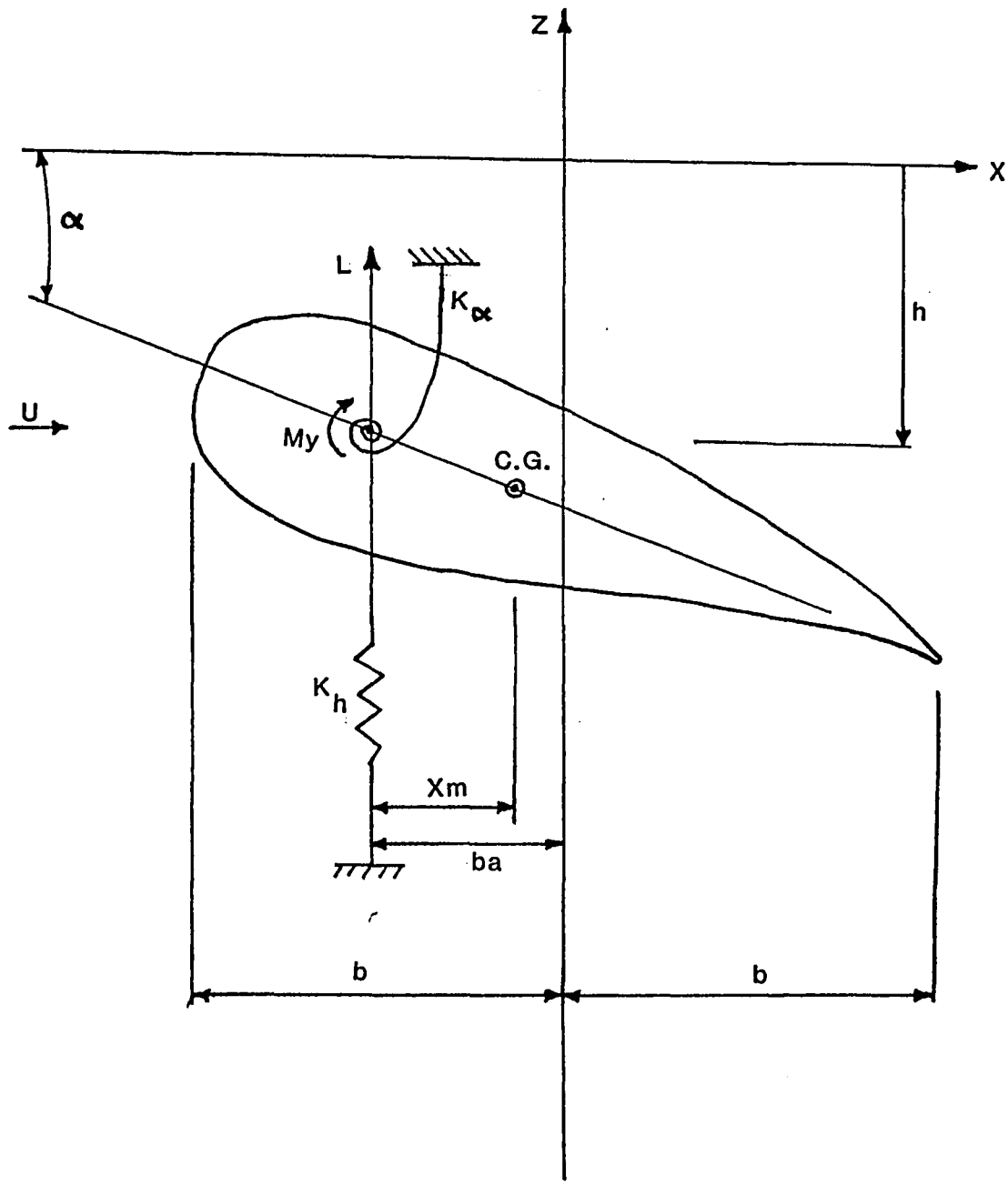

Figure 4-1. The Blade with Two Degrees of Freedom

5. Aerodynamic Tools

At this time one must wonder what type of oscillations a blade exhibits upon the substitution of the relations for the aerodynamic forces (lift and moment) in Equations 4.7 and 4.9.

Obtaining an equation that fully describes the aerodynamic lift and moment for a blade is obviously an impossible task and certain assumptions have to be made. At low speeds (subsonic) the flow can be considered incompressible. Bisplinghoff, et al [5] offer the following relationships for lift and pitching moment (due to pitching and vertical translation) for thin airfoils oscillating in incompressible flows

$$L=\pi\rho b^2[\ddot{h}+U\dot{\alpha}-ba\ddot{\alpha}] + 2\pi\rho UbC(k)[\dot{h}+U\alpha+b(1/2-a)\dot{\alpha}] \quad (5.1)$$

$$M=\pi\rho b^2[ba\ddot{h}-Ub(1/2-a)\dot{\alpha}-b^2(1/8+a^2)\ddot{\alpha}]+2\pi\rho Ub^2(a+1/2)C(k)[\dot{h}+U\alpha+b(1/2-a)\dot{\alpha}] \quad (5.2)$$

where C(K) is the Theodorsen's function

$$C(k)=c_1+ic_2=[H_1^{(2)}(k)]/[H_1^{(2)}(k)+iH_0^{(2)}(k)] \quad (5.3)$$

and

$$H_n^{(2)}(k) = J_n - iY_n \ . \quad (5.4)$$

$H_n^{(2)}(k)$ are the Hankel functions of first and second kind, i.e. a combination of Bessel functions of first and second kind. Substituting, we get

$$C(k)= [\ J_1(k)-iY_1(k)\ ]/[\ [J_1(k)+Y_0(k)] + i[J_0(k)-Y_1(k)]\ ] \quad (5.5)$$

$$C(k)= [J_1(k)-iY_0(k)][\ [J_1(k)+Y_0(k)] -i[J_0(k)-Y_1(k)]\ ] \ / \ [\ [J_1(k)+Y_0(k)]^2 + [J_0(k)-Y_1(k)]^2\ ] \quad (5.6)$$

The differential equations 4.7 and 4.9 are solved with the help of a Runge Kutta differential system simulator program (DSS/2 [19]). The

results are shown in Figure 5.1. The phase plane diagrams for α and h show that this system simply grows in amplitude. The oscillations resulting from the system above do not behave like the limit cycle oscillations.

After numerous runs with different blade characteristics no sign of the limit cycles appeared in the results. Therefore the hope for finding limit cycle oscillations in the flutter of blades using analytical expressions for lift and moment will be abandoned. The type of mechanism that is needed for the existence of the limit cycles does not exist in our lift and moment expressions. The flow and blade characteristics used in this analysis are listed in Table A-1. These values have been estimated by taking the blade to be a rectangular piece of steel. The blade characteristics can be found by the following equations [18]

$$K_\alpha = \tfrac{1}{3} (2b)\, h^3\, G \,/\, l \qquad (5.7)$$

$$K_h = 3\, E\, I \,/\, l^3 \qquad (5.8)$$

$$I_\alpha = 1/2\ m \left[(2b)^2 + h^2 \right] . \qquad (5.9)$$

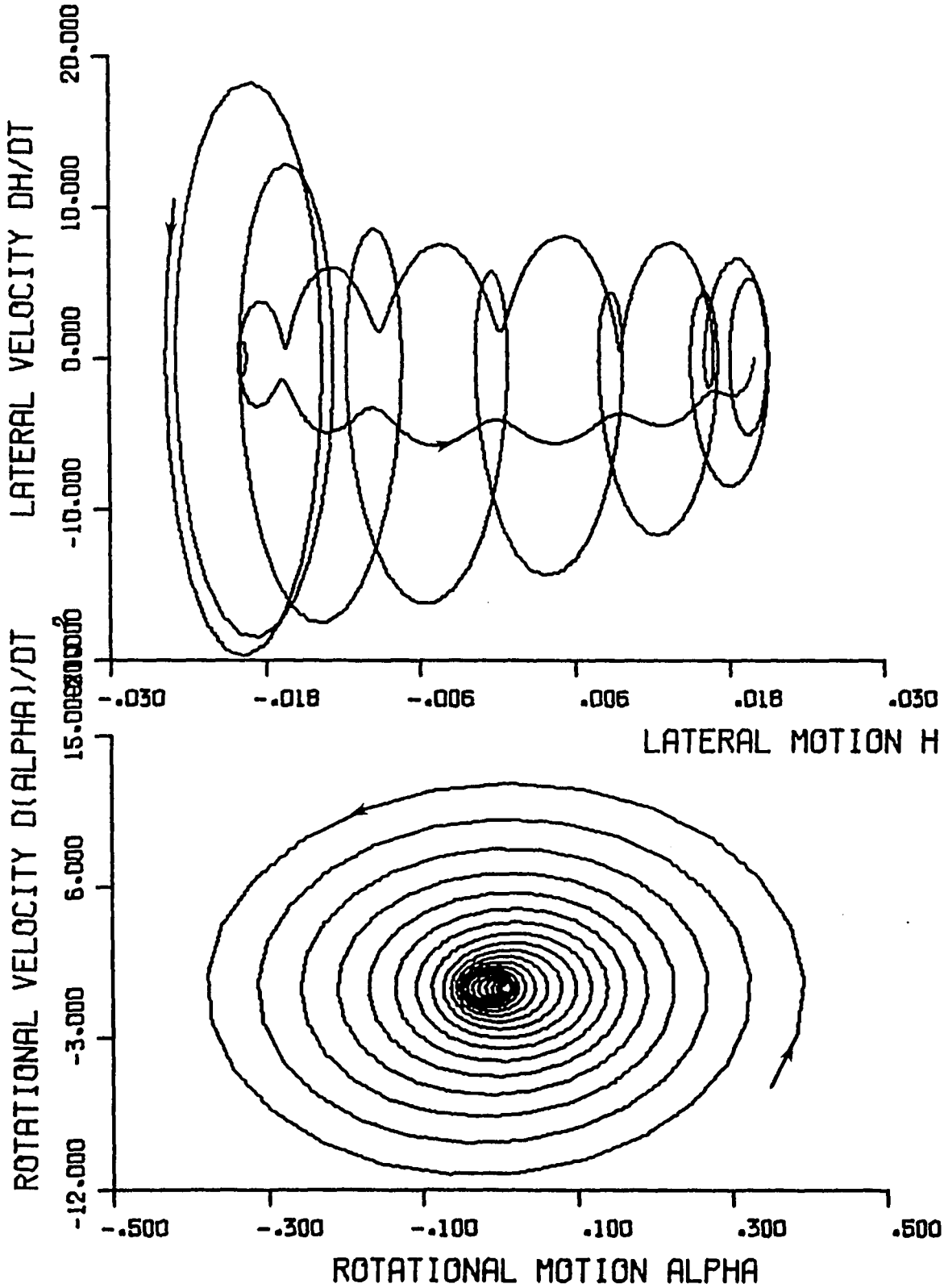

Figure 6-1. Phase Plane Diagrams

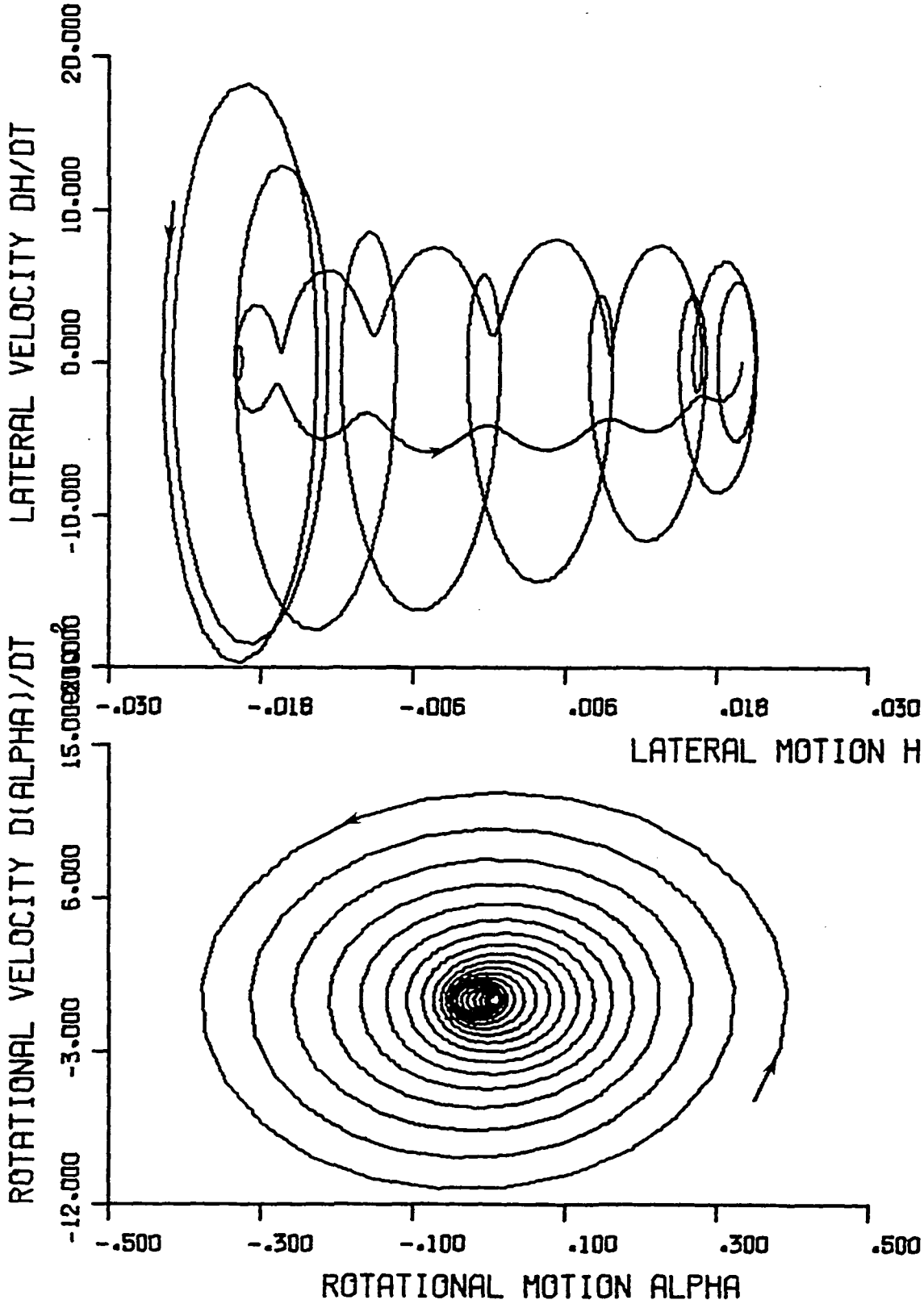

Figure 5-1. Phase Plane Diagrams

6. Analysis Using Static Lift and Moment Curves

The possibility of using experimental values for the lift and moment in Equations 4.7 and 4.9 will next be investigated. Abbott et al [1] includes an extensive summary of airfoil data and aerodynamic characteristics of wing sections. By the method of least squares [2] a fourth order polynomial will be fitted to the lift coefficient (C_l) and the moment coefficient (C_m) data. The lift and moment coefficients are plotted as functions of the angle of attack α. The interval of alpha has to be chosen big enough such that the lift and the moment curves are non-linear in this interval; since the limit cycle exists only in non-linear systems. The curves will be fitted through the points using

$$y = c_1 + c_2\alpha + c_3\alpha^2 + c_4\alpha^3 \tag{6.1}$$

$$b_{ij} = \sum_{k=1}^{N} \alpha_k^{i+j-2} \tag{6.2}$$

$$V_1 = \sum_{k=1}^{N} \alpha_k^{i-1}\, y_k \tag{6.3}$$

$$\underline{b}\ \underline{c} = \underline{V} \tag{6.4}$$

where N is the number of the points recorded.

The equations 6.1 through 6.4 are solved (for C_i) for NACA 4424, NACA 63-206, NACA 664-021 and NACA 4418. The data for the blades, obtained from Abbott's book are shown in Tables A-2 through A-5. Since we are interested in seeing the behavior of the system for different blades, care is taken to choose blades which have different aerodynamic behavior.

The following expressions for C_m and C_l are found

1- for NACA 4424 wing section

$$c_l = 1.9 + 6.22\alpha + 14.33\alpha^2 - 49.75\alpha^3 - 706.29\alpha^4 \quad (6.5)$$

$$c_m = -0.34 - 0.08\alpha + 0.38\alpha^2 + 0.29\alpha^3 + 18.17\alpha^4 \quad (6.6)$$

2- for NACA 63-206 wing section

$$c_l = 1.46 + 7.0\alpha - 6.12\alpha^2 - 197.25\alpha^3 - 808.48\alpha^4 \quad (6.7)$$

$$c_m = -0.22 - 0.30\alpha - 4.83\alpha^2 - 23.9\alpha^3 + 9.78\alpha^4 \quad (6.8)$$

3- for NACA 664-021 wing section

$$c_l = -0.02 + 5.40\alpha + 0.98\alpha^2 - 13.23\alpha^3 - 10.10\alpha^4 \quad (6.9)$$

$$c_m = -0.0009 + 0.58\alpha + 0.66\alpha^2 - 8.24\alpha^3 - 11.42\alpha^4 \quad (6.10)$$

4- for NACA 4418 wing section

$$c_l = 0.42 + 6.11\alpha - 2.82\alpha^2 - 21.67\alpha^3 + 1.66\alpha^4 \quad (6.11)$$

$$c_m = -0.08 + 0.04\alpha + 0.36\alpha^2 + 0.64\alpha^3 - 4.39\alpha^4 \; . \quad (6.12)$$

The plots of these coefficients versus α are shown in Figures 6.1 through 6.4. The lift and pitching moment are given by the following expressions

$$L = 1/2\,\rho\, U^2\, S\, \text{abs}(\cos\alpha)\, c_l \quad (6.13)$$

$$M = 1/2\,\rho\, U^2\, S\, \text{abs}(\cos\alpha)\, b\, c_m \quad (6.14)$$

where

$$U = \mu g_c R_e \; / \rho\, D \; . \quad (6.15)$$

These expressions are used in Equations 4.7 and 4.9 and the resulting differential equations are simulated. Again, no limit cycle appears for any of the four blades investigated. This is again due to the fact that the energy injection/suction that is essential to the existence of the limit cycles is lacking so far in our model. However, the question that arises is how important is this damping (energy injection/suction mechanism) compared to other aerodynamic or spring forces.

To answer this question, we introduce the Den Hartog [7] damping coefficient to our equations as suggested by Lubomski [14]. The equation of motion becomes

$$I_\alpha \ddot{\alpha} - (c_1 - c_2 \alpha^2) \dot{\alpha} + K_\alpha \alpha = M \qquad (6.16)$$

This equation is plotted for the four blades above. We chose four different blades with four different moment diagrams and yet all these blades show a stable limit cycle when the energy injection/ suction mechanism appears in the equation of motion. Moreover, by using a linear moment versus α relationship in place of a more realistic non-linear expression, the limit cycle is still persistent, as shown in Figure 6-5. Therefore, the conclusion is that if the aerodynamic forces alternatively extract and inject energy into the isolated blade, a persistent limit cycle can result which is unaffected by the details of the specific situation. This is despite the fact that the amount of the aerodynamic damping in each cycle is small compared to the inertia and spring forces. This is consistent with the measurements taken from the turbine blades where the aerodynamic damping is found to be very small.

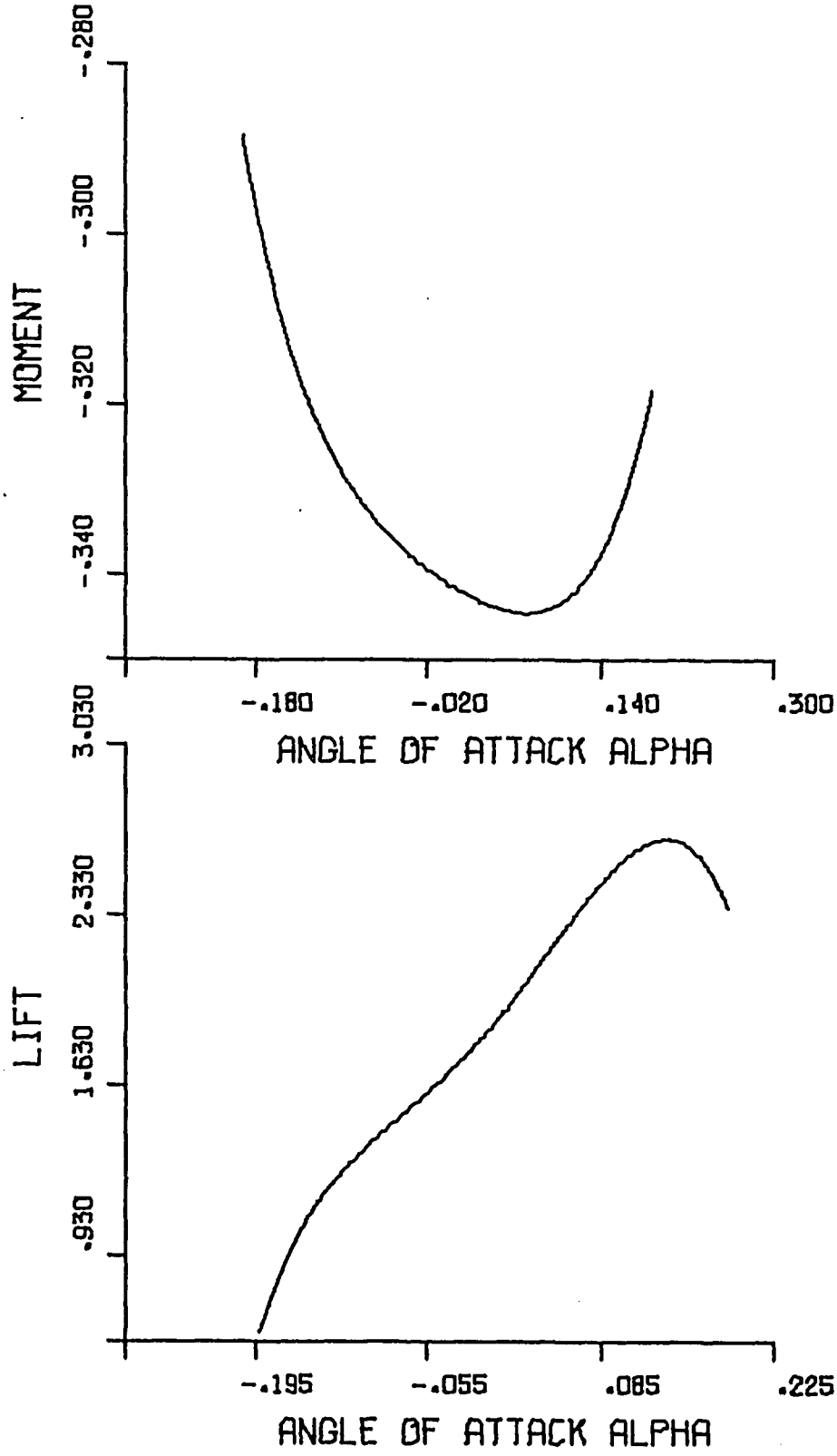

Figure 6-1. Blade NACA.4424

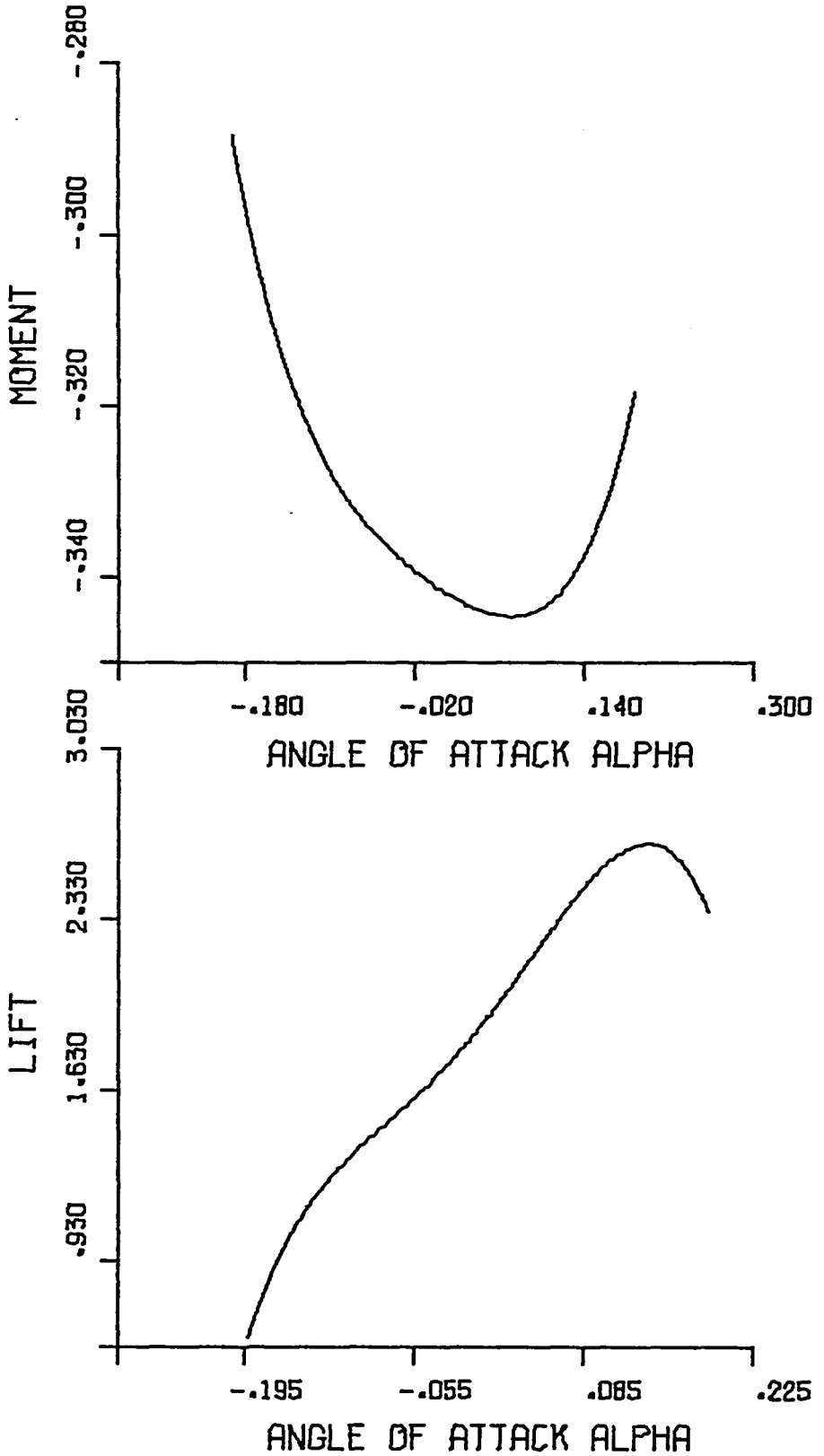

Figure 6-1. Blade NACA.4424

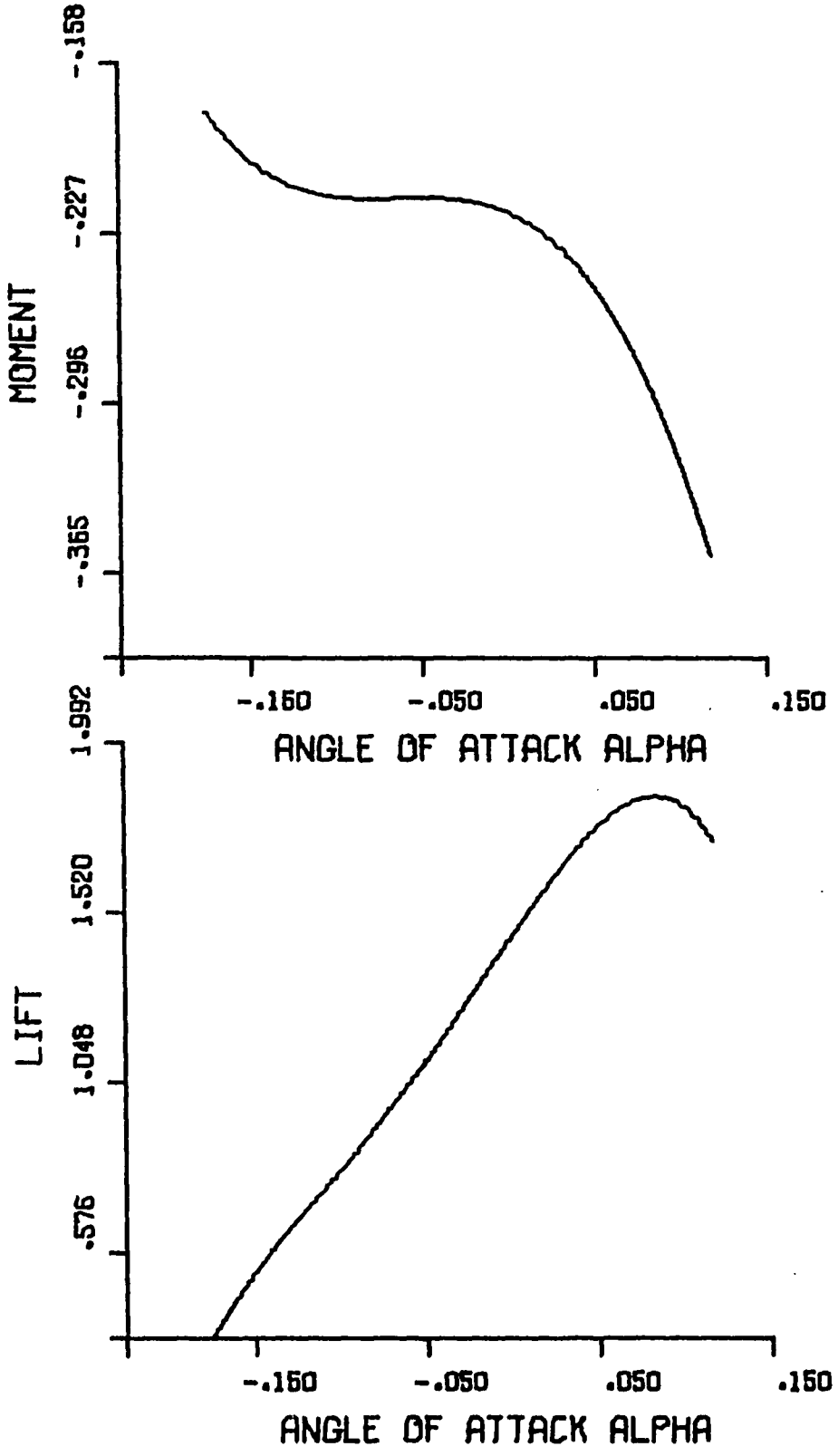

Figure 6-2. Blade NACA 63-206

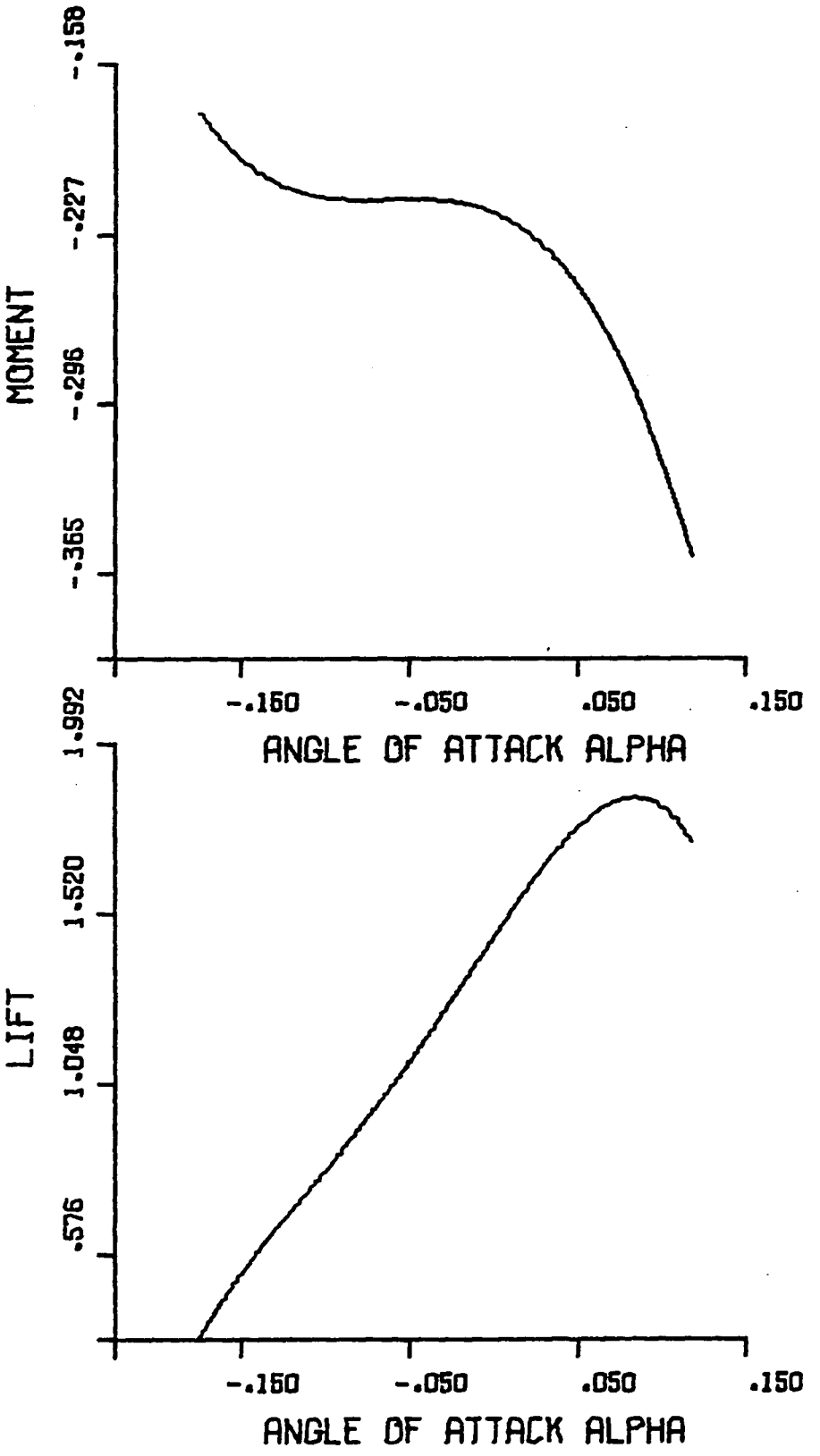

Figure 6-2. Blade NACA 63-206

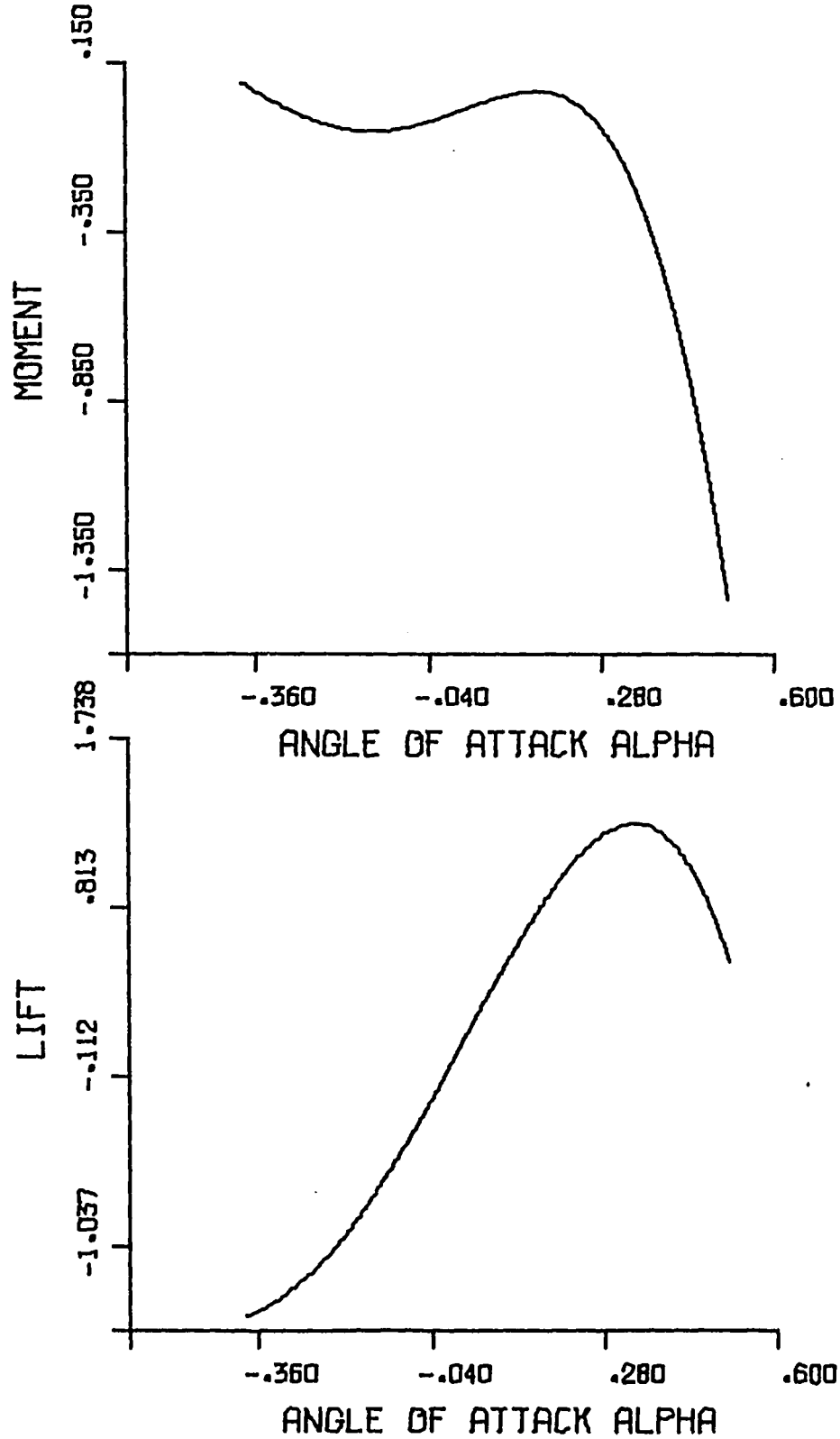

Figure 6-3. Blade NACA 664-021

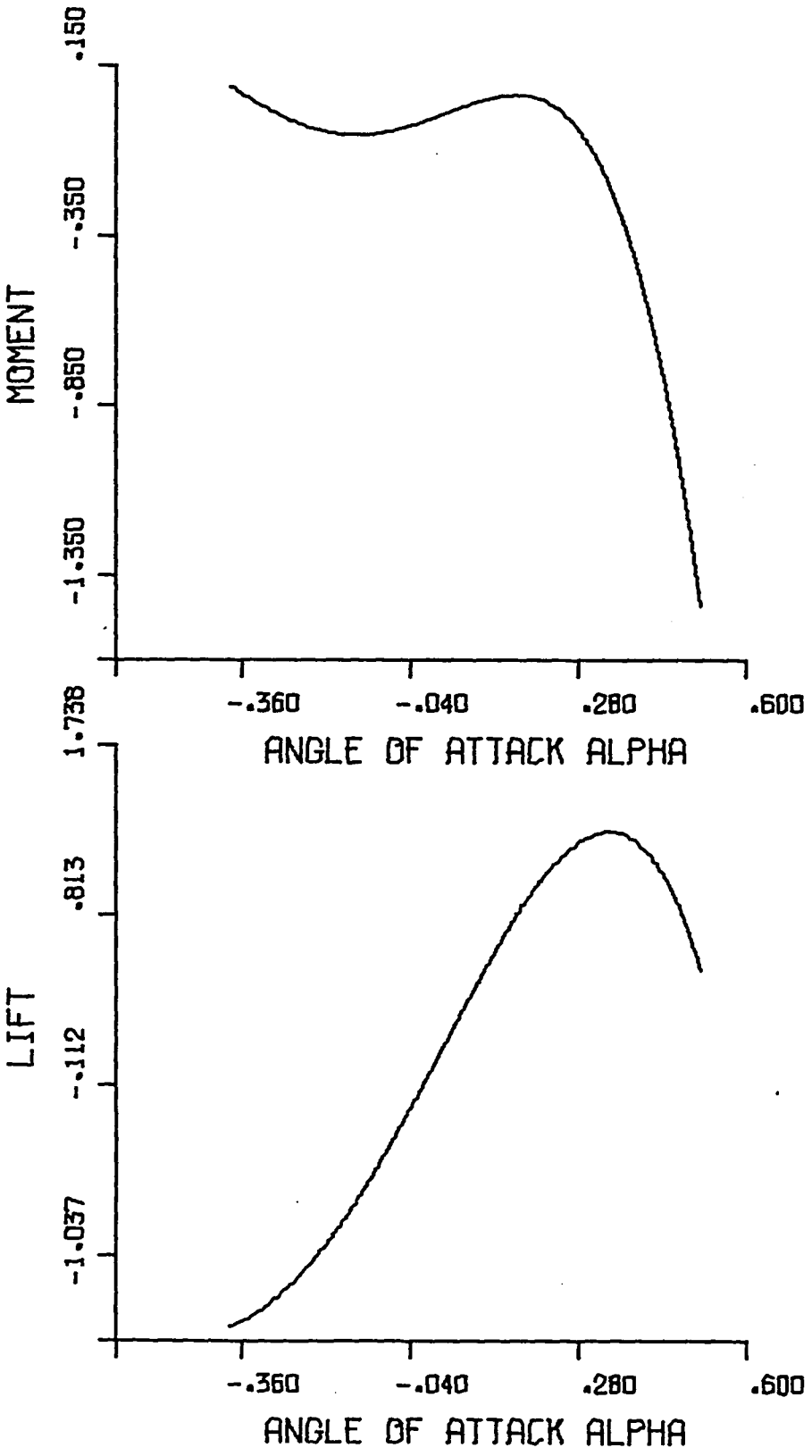

Figure 6-3. Blade NACA 664-021

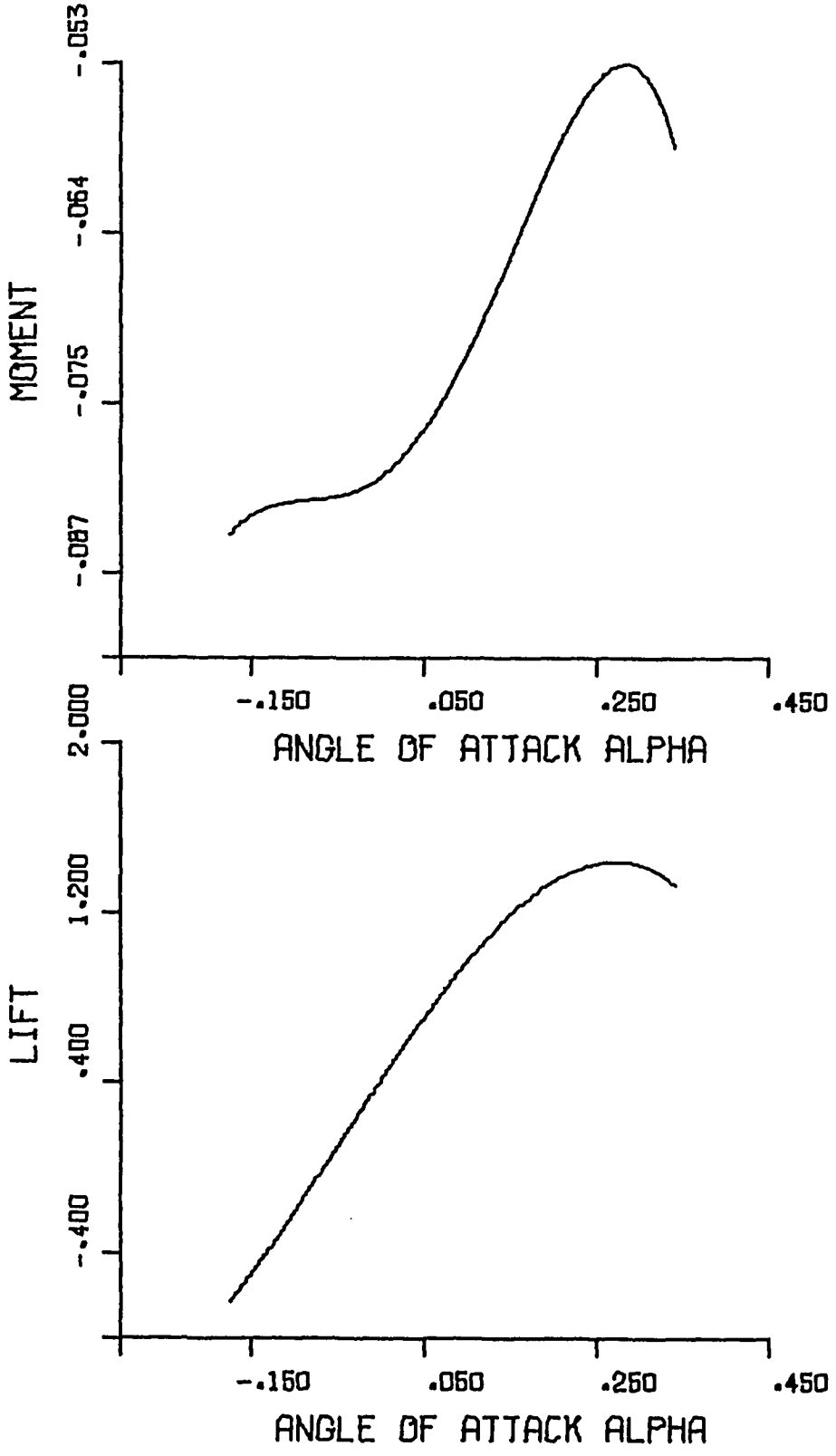

Figure 6-4. Blade NACA 4418

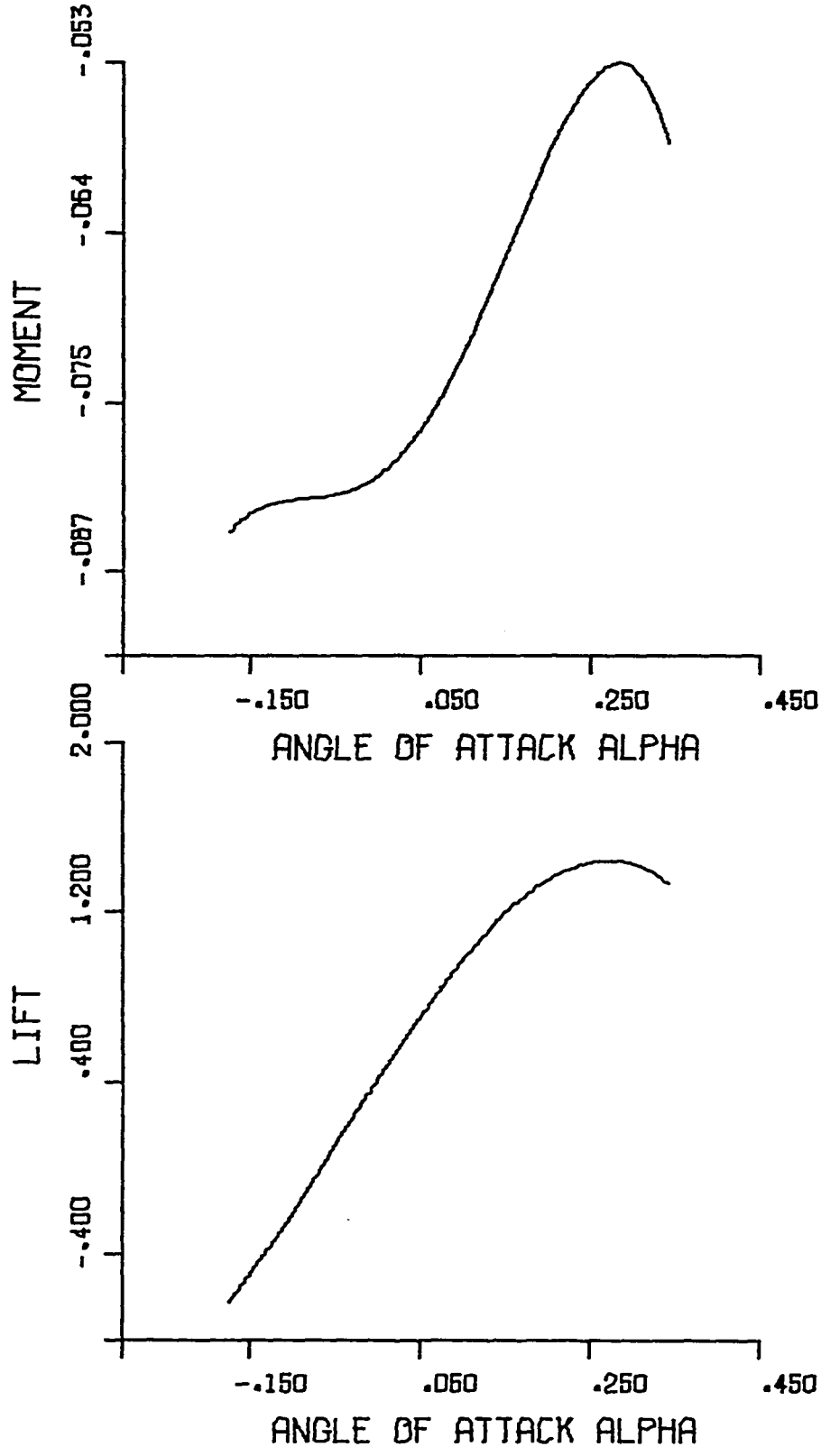

Figure 6-4. Blade NACA 4418

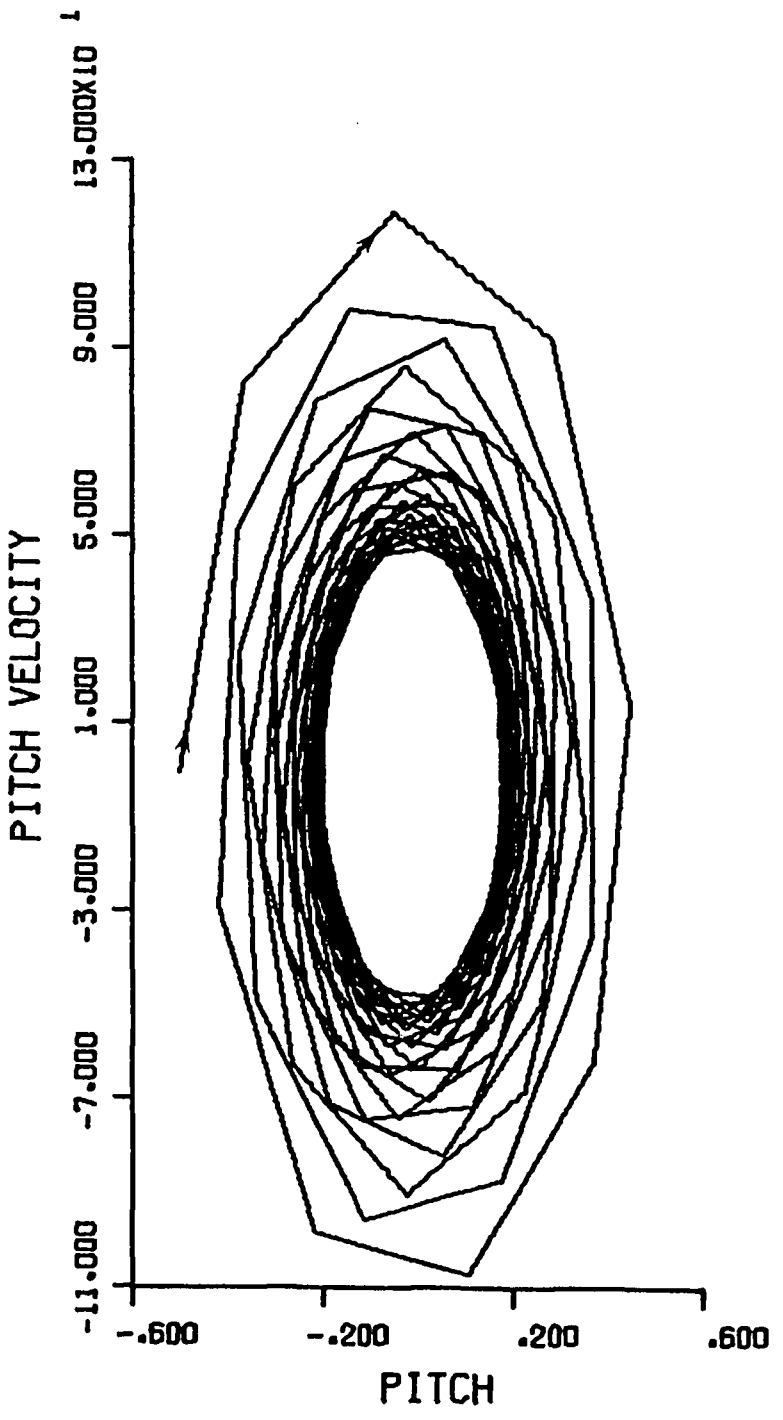

Figure 6-5A. Using Blade NACA 4424 in the Equations

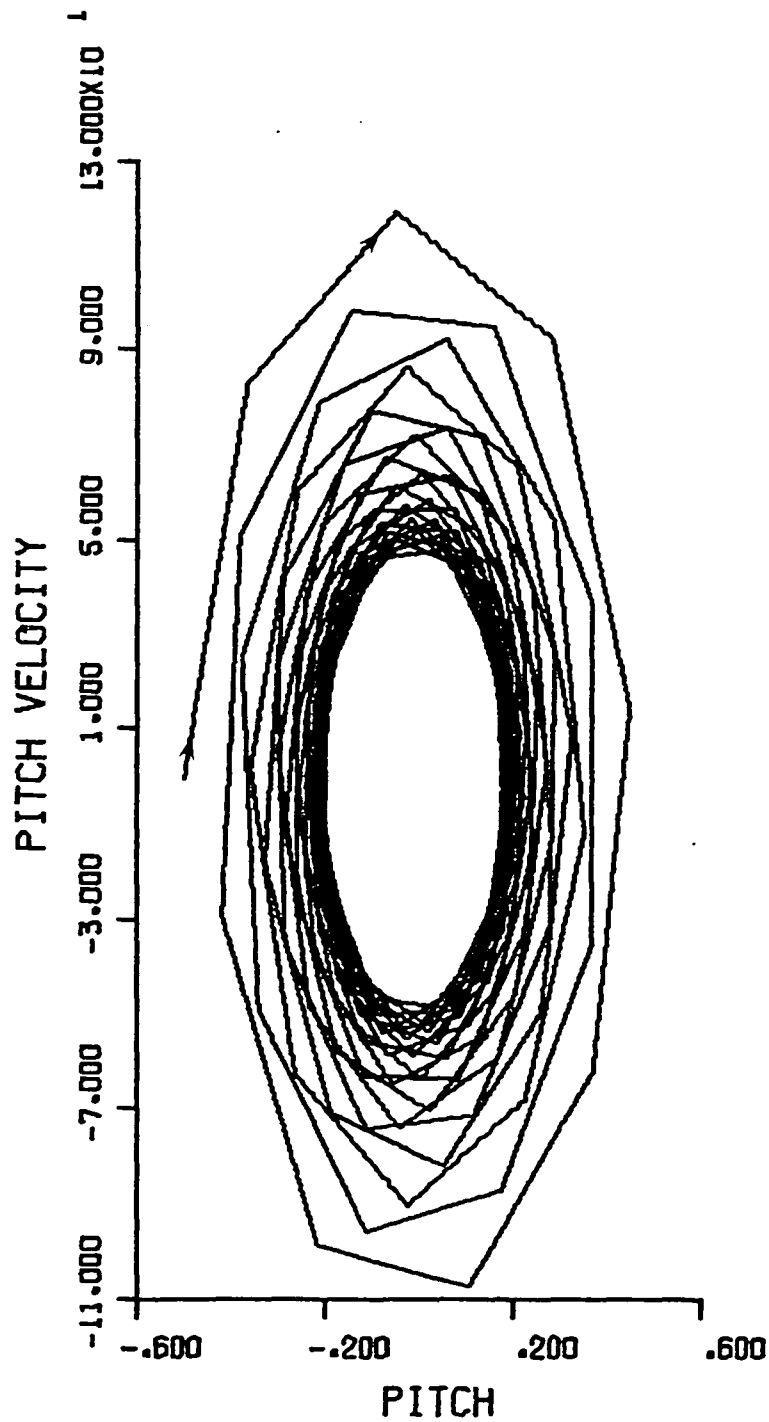

Figure 6-5A. Using Blade NACA 4424 in the Equations

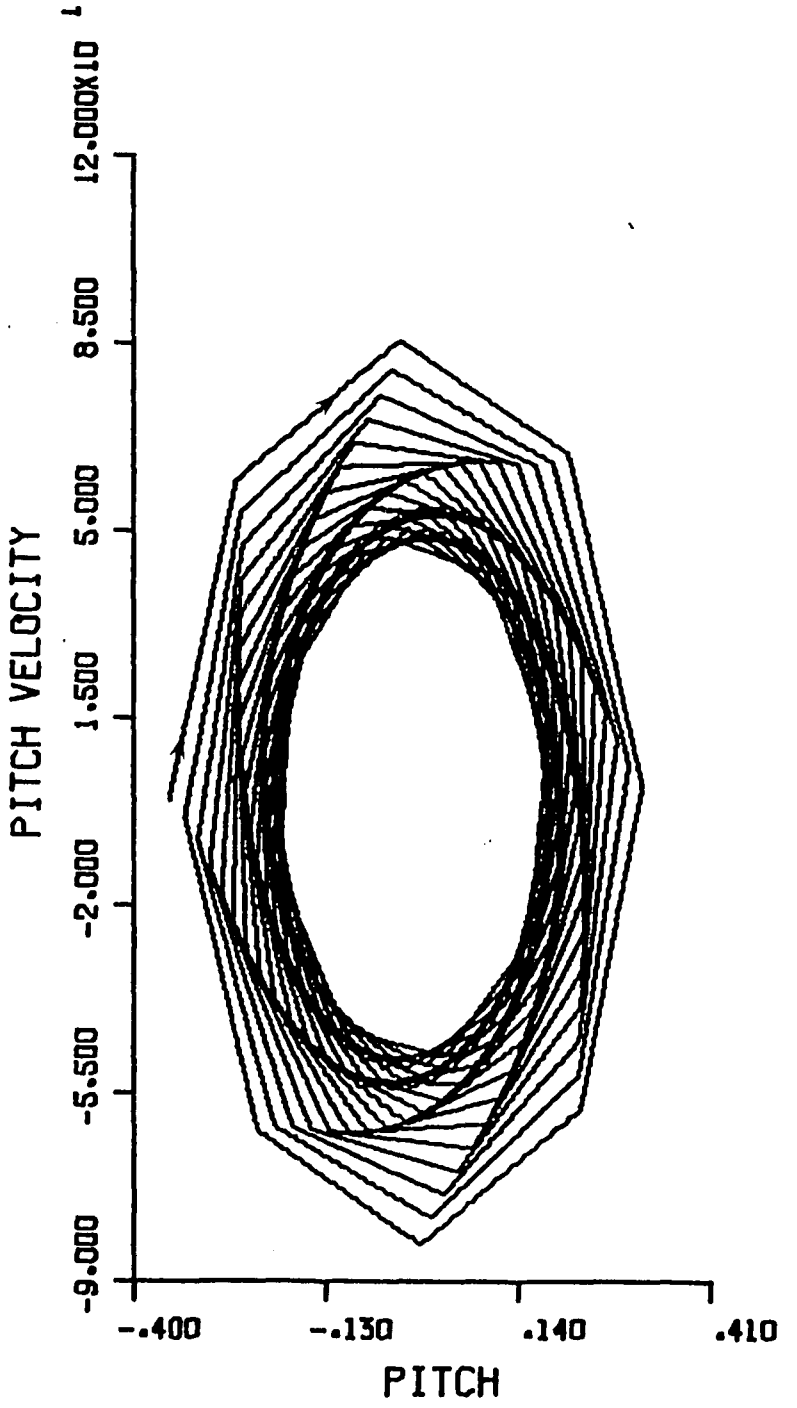

Figure 6-5B. Using Blade 63-206 in the Equations

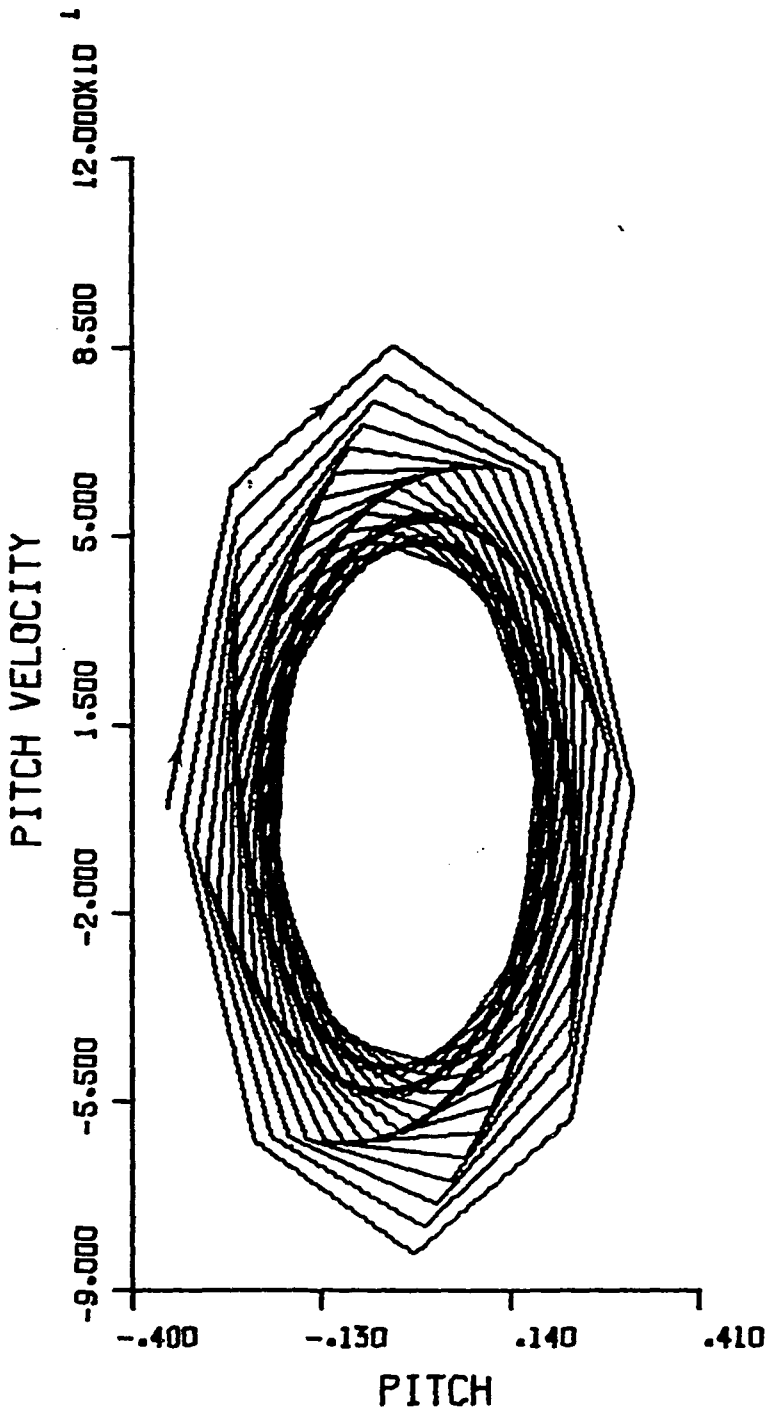

Figure 6-5B. Using Blade 63-206 in the Equations

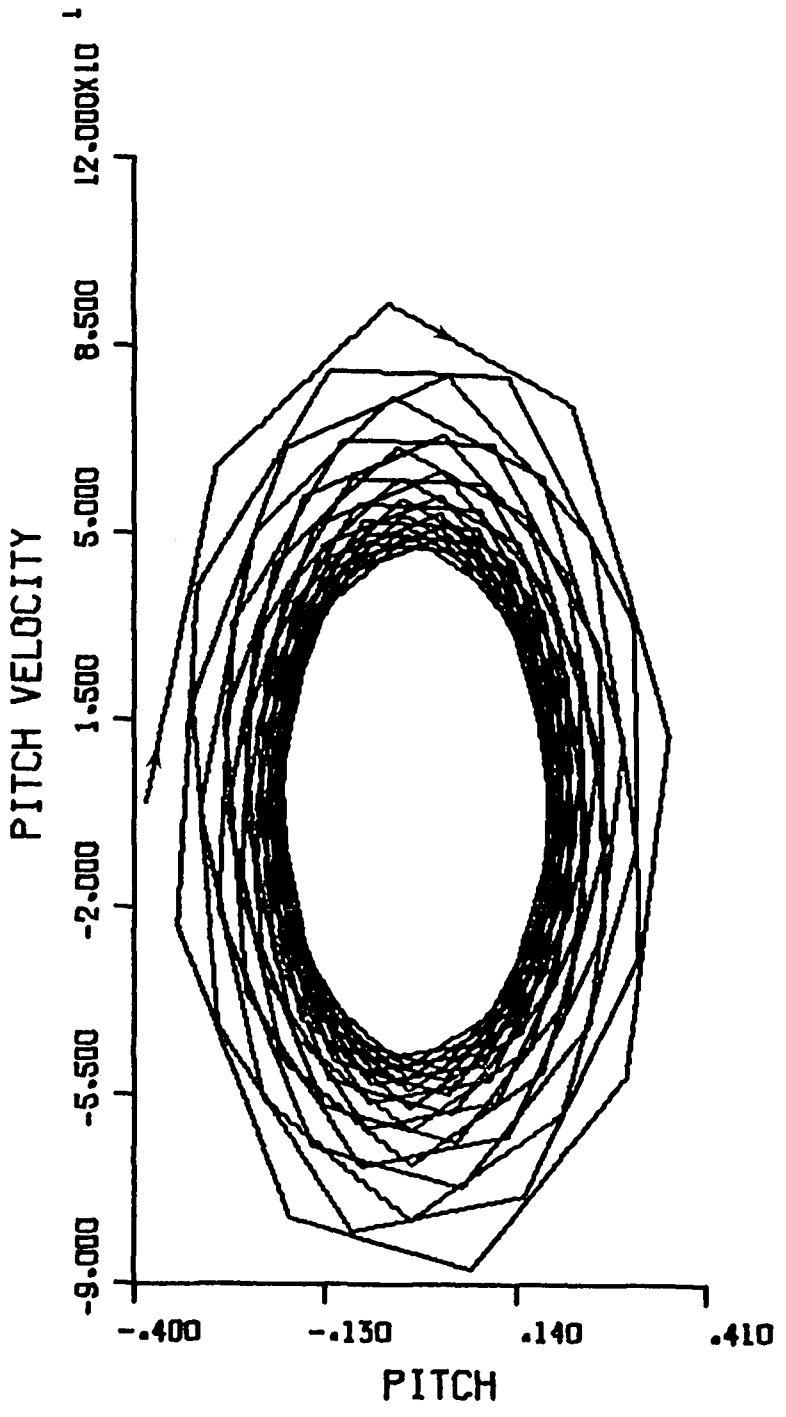

Figure 6-5C. Using Blade NACA 664-021 in the Equations

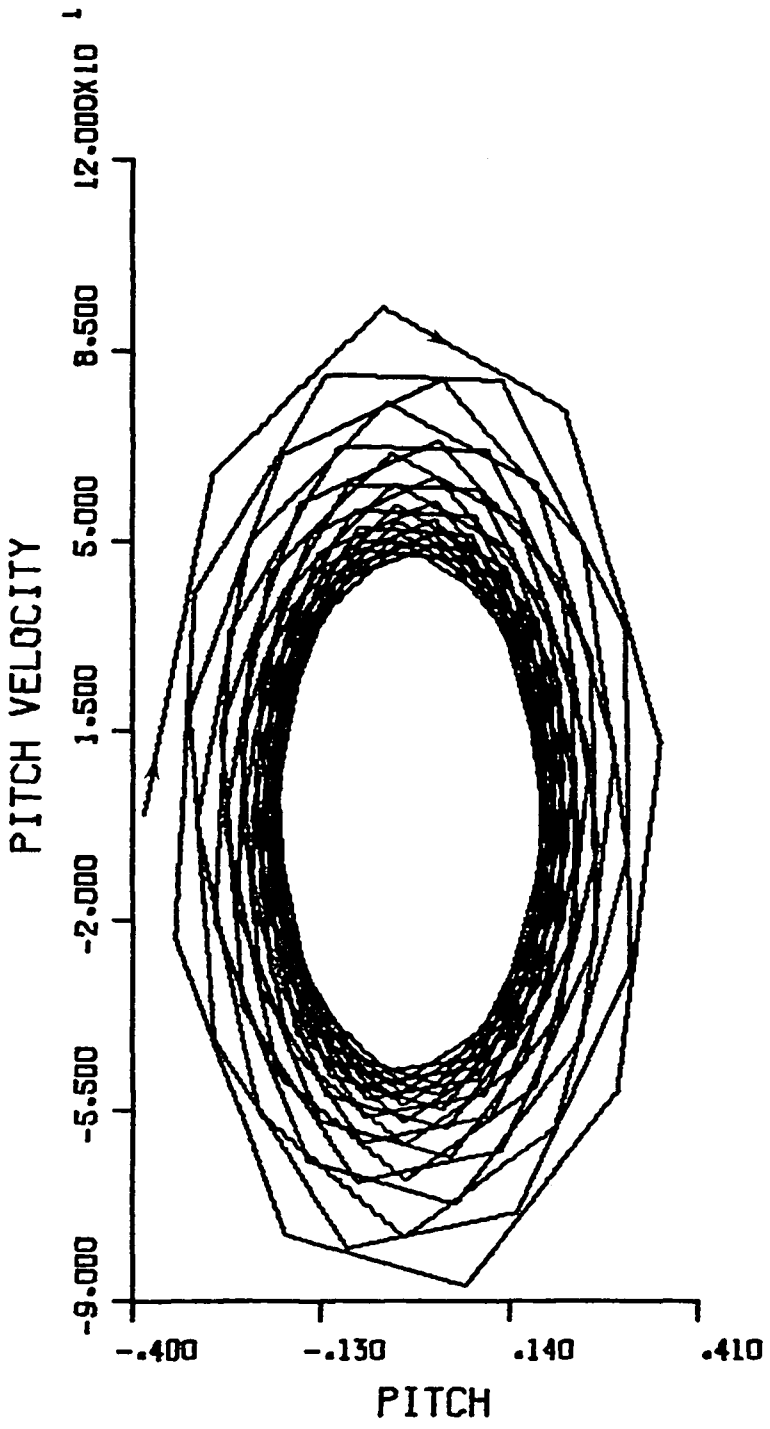

Figure 6-5C. Using Blade NACA 664-021 in the Equations

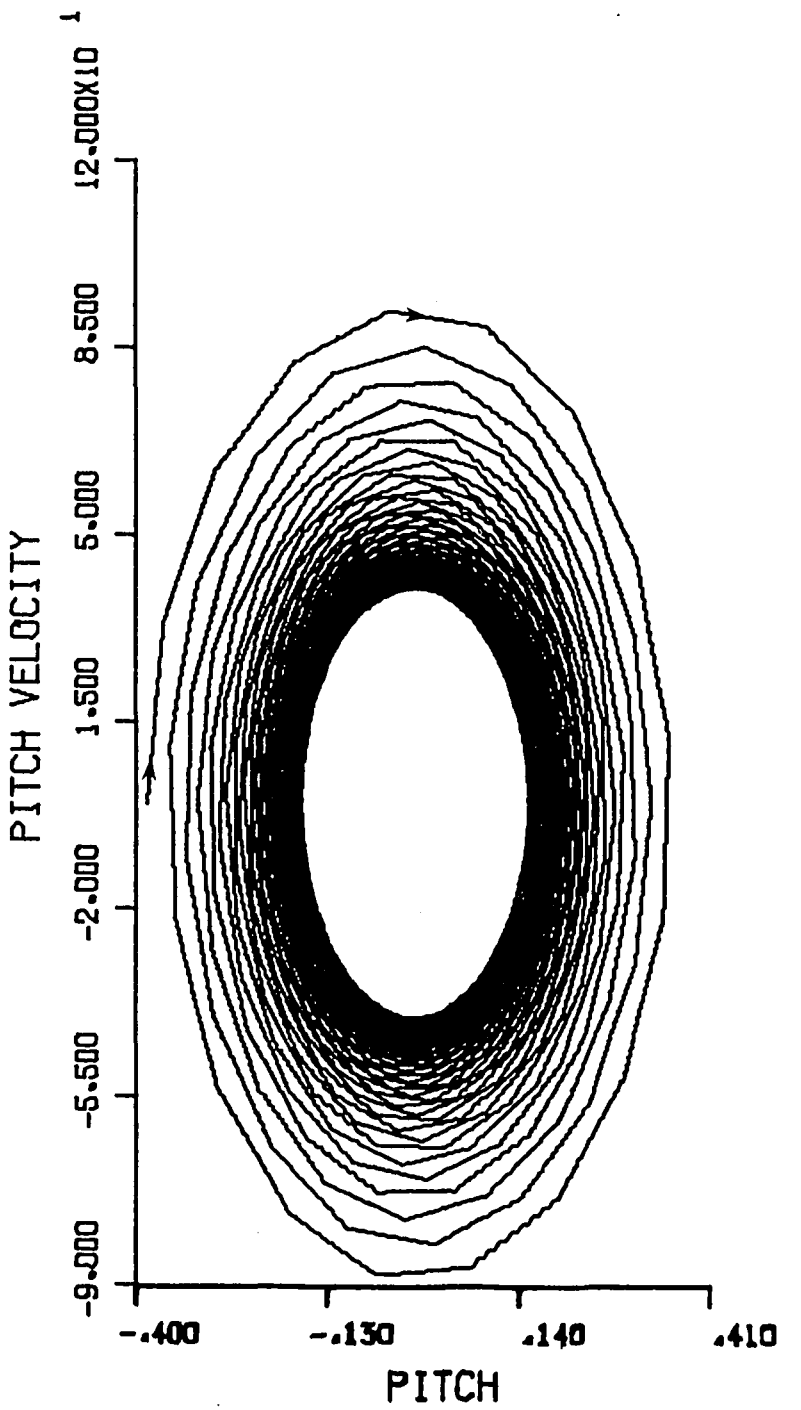

Figure 6-5D. Using a Linear Blade in the Equations

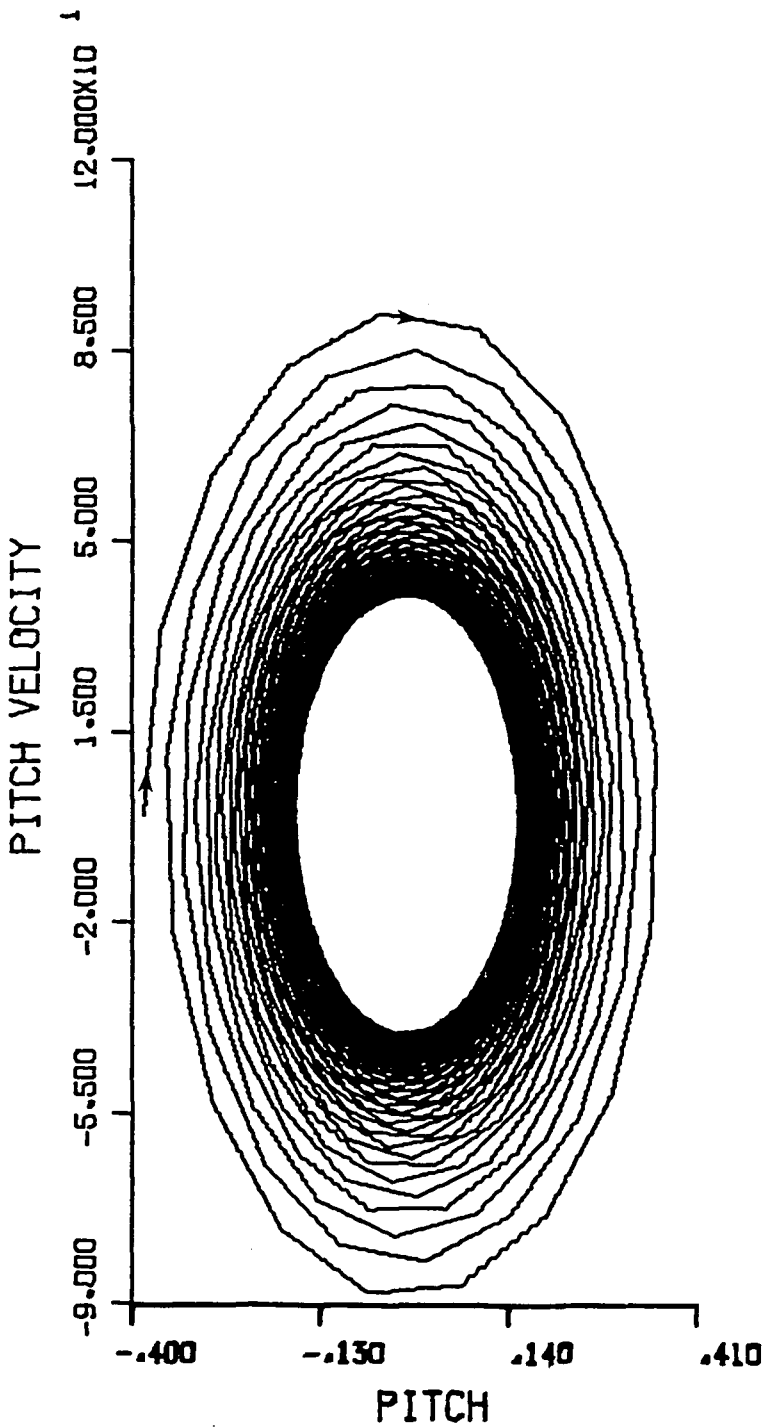

Figure 6-5D. Using a Linear Blade in the Equations

7. Modeling of Vortex-Induced-Like Fan Flutter

Vortex-induced oscillations can best be modeled mathematically by the use of two coupled ordinary differential equations in terms of α (the mechanical oscillator) and a flow variable c_L (the wake oscillator). The flow variable c_L is directly related to the aerodynamic excitation of the blade

$$\ddot{\alpha} + 2\beta\dot{\alpha} + \alpha = a\, c_L \tag{7.1}$$

$$\ddot{c}_L + f(\dot{c}_L) + w_n^2\, c_L = b\dot{\alpha} \tag{7.2}$$

$$\dot{x} = dx / d\tau = (1 / w_n)\, dx / dt\ . \tag{7.3}$$

Only the coefficient of damping in the wake oscillator $f(\dot{c}_L)$ is non-linear. In Section 3, different forms of $f(\dot{c}_L)$ by different authors were discussed. It was also discussed that all these different damping terms produce the same results and we will not restrict ourselves to the use of one or another. The model by Hartlen and Currie [10] will be used in the representation of the behavior of the cascade because of it's simplicity, since the non-linearity used in this model is of the Van der Pol type.

Equations 7.1 through 7.3 exhibit the type of phenomena that have been recorded in the flutter of turbine blades. If these two equations are used for every blade around the rotor of a turbine engine, compressor or fan section to represent it's behavior, the model will predict that every one of the twenty four blades around the rotor exhibits limit cycle flutter. It has been observed that some blades flutter, some blades vibrate less violently and some are virtually

still. The model must allow different forms of oscillations. A model must be developed that, given a different stiffness for each blade around the rotor, will predict their behavior individually. We must therefore tune Equations 7.1 through 7.3 to perform as such a model.

Two control system techniques will be used to search for a model that represents the mistuned rotor: the describing function technique and the linearization method (along with Routh's criteria).

8. The Describing Function Technique

The method of Describing Functions is a control system engineering approximate technique for predicting the existance of limit cycle. This method, however, is not accurate for a transfer function G(s) which is not strongly low pass. Figure 8-1(A) is the block diagram of the un-normalized equations

$$\ddot{\alpha}+2\beta\dot{\alpha}+ =ac_L \quad ; \quad a=Ew_n^2=nU^2w_n^2/w_L^2 \tag{8.1}$$

$$\ddot{c}_L-Aw_n\dot{c}_L+(B/w_n)\dot{c}_L^3+w_n^2c_L=b\dot{\alpha} \quad ; \quad b=Dw_n/w_L \tag{8.2}$$

which can be transformed to figure 8-1(B). The transfer function (G) becomes

$$G(s)=[s^3+2\beta s^2+s]/[(s^2+w_n^2)(s^2+2\beta s+1)-DEw_n^3s] \tag{8.3}$$

substituting jw for s we get

$$G(j\,w) = (p_1 + j\,p_2) / (p_3 + j\,p_4) = [(p_1p_3 +p_2p_4 + j(p_2p_3-p_1p_4)]/[p_3^2 +p_4^2] \tag{8.4}$$

where

$$p_1 = - 2\,\beta\,w^2 \tag{8.5}$$

$$p_2 = w - w^3 \tag{8.6}$$

$$p_3 = w^4 - (w_n^2 + 1)\,w^2 + w_n^2 \tag{8.7}$$

$$p_4 = - 2\beta w^3 + (2\beta\,w_n^2 - D\,E\,w_n^3)\,w\ . \tag{8.8}$$

To find w at the real axis crossings of G(jw) we set

$$p_2\,p_3 - p_1\,p_4 = 0 \tag{8.9}$$

which leads to

$$w^6+(4\beta^2-2-w_n^2)w^4+[1+(2-4\beta^2)w_n^2+2\beta DEw_n^3]w^2-w_n^2=0\ . \tag{8.10}$$

This equation can be solved for the frequency at which the Nyquist plot of G crosses the x axis (which is the Nyquist plot of the non-linear

block). To find the real axis crossing

$$\alpha = (p_1\ p_3 + p_2\ p_4) \ / \ (p_3^2+p_4^2) \tag{8.11}$$

$$\alpha=[DEw_n^3w^2(w^2-1)]/[[w^4-(1+w_n^2)w^2+w_n^2]+[-2\beta w^3+(2\beta w_n^2-DEw_n^3)w]^2] \ . \tag{8.12}$$

A limit cycle probably exists at the point of the intersection of G(jw) and $-1/\mathcal{Z}(a,w)$. We can therefore find (-1/describing function) of the non-linearity and find it's intersection with G(jw). w_n can therefore be adjusted in such a manner that the Nyquist plot of G(jw) intersects or misses $-1/\mathcal{Z}(a,w)$. The w_n that causes G and $-1/\mathcal{Z}$ to cross, corresponds to the blades on the rotor that do not exhibit flutter. If this method is successful, the designer of bladed cascades can avoid the construction of the blades whose natural frequencies cause G and $-1/\mathcal{Z}$ to intersect and therefore exhibit limit cycle flutter. To find the describing function of the non-linearity

$$F = - A\ w_n\ \dot{c}_L + (B/w_n)\ \dot{c}_L^3 \tag{8.13}$$

$$\dot{c}_L = a \sin(\theta) \tag{8.14}$$

$$F = - A\ a\ w_n \sin(\theta) + (Ba^3/w_n) \sin^3(\theta) \tag{8.15}$$

the first coefficient of the Fourier series is

$$-(1/\pi)\left[\int_{-\pi}^{\pi}(-Aaw_n\sin\theta+(Ba^3/w_n)\sin^3\theta)\cos\theta\ d\theta + \int_{-\pi}^{\pi}(-Aaw_n\sin\theta+(Ba^3/w_n)\sin^3\theta)\sin\theta\ d\theta\right] \tag{8.16}$$

$$= \theta - A\ w_n\ a + (3\ B\ a^3)/(4\ w_n) \tag{8.17}$$

$$\mathcal{Z}(a) = - A\ w_n + (3\ B\ a^2)/(4\ w_n) \tag{8.18}$$

$$-1/\mathcal{Z}(a) = w_n \ / \ (Aw_n^2 - 3/4\ B\ a^2) \ . \tag{8.19}$$

The describing function is a function of a only (ie. w is absent), which means that it coincides with the real axis. We can therefore use equation 8.12 in order to find the intersection of G(jw) and $-1/\mathcal{Z}(a)$ (where a limit cycle may exist). Figure 8-2(A) is the plot of

$-1/\mathcal{Y}$ against a. Figure 8-2(B) is a plot of $-1/\mathcal{Y}(w)$. If by adjusting w_n we can make the Nyquist plot of G cross the real axis in the region R, there will be no limit cycle possible. Figure 8-2(B) shows that as A (the negative damping) is decreased, the gap R widens causing more Nyquist plots of G to miss the describing function - corresponding to the oscillations that decay or grow. This is in agreement with the actual events since by reducing the negative damping, the positive damping B becomes more effective causing the oscillations to die out. If this technique of tuning is to work, as the w_n is changed the axis crossings of G(jw) must be distinct. This is demonstrated in tables 8-1 and 8-2 where it is seen that the transfer function crosses the real axis at values relatively separated as w_n and DE are varied. The values of w_n that cause G(jw) to cross the real axis in the region R correspond to the natural frequencies of the blades whose oscillations die out and vice versa. The Nyquist plots of three different natural frequencies are plotted in figure 8-3. The coupling and damping variables are chosen such that the describing function of the non-linearity turns at a value equal to $\mathcal{Y}$. According to this plot the equations 8-1 and 8-2 exhibit a limit cycle flutter with blades whose natural frequencies are 1.39 and 1.46 while the oscillations die out with $w_n = 1.26$. The Nyquist plot of each w_n crosses the real axis at three different locations, two of which are unstable.

The simulation of the blades by numerical techniques, using the values obtained by this method, do not agree with the findings above. The limit cycle existed even in the regions of frequencies for which the

describing function technique predicted otherwise.

The discouraging results of this method may be blamed on the fact that the describing function method works best only with G(jw) of a low pass system. Figure 8-4 is the Bode plot of G(s). As this plot suggests, the describing function is not strongly low pass. Due to the nature of the system, this method can not show us the sensitivity of flutter to different natural frequencies. The linearization method will next be tried.

w_n	Axis Crossings (triple roots)		
0.0500	-88668.8947	-88668.8947	-88668.8947
0.1000	-11001.1233	-11001.1233	-11001.1233
0.2000	-1333.9163	-1333.9163	-1333.9163
0.3000	-374.9033	-374.9033	-374.9033
0.4000	-146.1863	-146.1863	-146.1863
0.5000	-67.0063	-67.0063	-67.0063
0.6000	-33.2953	-33.2953	-33.2953
0.7000	-17.0043	-17.0043	-17.0043
0.8000	-8.5821	-8.5821	-8.5821
0.9000	-4.3522	-4.3522	-4.3522
1.0000	-2.5111	-2.5111	-2.5111
1.1000	-1.6947	-1.6947	-1.6947
1.2000	-1.2517	-1.2517	-1.2517
1.3000	3.2060	-0.9693	1.2640
1.4000	3.7448	-0.7718	0.9278
1.5000	4.0258	-0.6264	0.7302
1.6000	4.1689	-0.5159	0.5930
1.7000	4.2268	-0.4301	0.4912
1.8000	4.2299	-0.3625	0.4129
1.9000	4.1969	-0.3084	0.3511
2.0000	4.1404	-0.2648	0.3015
2.1000	4.0686	-0.2291	0.2612
2.2000	3.9871	-0.1997	0.2281
2.3000	3.9001	-0.1752	0.2005
2.4000	3.8101	-0.1547	0.1774

Table 8-1, The Sensitivity of the Axis Crossings to the Frequency (DE= 0.09, BETA= 0.05)

DE	Axis Crossings (triple roots)		
0.0500	6.6666	-1.7233	1.6963
0.1000	3.1829	-0.7670	0.9773
0.2000	1.3785	-0.4467	0.7720
0.3000	-0.3363	-0.3363	-0.3363
0.4000	-0.2765	-0.2765	-0.2765
0.5000	-0.2379	-0.2379	-0.2379
0.6000	-0.2105	-0.2105	-0.2105
0.7000	-0.1898	-0.1898	-0.1898
0.8000	-0.1734	-0.1734	-0.1734
0.9000	-0.1602	-0.1602	-0.1602
1.0000	-0.1491	-0.1491	-0.1491
1.1000	-0.1398	-0.1398	-0.1398
1.2000	-0.1317	-0.1317	-0.1317
1.3000	-0.1247	-0.1247	-0.1247
1.4000	-0.1185	-0.1185	-0.1185
1.5000	-0.1130	-0.1130	-0.1130
1.6000	-0.1081	-0.1081	-1.1081
1.7000	-0.1036	-0.1036	-0.1036
1.8000	-0.0996	-0.0996	-0.0996
1.9000	-0.0959	-0.0959	-0.0959
2.0000	-0.0925	-0.0925	-0.0925
2.1000	-0.0894	-0.0894	-0.0894
2.2000	-0.0865	-0.0865	-0.0865
2.3000	-0.0838	-0.0838	-0.0838
2.4000	-0.0814	-0.0814	-0.0814

Table 8-2, The Sensitivity of the Axis Crossings to the Coupling Factors (w_n= 1.36, BETA= 0.05)

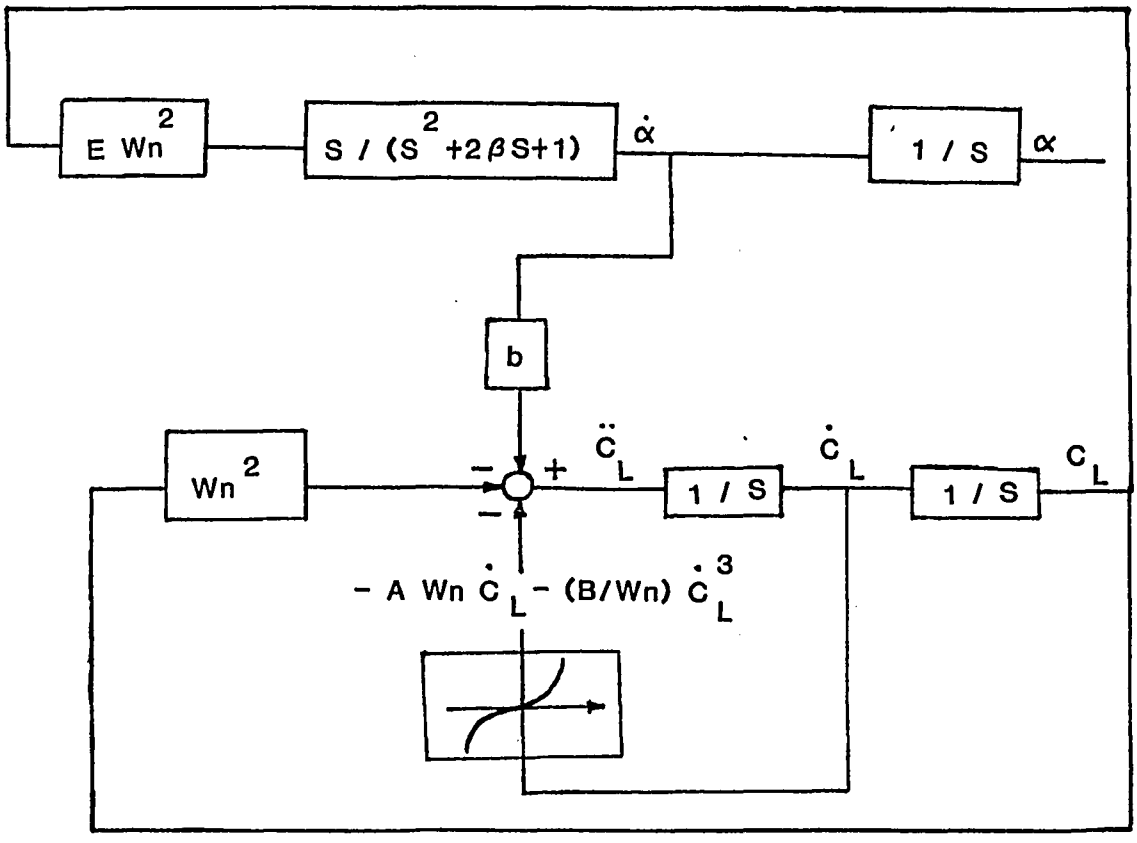

8-1a

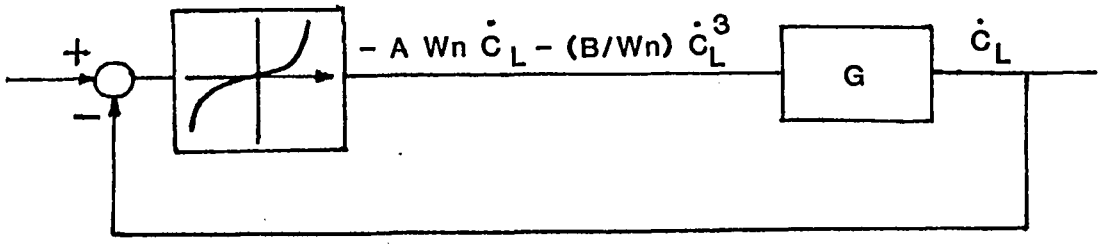

8-1b

Figure 8-1. The Block Diagram of the System

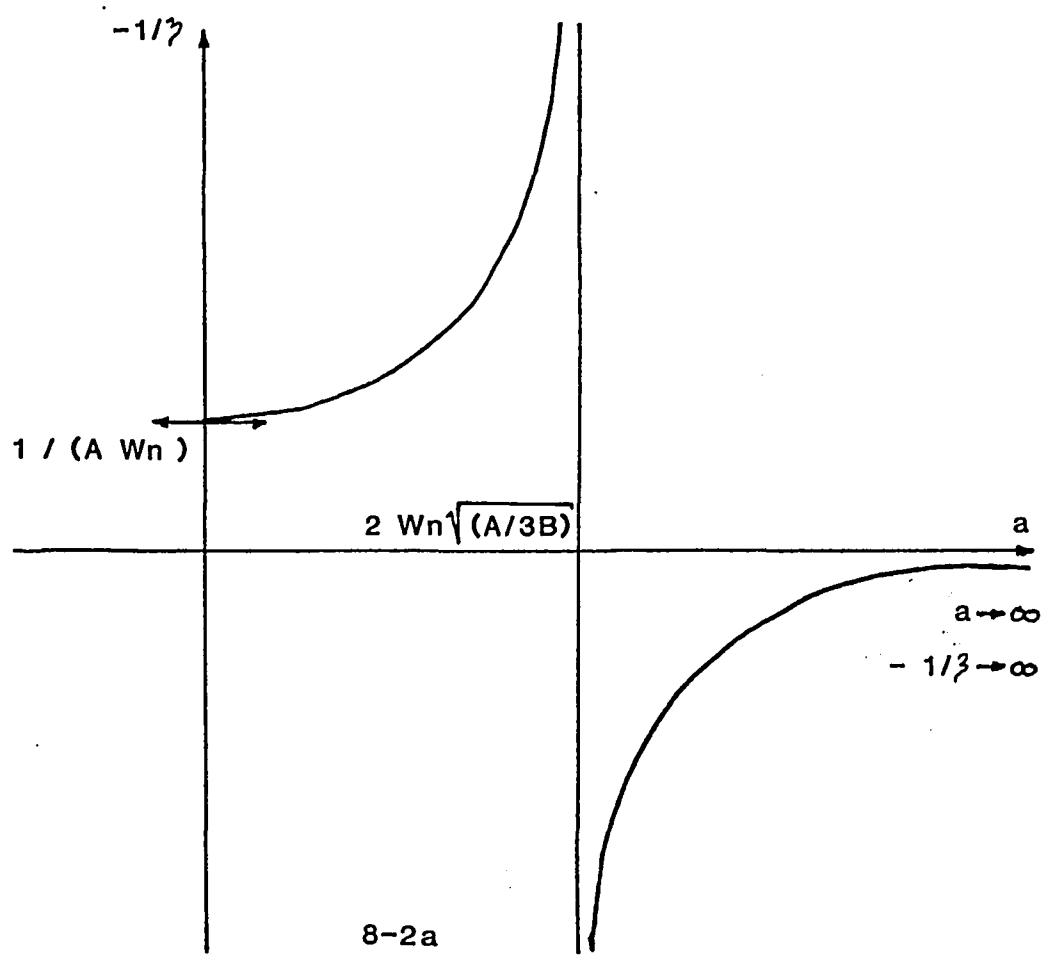

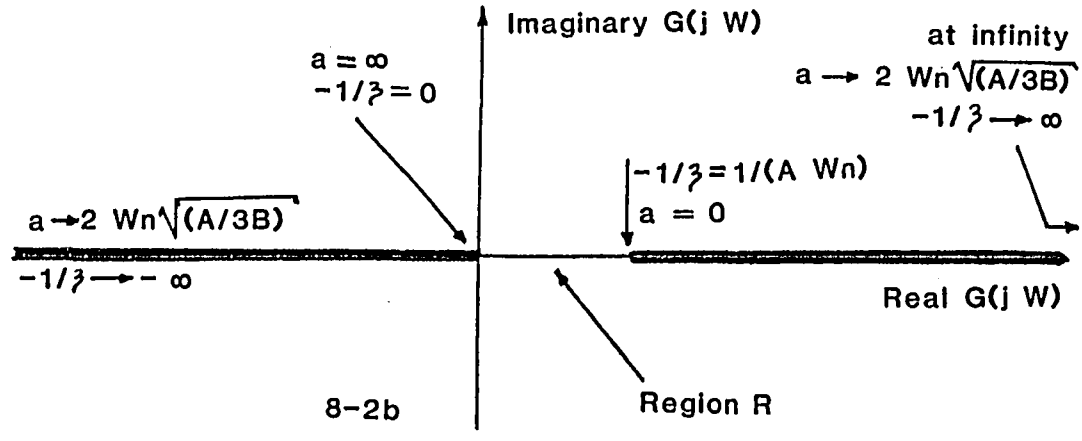

Figure 8-2. The Describing Function of the System

Figure 8-3. The Nyquist Plot

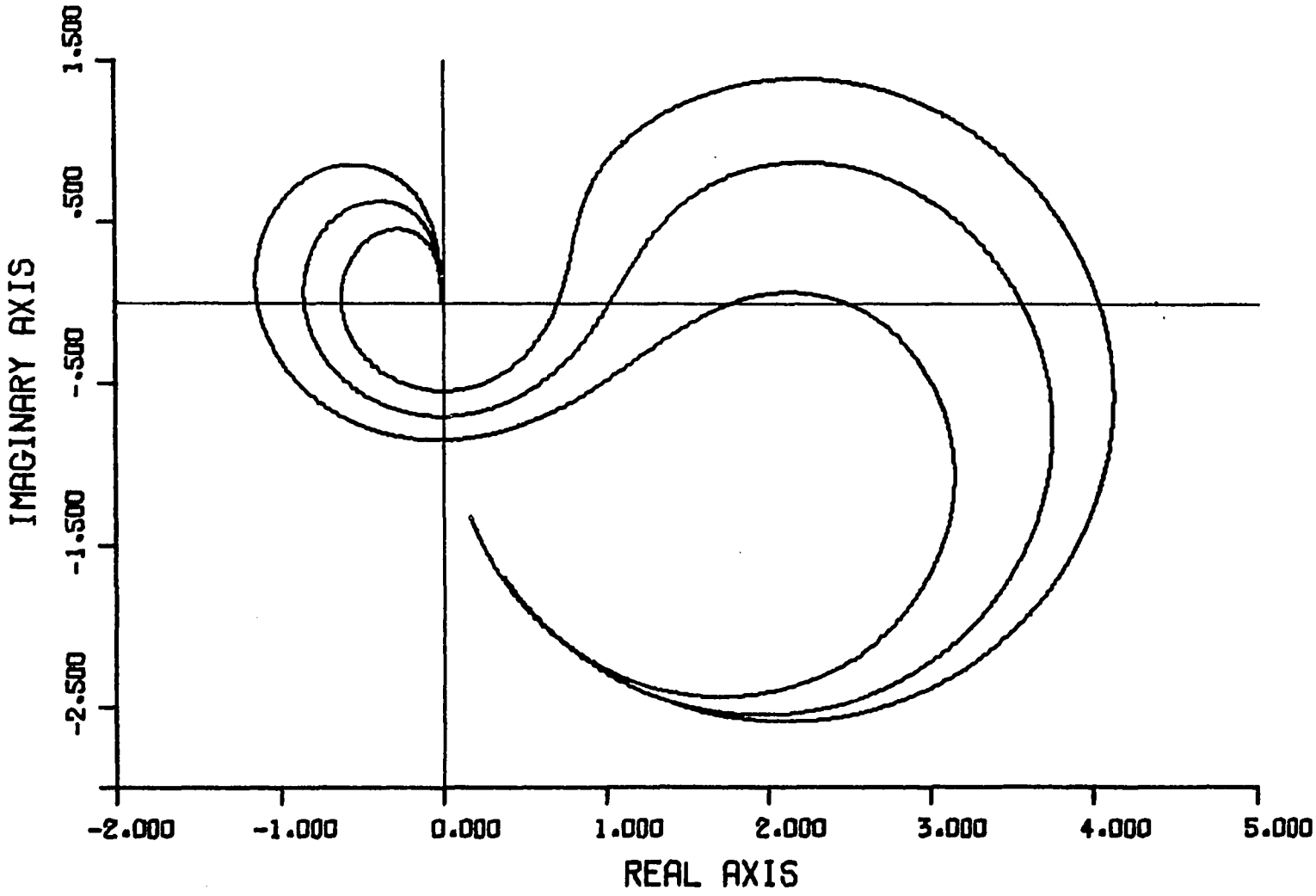

Figure 8-3. The Nyquist Plot

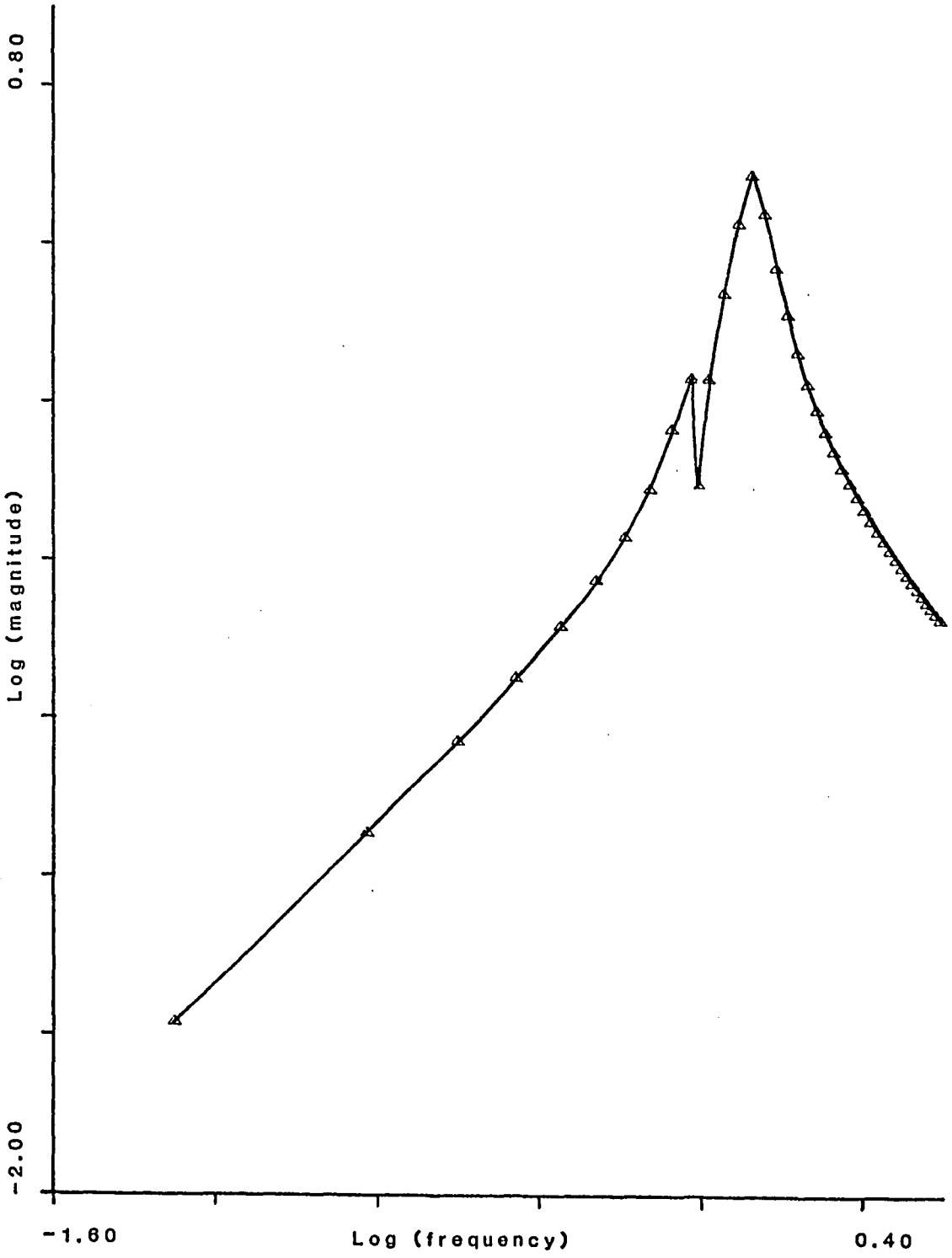

Figure 8-4. The Bode Plot of Magnitude

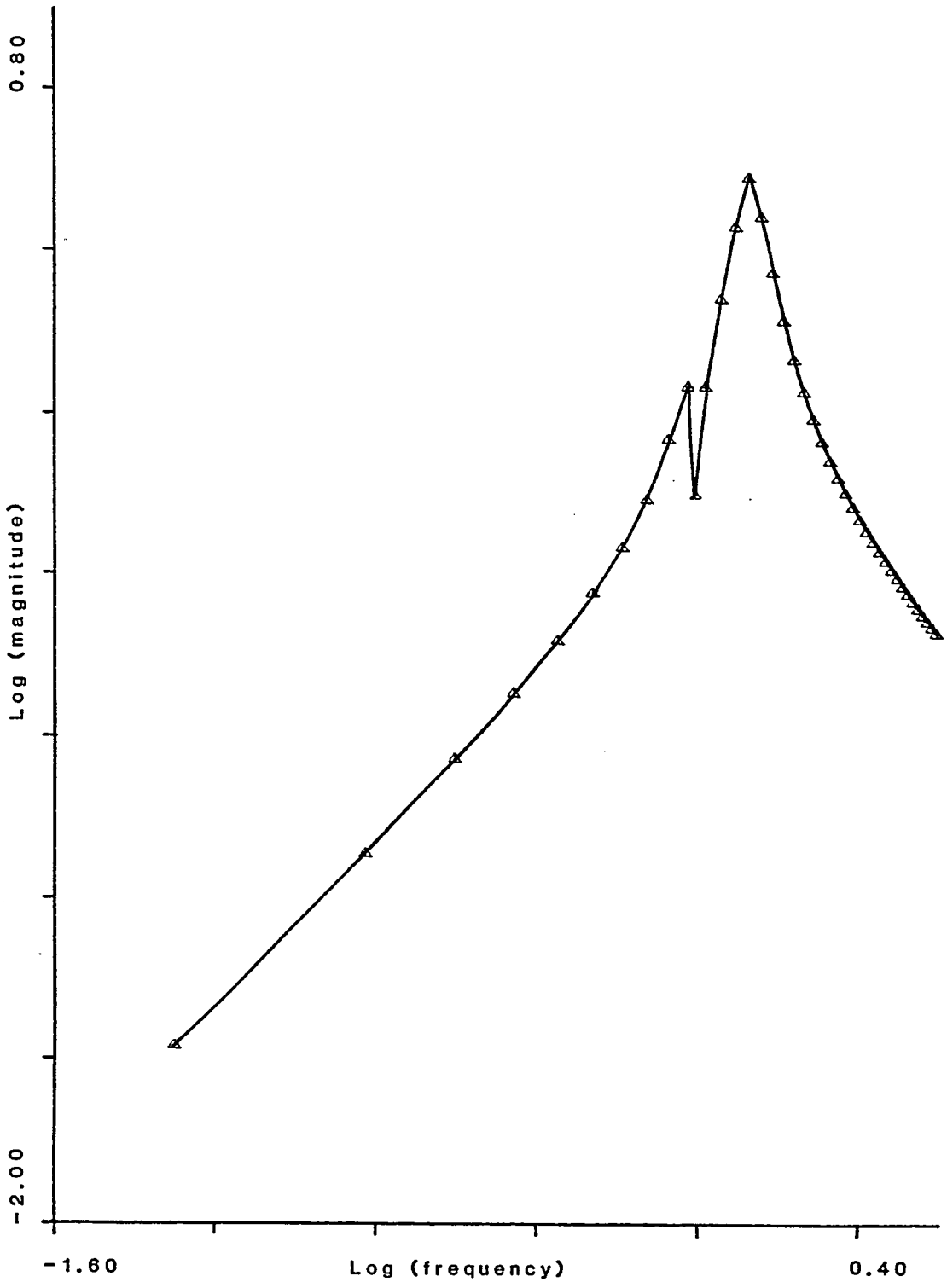

Figure 8-4. The Bode Plot of Magnitude

9. The Linearization Approach

The properties of a non-linear system can be estimated by the behavior of it's linear approximation in the vicinity of the equilibrium point. If, for instance, the equations exhibit an oscillation that dies out, the linearized equations must do the same near the origin. We can, therefore, establish the possibility of decaying oscillations by linearizing the system and finding the set of parameters that force the oscillation of the linear system to decay. Obviously in the fan flutter problem the parameters of the system are set by the physical events that take place. Our goal is to find out if the equations of motion chosen can represent the types of oscillations that are displayed by the blades in the cascade.

We begin by linearizing the system and finding the characteristic equation of the linearized model. If we can find a set of parameters that cause the characteristic equation to have eigenvalues with negative real parts only, then the system is stable (spirals to the equilibrium point)

$$\ddot{\alpha} + 2\beta\dot{\alpha} + \alpha = E\, w_L\, w_n^2\, c_L \tag{9.1}$$

$$\ddot{c}_L - A w_n \dot{c}_L + (B/w_n)\dot{c}_L^3 + w_n^2 c_L = (D w_n / w_L)\,\dot{\alpha} \tag{9.2}$$

$$\dot{\alpha}_1 = \alpha_2 \tag{9.3}$$

$$\dot{\alpha}_2 = -2\beta\alpha_2 - \alpha_1 + E\, w_L\, w_n^2\, \alpha_3 \tag{9.4}$$

$$\dot{\alpha}_3 = \alpha_4 \tag{9.5}$$

$$\dot{\alpha}_4 = A w_n \alpha_4 - (B/w_n)\alpha_4^3 - w_n^2 \alpha_5 + (D w_n / w_L)\alpha_2 \tag{9.6}$$

for the equilibrium point

$$\alpha_1 = \alpha_2 = \alpha_3 = \alpha_4 = 0 \ . \tag{9.7}$$

The Jacobian becomes

$$r_{ij}=\partial\alpha_i/\partial\alpha_j \quad \text{(using equation 9.7 and i,j=1,2,3,4)} \tag{9.8}$$

$$J = [\ r_{ij}\ ] \tag{9.9}$$

$$J = \begin{vmatrix} -\lambda & 1 & 0 & 0 \\ -1 & -2\beta-\lambda & Ew_L w_n^2 & 0 \\ 0 & 0 & -\lambda & 1 \\ 0 & Dw_n/w_L & -w_n^2 & Aw_n-\lambda \end{vmatrix} = 0 \ . \tag{9.10}$$

The characteristic equation becomes

$$\lambda^4+(2\beta-Aw_n)\lambda^3+(1-2\beta Aw_n+w_n^2)\lambda^2+(-Aw_n+2\beta w_n^2-DEw_n^3)\lambda+w_n^2=0 \ . \tag{9.11}$$

For a stable spiral in the vicinity of the origin, equation 9.11 must have eigenvalues with negative real parts. The Routh's criterion can now be used to determine the conditions that must be satisfied to obtain negative eigenvalues

$$\begin{array}{ll} 1 & f_4 \qquad w_n^2 \\ f_1 & f_5 \\ f_2 & w_n^2 \\ f_3 & \\ w_n^2 & \end{array} \tag{9.12}$$

where

$$f_1=2\beta - A\ w_n \tag{9.13}$$

$$f_2=[2\beta-4\beta^2Aw_n+2\beta A^2w_n^2+(DE-A)w_n^3]/f_1 \tag{9.14}$$

$$f_3=(DEA-D^2E^2)w_n^6+(-2\beta A^2DE-2\beta A+2\beta DE)w_n^5+$$
$$(4\beta DEA + 4\beta^2A^2 - ADE)w_n^4 + (-2\beta DE - 8\beta^3A - 2\beta A^3 + 4\beta A)w_n^3 \tag{9.15}$$

$$f_4= 1 - 2\beta A\ w_n + w_n^2 \tag{9.16}$$

$$f_5 = - A w_n + 2\beta w_n^2 - D E w_n^3 . \qquad (9.17)$$

Routh's criterion states that for the roots of the characteristic equation to have negative real parts, the terms in the first column of the equations 9.12 must have the same sign. The same restriction should hold for the coefficients of the characteristic equation. This means that the equations 9.13 through 9.17 must all have a positive value.

In summary, we have come to the conclusion that if the coupled equations 9.1 and 9.2 are to represent a decaying motion, f_1 through f_5 must all be positive. At first glance this looks like a very stiff requirement. There are, however, many values of the parameters A, β, D, E and w_n that satisfy these requirements. This was investigated by trying different sets of parameters by a high speed computer. A neighborhood of the values of the parameters that were of interest was chosen and equations 9.13 through 9.17 were computed. If the signs of f_1 through f_5 turned positive the parameters used to compute these functions cause the system to decay.

In the process of linearization, B (the coefficient of non-linearity) is eliminated. It must be noted that knowing a precise value of this damping parameter is not necessary for determining the decaying system. B simply determines the amplitude of the limit cycle. When the phase plane of the system grows, the unstable spiral finally reaches the isolated closed trajectory. This is because at this time $B\dot{c}_L^3$ becomes large enough that the energy taken out by this term balances the energy put in by $-A\dot{c}_L$. The smaller the parameter B, the bigger the amplitude

of the limit cycle.

The parameters listed in table A-6 were found in the fashion described above. With these parameters we are now interested in finding out the limits of natural frequencies (w_n) that cause the system to flutter or to decay.

Figure 9-1 is a plot of f_1, f_2, f_3, f_4 and f_5 versus w_n for the parameters of table A-7. In the region of

$$1.147 < w_n < 1.442 \qquad (9.18)$$

all of the requirements of the Routh's criterion are satisfied. That is to say that for the system parameters of table A-7, the system is tuned in such a way that the blades with natural frequencies outside of the region of equation 9.18 flutter. The blades in the fan, of course, oscillate at much higher frequencies. We simply have chosen to work with such small numbers since our computing capabilities are limited. For the twenty four blade problem that will be simulated next, choosing such small values for w_n is the only way to keep the program within our computing capabilities.

The results of the numerical simulation of the blades confirm our conclusions. Two points, one inside and one outside of the region of equation 9.18, are chosen. Figure 9-2 is the simulation of the system with w_n= 1.08 (outside the region) and figure 9-3 is the system with w_n= 1.20 (inside the region). A reasonable difference of 10% between the stiffnesses of the two blades produces the two different behaviors, as

witnessed in the fans and compressors.

An unstable inner ring is seen in figure 9-2. This unstable limit cycle was predicted by the describing function technique.

It is also of interest to note that the equations of motion exhibit beating (figure 9-3), a phenomenon that is often seen in the flutter of the fans.

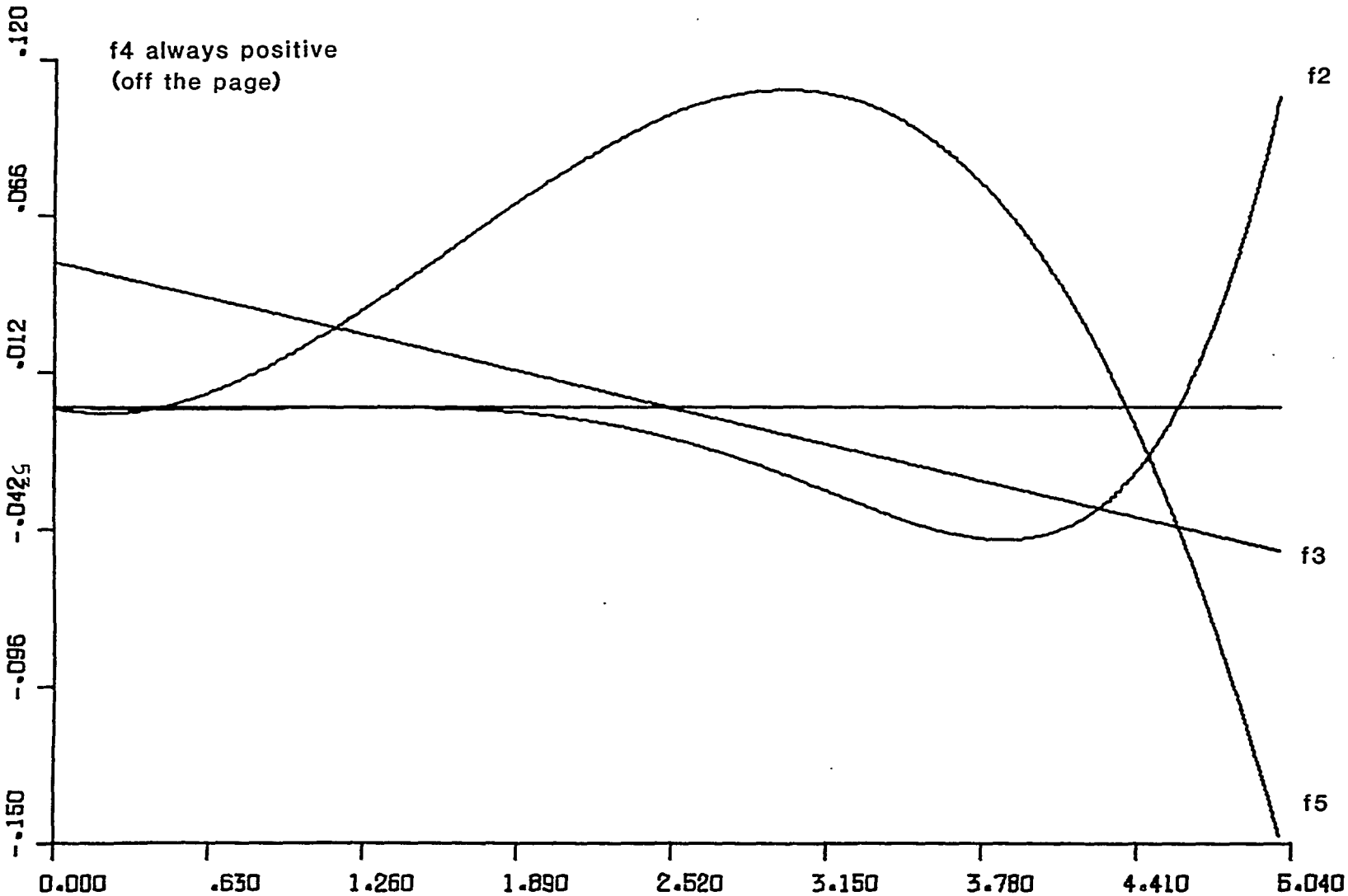

Figure 9-1. Equations 9.13 Through 9.17 Versus Wn

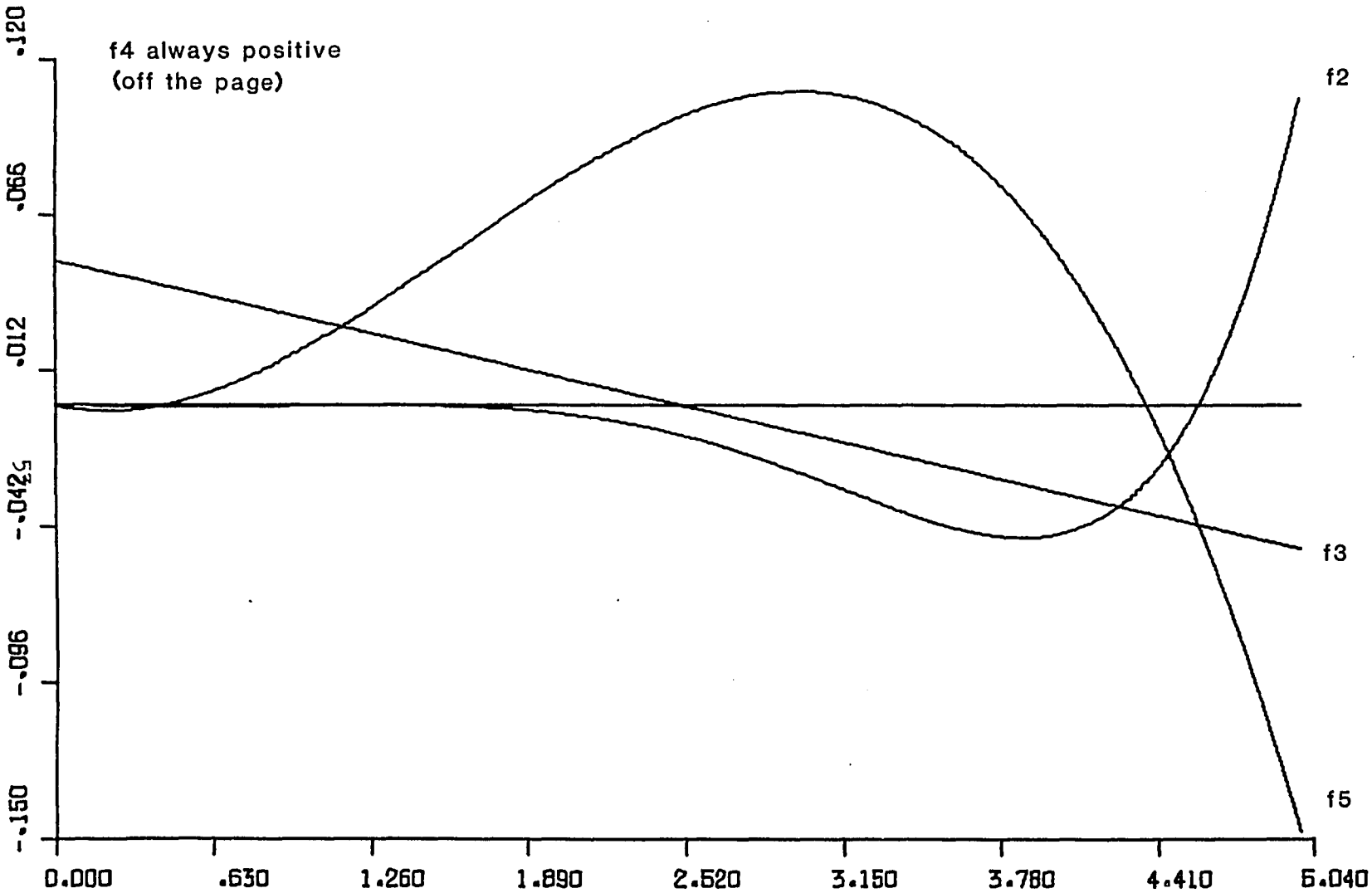

Figure 9-1. Equations 9.13 Through 9.17 Versus Wn

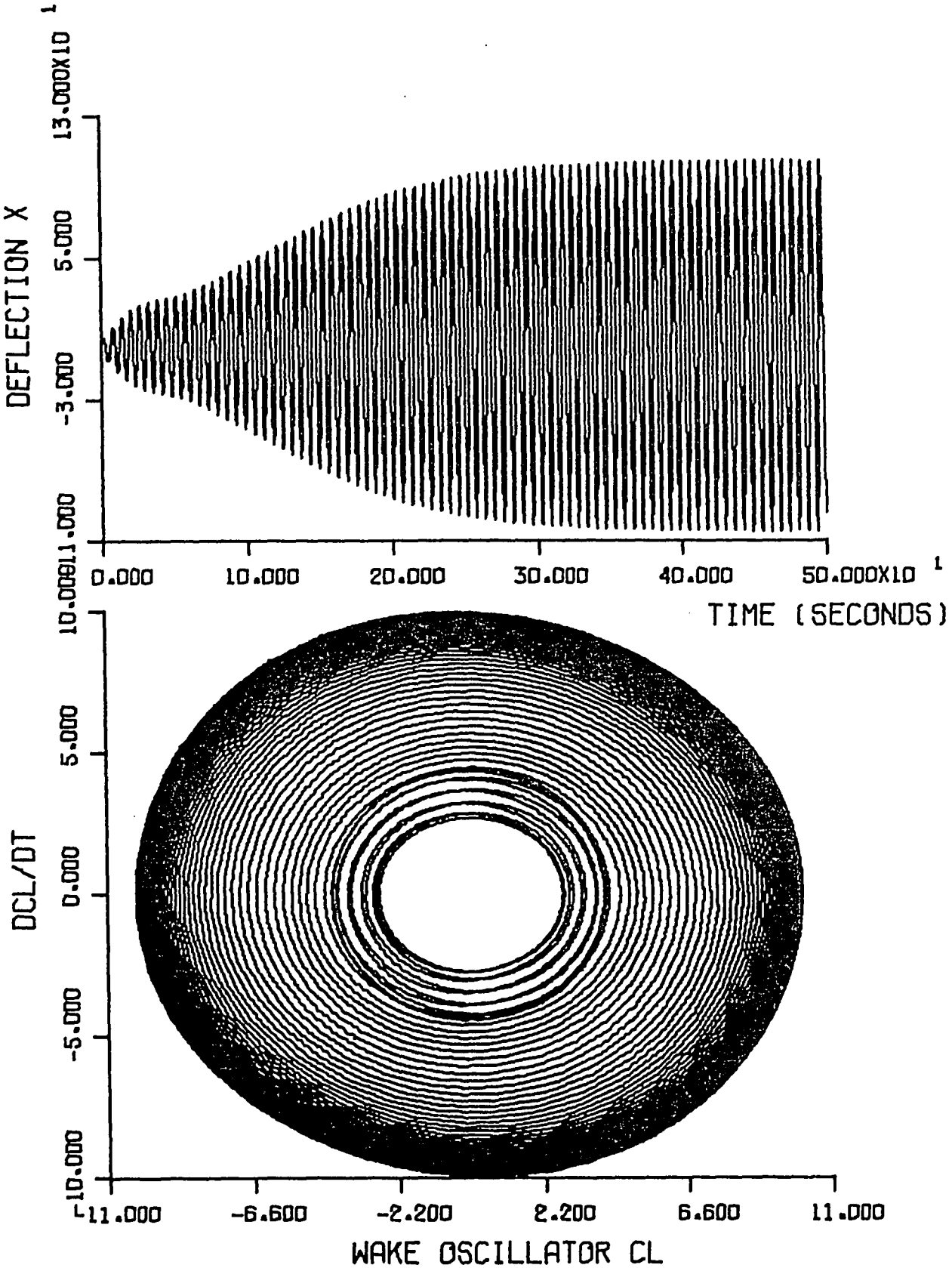

Figure 9-2. Blade with Wn = 1.08

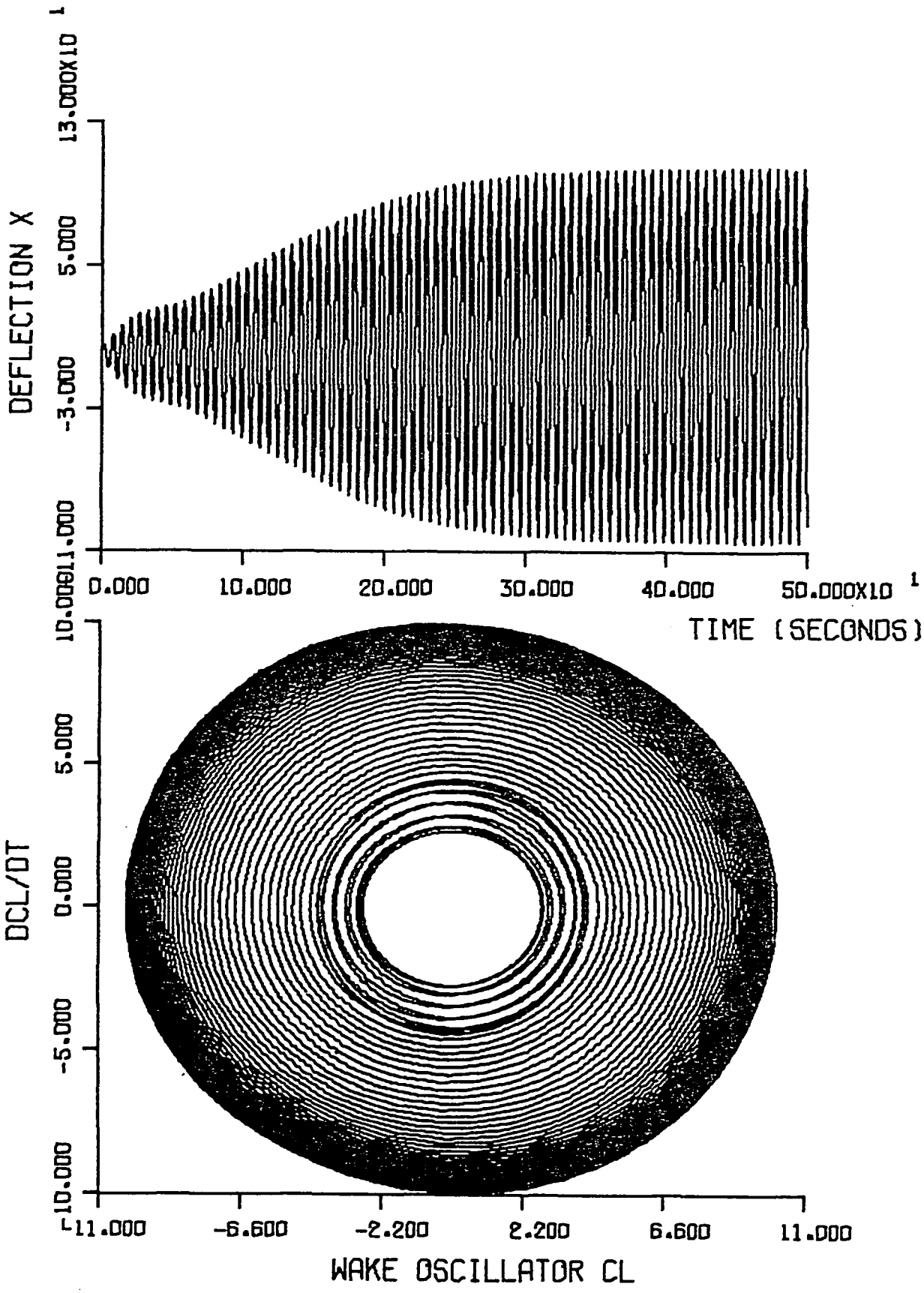

Figure 9-2. Blade with Wn = 1.08

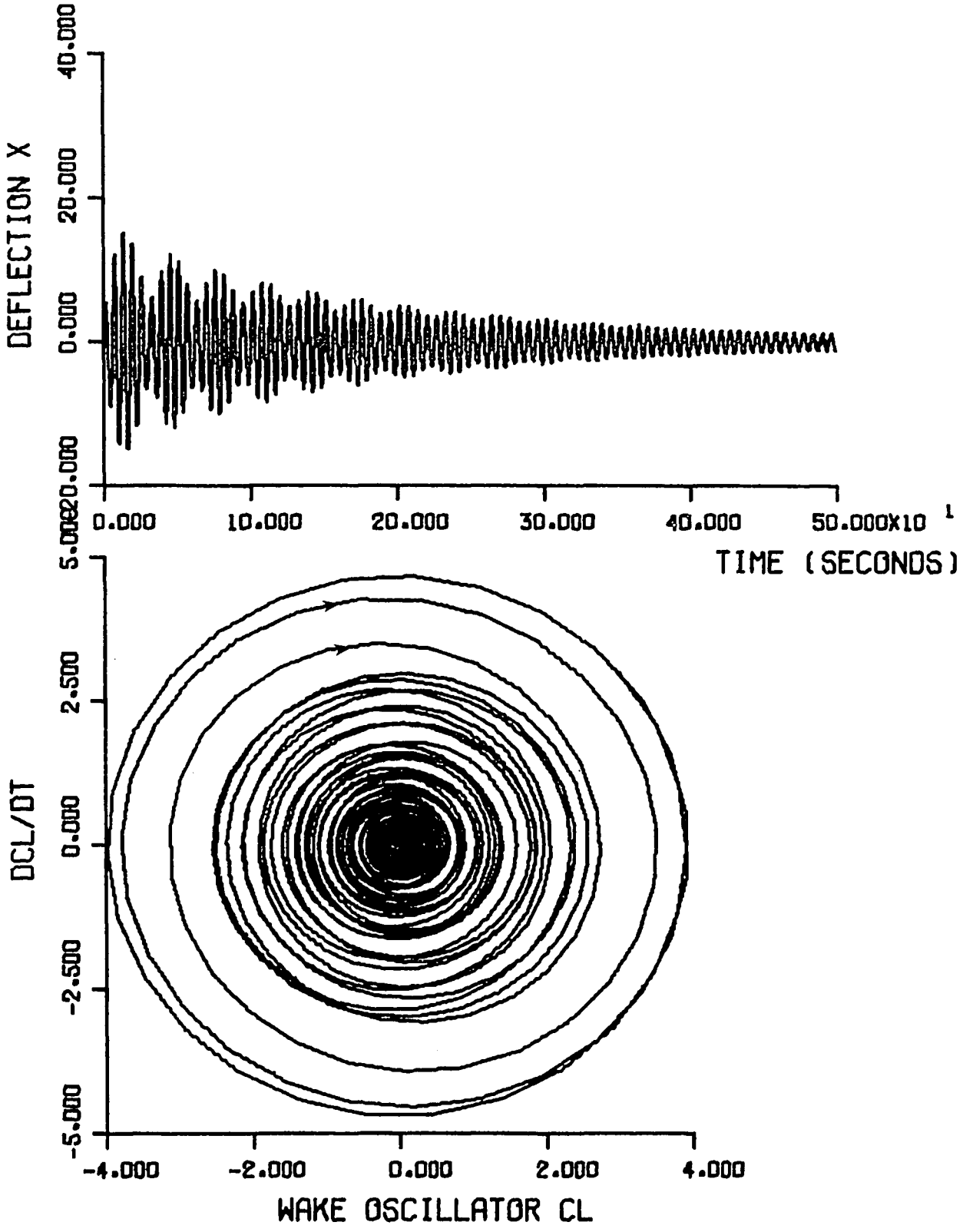

Figure 9-3. Blade with Wn : 1.20

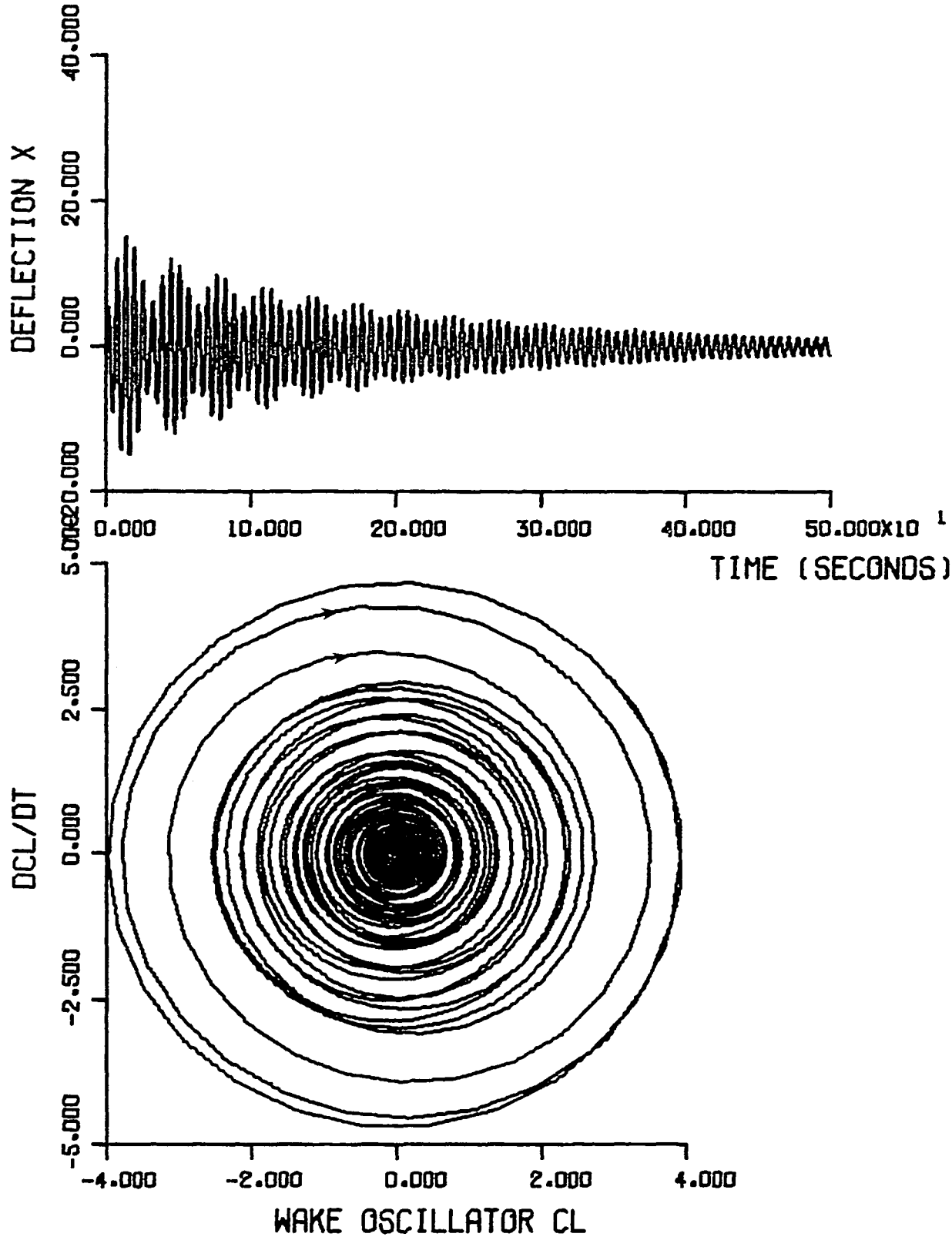

Figure 9-3. Blade with Wn = 1.20

10. Conclusions

The equations of motion of each individual blade are coupled to the equations of the neighboring blades in the following fashion

$$\ddot{\alpha}(1)+2\beta\dot{\alpha}(1)+\alpha(1)=Ew_L w_n^2(1)c_L(24) \tag{10.1}$$

$$\ddot{\alpha}(I)+2\beta\dot{\alpha}(I)+\alpha(I)=Ew_L w_n^2(I)c_L(I-1) \quad I=2,3,\ldots,24 \tag{10.2}$$

$$\ddot{c}_L(I)-Aw_n(I)\dot{c}_L(I)+[B/w_n(I)]\dot{c}_L^3(I)+w_n^2(I)c_L(I)=[Dw_n(I)/w_L]\dot{\alpha}(I+1)$$

$$I= 1,2,3,\ldots,23 \tag{10.3}$$

$$\ddot{c}_L(24)-Aw_n(24)\dot{c}_L(24)+[B/w_n(I)]\dot{c}_L^3(24)+w_n^2(24)c_L(24)=[Dw_n(24)/w_L]\dot{\alpha}(1)\ . \tag{10.4}$$

It is not easy to agree upon a form of coupling between the equations. In the equations above, the wake oscillator position (c_L) of any blade around the rotor has been coupled to the previous blade. Each blade also has velocity coupling ($\dot{\alpha}$) with the adjacent wake oscillator. The method of section 9 can successfully be applied to equations with any form of coupling.

Figure 10-1 is a plot of position versus time for a twenty four blade rotor. Table A-7 lists the natural frequency of each blade. These natural frequencies are randomly chosen, such that a maximum difference of 10% exists among them. Taking the effect of coupling into consideration, the results shown, agree with the prediction of figure 9-1.

Figure 10-1 shows that as a result of this work, we can precisely tune any blade (with any natural frequency) around the rotor to exhibit

the observed behavior of limit cycle flutter. The aerodynamic coupling and damping parameters must be furnished to the model. These parameters must be evaluated experimentally.

Working backward (ie. having the natural frequency of a number of blades around a mistuned assembly), we can tune every blade in the following way:

A- The aerodynamic damping and coupling parameters in the chosen equations of motion (ie. equations 9.1 and 9.2) should first be found for a specific situation.

B- The Jacobian (equation 9.10) is then written which leads to the characteristic equation 9.11.

C- A plot of the functions resulting from Routh's criterion is made (figure 9.1). The range of the natural frequencies that cause all of these functions to have a positive value is determined.

D- The blades whose natural frequencies fall in this range show decaying oscillations, the rest flutter.

Figure 10-1. Deflection Versus Time for Each Blade

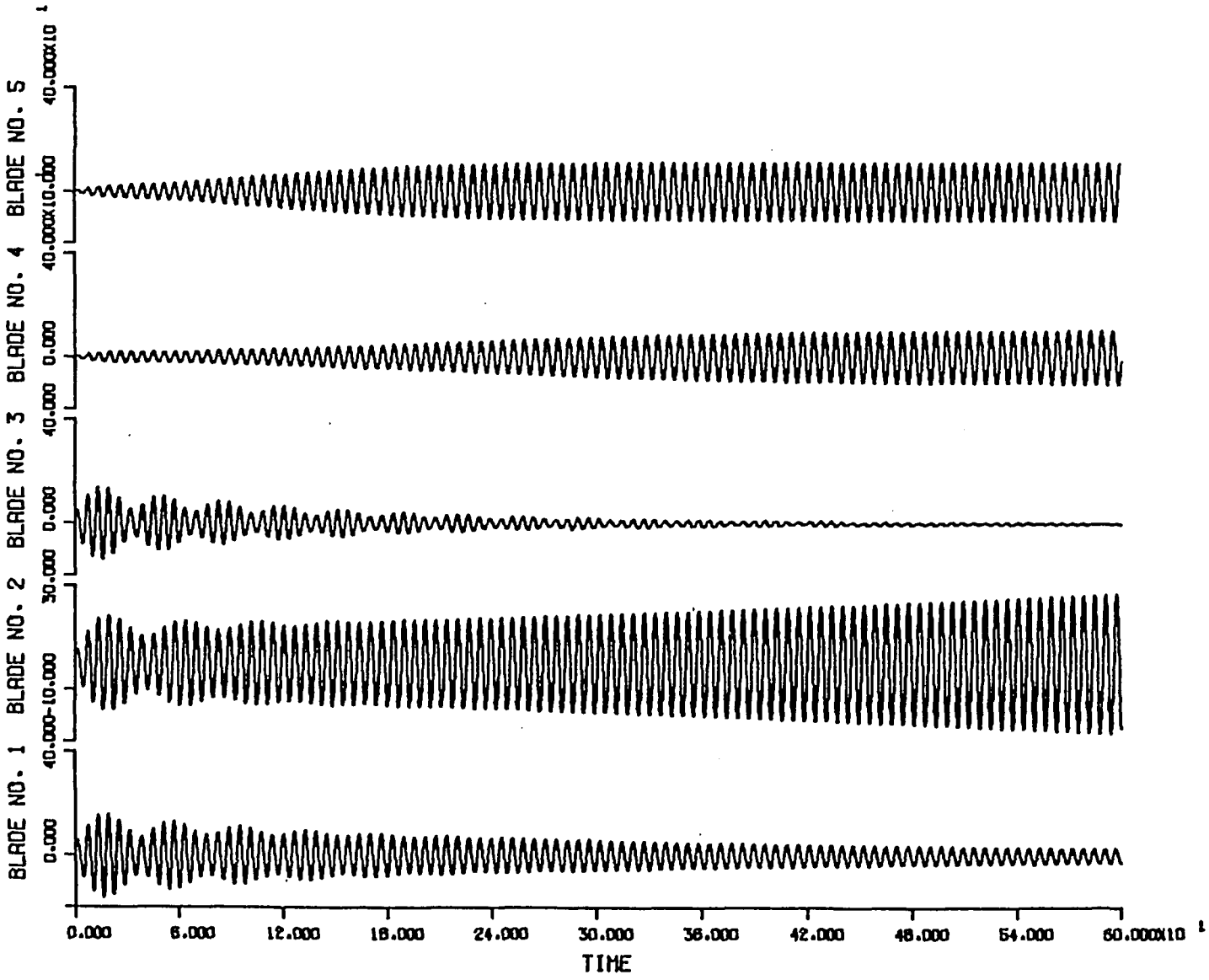

Figure 10-1. Deflection Versus Time for Each Blade

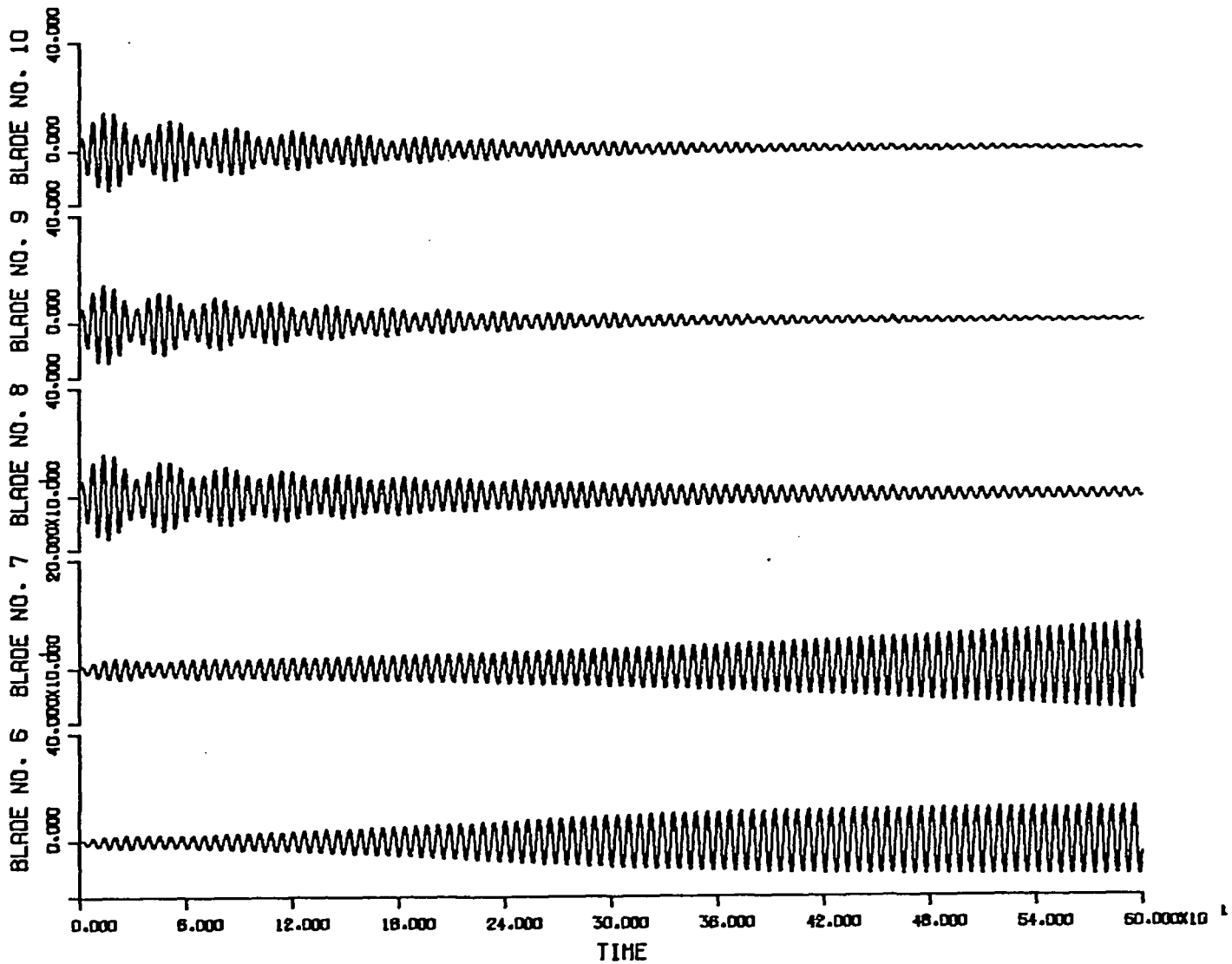

Figure 10-1. Continued

Figure 10-1. Continued

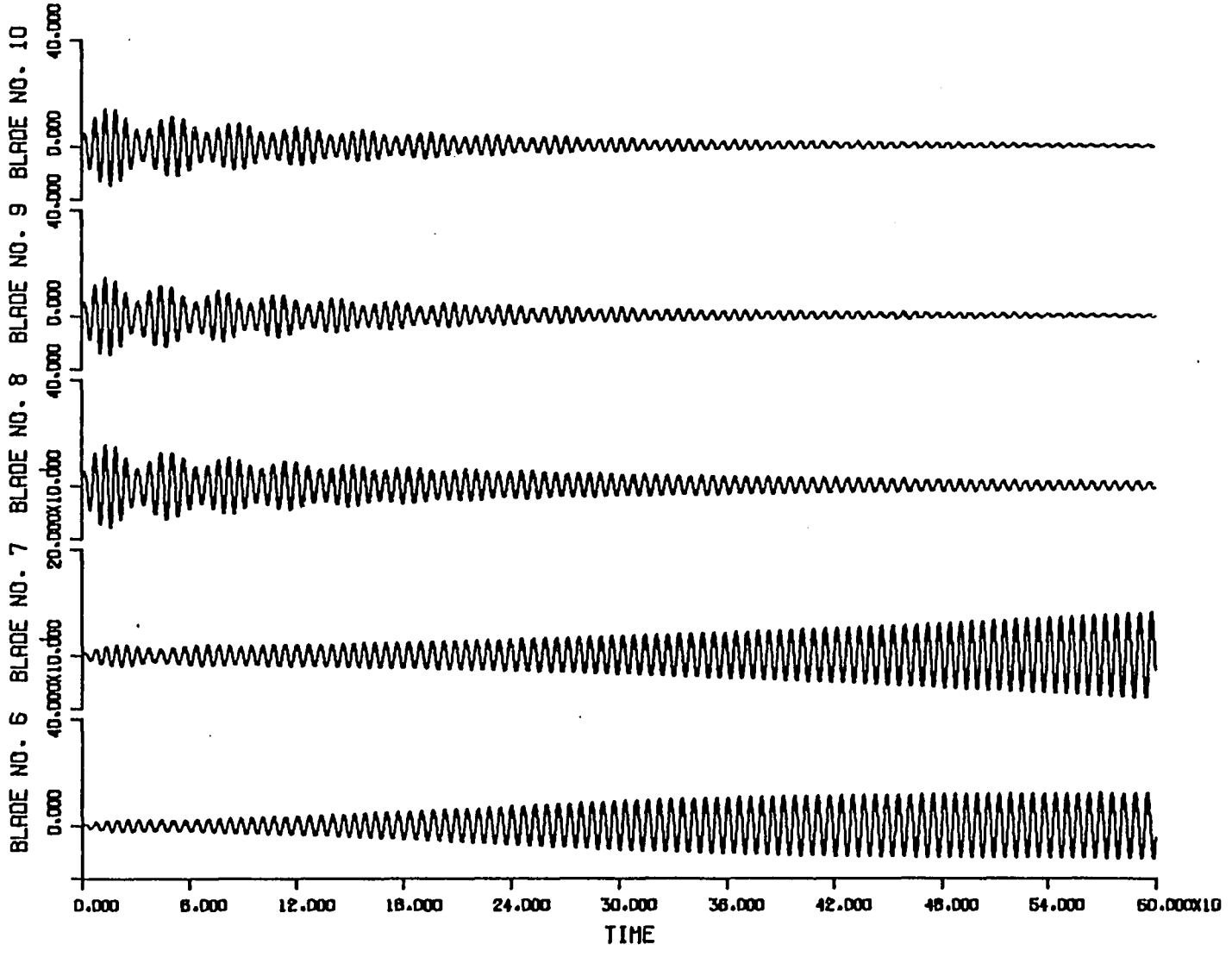

Figure 10-1. Continued

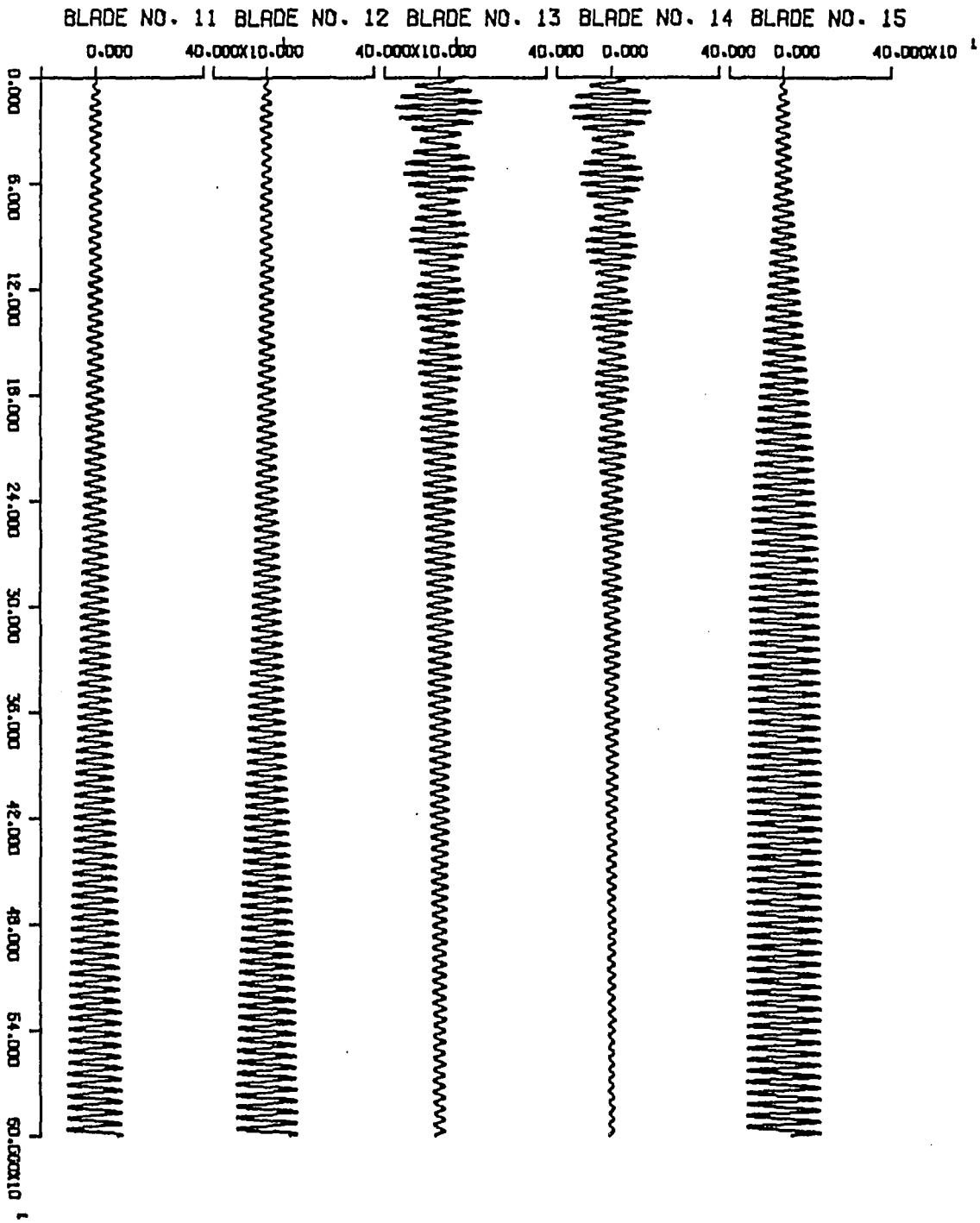

Figure 10-1. Continued

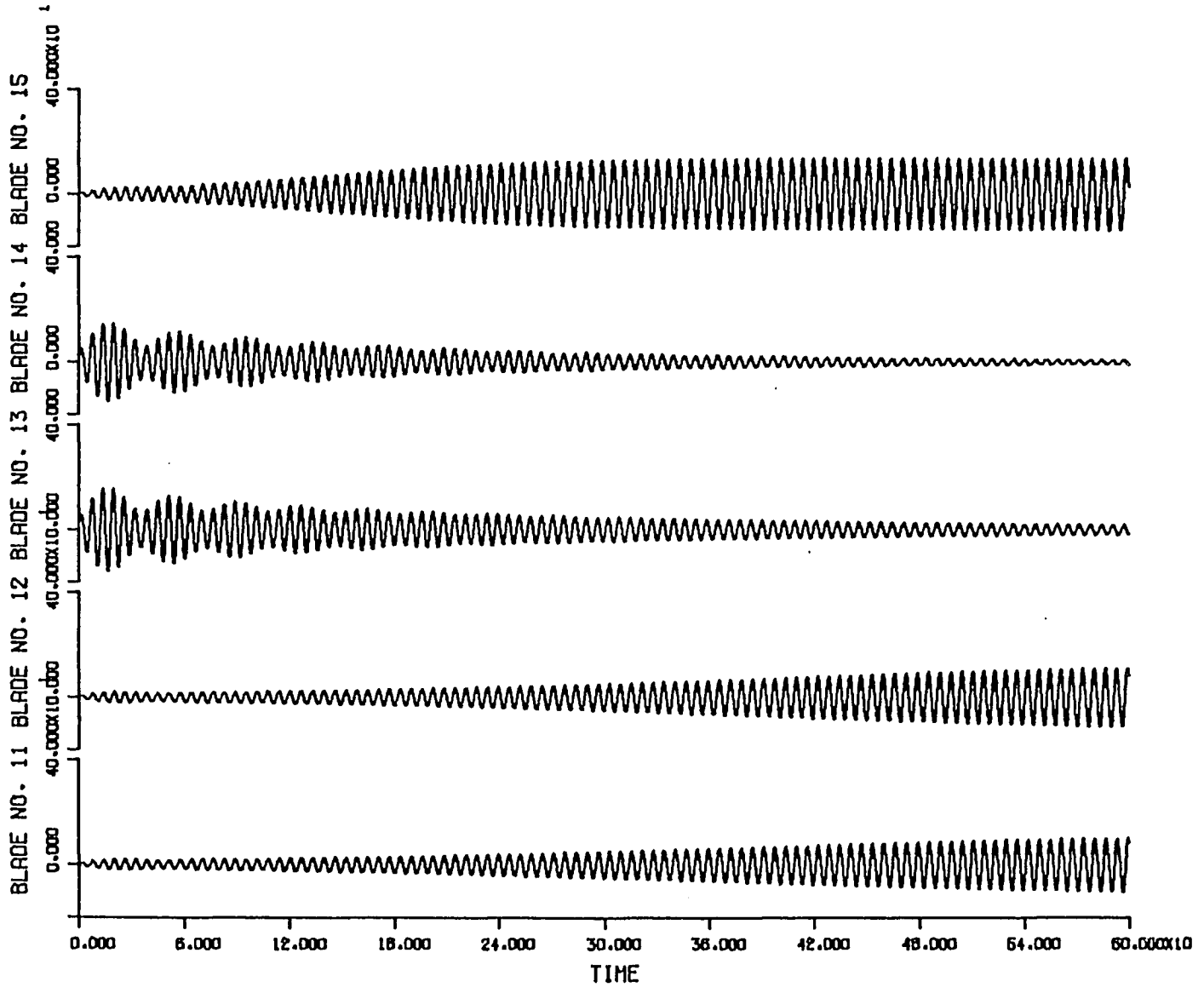

Figure 10-1. Continued

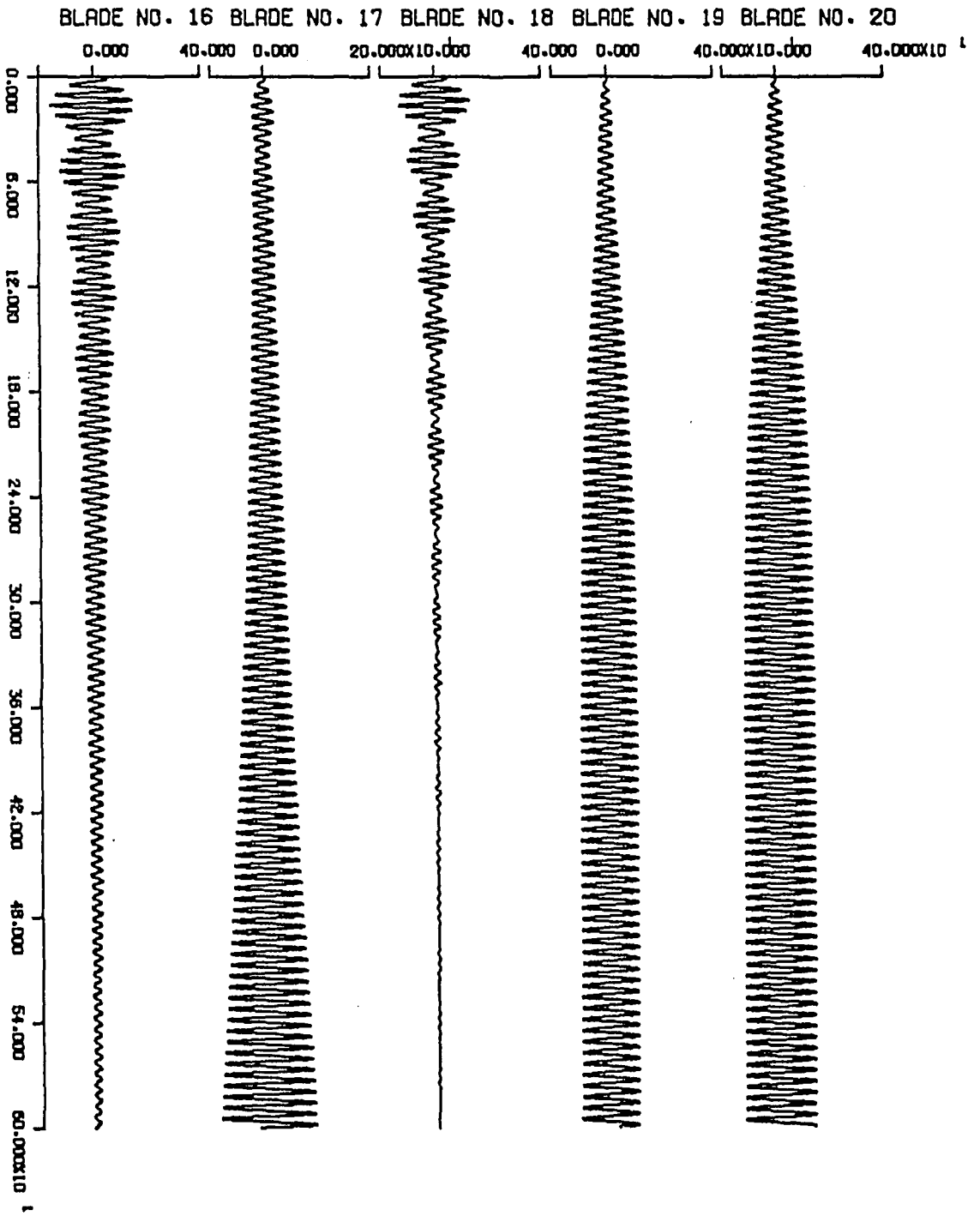

Figure 10-1. Continued

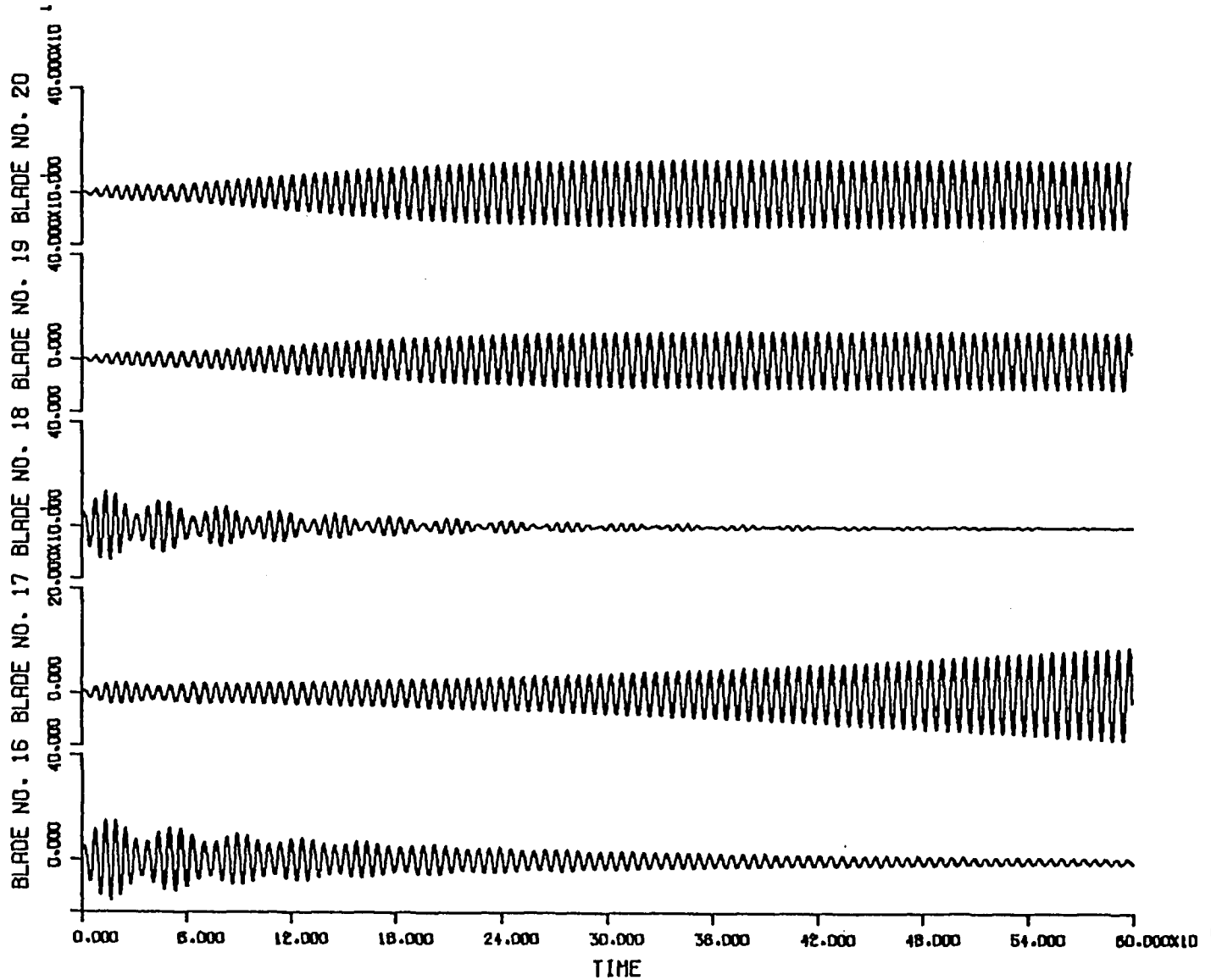

Figure 10-1. Continued

Figure 10-1. Continued

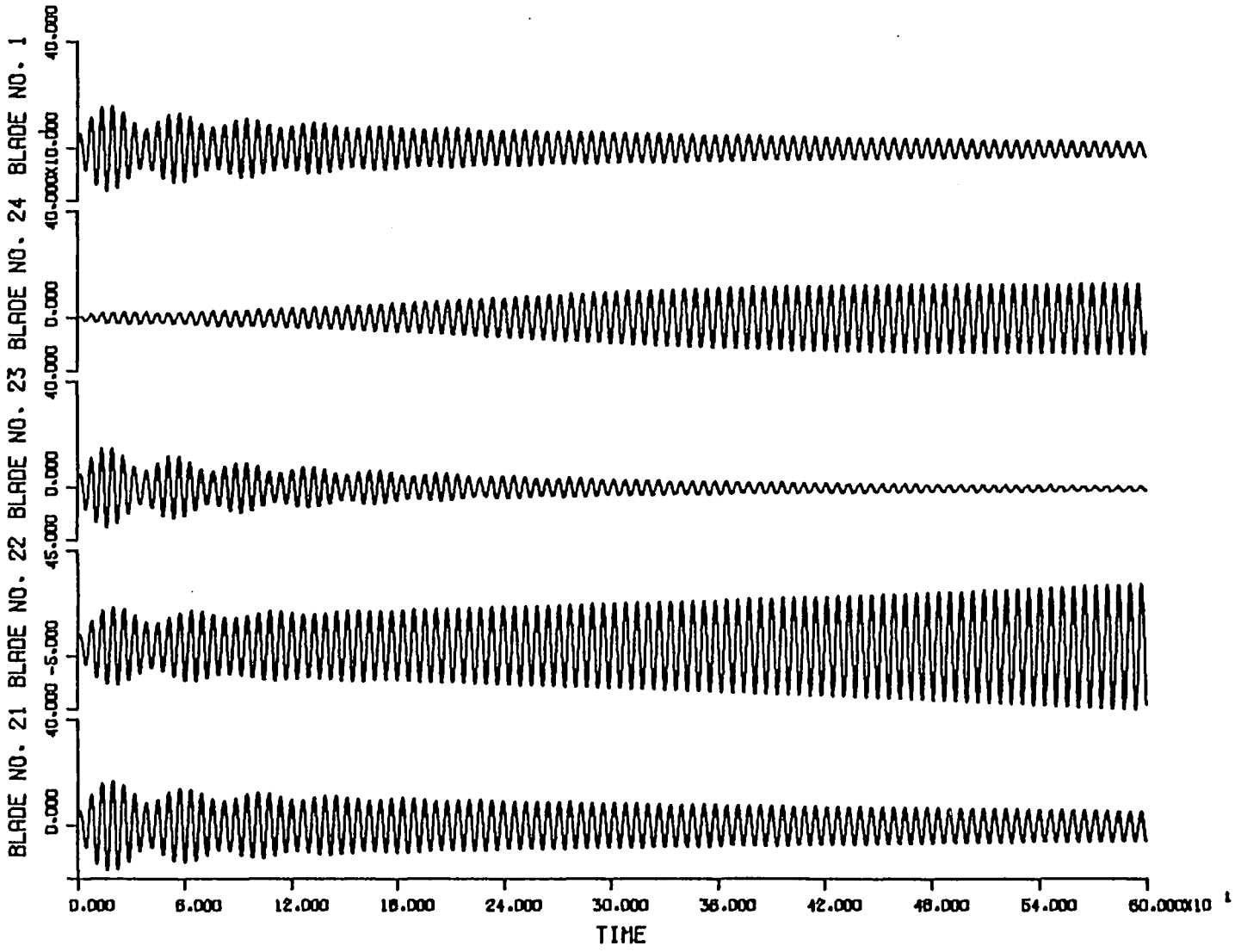

Figure 10-1. Continued

List of References

(1) Abbott, I.H. and A.E. Von Doenhoff "Theory of wing Sections", Dover Publications, Inc., 1959.

(2) Bechett, R. and J. Hurt "Numerical Calculations and Algorithms", McGraw Hill, 1967.

(3) Berger, E. "On Some Progress in Fluid Oscillator Model Theory", IUTAM symposium on Flow-Induced Vibrations, Karlsruhe, Germany, 1979.

(4) Blevins, R.D. "Flow-Induced Vibrations", Van Nostrand Reinlold Company, 1977

(5) Bisplinghoff, R.L., H. Ashley and R. L. Halfman "Aeroelasticity", Addison-Wesley Publishing Company, 1955.

(6) Currie, I.G., R.T. Hartlen and W. W. Martin "The Response of Circular Cylinders to Vortex Shedding", IUTAM symposium on Flow-Induced Structural Vibrations, Karlsruhe, Germany, 1972.

(7) Den Hartog, J.P. "Mechanical Vibrations", 3rd edition, McGraw Hill, 1947.

(8) Ewins, D.J. "Vibration Characteristics of Bladed Disc Assemblies", Journal of Mechanical Engineering Science, 1975, No. 3, pp. 165-186

(9) Griffin, O.M., R. A. Skop anf G.H. Koopman, "The Vortex Excited Resonant Vibrations of Circular Cylinders", Journal of Sound and Vibration, 1973, No. 31, pp. 235-249.

(10) Hartlen, R.T. and I.G. Currie, "Lift-Oscillator Model of Vortex- Induced Vibrations", Journal of the Engineering of Mechanics, Division of ASCE, EM5, October 1970, pp. 557-591.

(11) Iwan, W.D. and R.D. Blevins "A Model for Vortex-Induced Oscillation of Structures", Journal of Applied Mechanics, September 1974, pp. 581-586.

(12) Kryloff, N. and N. Bogoliuboff "Introduction to Non-Linear Mechanics", Princton University Press, 1943.

(13) Landl, R. "A Mathematical Model for Vortex-Excited Vibration of Bluff Bodies", Journal of Sound and Vibration, 1975, No. 42, pp. 219-234.

(14) Lubomski, J. "The Character of F-100 Fan Flutter", unnumbered NASA-LRC report, April 15, 1977.

(15) Minorski, N. "Non-Linear Oscillations", D. Van Nostrand Company, Inc., 1962.

(16) Parkinson, G.V. "Non-Linear Oscillator of Flow-Induced Vibrations", IUTAM symposium on Flow-Induced Vibrations, Karlsruhe,

Germany, 1979.

(17) Parkinson, G.V. and J.D. Smith "The square Prism as an Aeroelastic Non-Linear Oscillator", Journal of Applied Mechanics, April 1963.

(18) Popov, E.V. "Introduction to Mechanics of Solids", Prentice-Hall, Inc., 1968.

(19) Sheiser, W.E., DSS/2 Differential System Simulator, Lehigh University, Bethlehem, Pa

(20) Skop, R.A. and O.M. Griffin "A Model for the Vortex-Excited Resonant Response of Bluff Cylinders", Journal of Sound and Vibration, 1973, No. 27, pp. 225-233.

(21) Stoker, J.J. "Non-Linear Vibrations", Inter Science Publishers Ltd., 1950.

(22) Truxal, J.C. "Control System Synthesis", McGraw Hill, 1955.

(23) Van der Pol, B. "Forced Oscillations in a System with Non-Linear Resistance", Phil. Mag., 1927.

(24) Vidyasagar, M. "Non-Linear System Analysis", Prentice-Hall, Inc., 1978.

Appendix - Parameter Values

Frequency of Oscillations	318.31	Cyc/Sec
Blade Mass	1.666	Slug
Density of Air	0.0481	$Slug/ft^3$
Sonic Speed	1057.49	ft/Sec
Mach Number	0.4	
Lateral Spring Constant k_h	2991.7	lb_f/ft
Torsional Spring Constant k	3.429	lb_f/ft
X_m	0.0166	ft
Semi-Chord b	0.0416	ft

Table A-1, The Flow and Blade Variables used in equations 4.7, 4.9, 5.1 and 5.2 to Produce Figure 5-1

Angle of Attack Degrees	Radians	Moment	Lift
-11.0	-0.192	-0.285	0.65
- 9.5	-0.166	-0.310	0.87
- 7.5	-0.1309	-0.320	1.35
- 5.5	-0.096	-0.326	1.35
- 3.5	-0.0611	-0.330	1.55
- 1.5	-0.0262	-0.340	1.78
0.7	0.01222	-0.345	1.98
2.7	0.0471	-0.345	2.21
3.2	0.0558	-0.344	2.32
4.7	0.6820	-0.344	2.32
5.2	0.09076	-0.344	2.49
6.7	0.11694	-0.342	2.60
7.2	0.12566	-0.340	2.65
8.7	0.15184	-0.328	2.55
9.2	0.1606	-0.328	2.55
10.8	0.1885	-0.320	2.35

Table A-2, Lift and Moment for NACA 4424 Wing Section

Angle of attack Degrees	Radians	Moment	Lift
-10	-0.1745	-0.18	0.35
- 8	-0.1396	-0.2	0.58
- 6	-0.1047	-0.21	0.79
- 4	-0.0698	-0.215	1.0
- 2	-0.0349	-0.22	1.2
0	0.	-0.221	1.45
2	0.0349	-0.225	1.68
4	0.0698	-0.26	1.85
5	0.0873	-0.3125	1.86
6	0.1847	-0.337	1.75
7	0.1222	-0.360	1.70

Table A-3, Lift and Moment for NACA 63-206 Wing Section

Angle of Attack Degrees	Radians	Moment	Lift
-22	-0.3840	0.0530	-1.35
-20	-0.3491	0.0540	-1.37
-18.5	-0.3230	-0.0120	-1.36
-17	-0.2971	-0.0121	-1.31
-16.3	-0.2845	-0.0122	-1.25
-15.5	-0.7053	-0.0120	-1.2
-14	-0.2443	-0.0118	-1.5
-13.2	-0.2304	-0.0118	-1.07
-12	-0.2094	-0.0117	-1.0
-10	-0.1745	-0.010	-0.87
- 8	-0.1396	-0.003	-0.7
- 7	-0.1222	-0.003	-0.62
- 5	-0.0863	0.01	-0.5
- 2	-0.0349	0.005	-0.22
0	0.0	0.0	0.0
1	0.0175	-0.011	0.1
2	0.0349	-0.012	0.2
4	0.0698	-0.0125	0.4
6	0.1047	-0.0117	0.53
8	0.1396	0.0	0.68
10	0.1745	0.005	0.83
12	0.2094	0.0	1.00
14	0.2443	0.005	1.12
15	0.2618	0.005	1.19
16	0.2793	0.005	1.22
17	0.2967	0.0	1.27
18	0.3420	0.005	1.28
20	0.3491	0.01	1.3
22	0.3840	0.75	1.21

Table A-4, Lift and Moment for Blade NACA 664-021 Wing Section

Angle of Attack Degrees	Radians	Moment	Lift
-10	-0.1745	-0.083	-0.62
- 8	-0.1396	-0.084	-0.46
- 4	-0.0698	-0.083	-0.2
- 2	-0.0349	-0.081	0.2
0	0.0	-0.079	0.4
2	0.0349	-0.077	0.6
4	0.0698	-0.076	0.8
6	0.1047	-0.075	1.0
8	0.1396	-0.072	1.19
10	0.1745	-0.059	1.3
12	0.2094	-0.054	1.39
14	0.2443	-0.053	1.42
16	0.2793	-0.059	1.40
18	0.3420	-0.060	1.38
20	0.3491	-0.060	1.28

Table A-5, Lift and Moment for Blade NACA 4418 Wing Section

Damping B	0.025
Negative Damping A	0.02
Coupling D	0.102
Coupling E	0.102
Eigenvalues of the Characteristic Equation with w_n = 1.20	-0.0084 - 1.20 j
	-0.0084 + 1.20 j
	-0.0046 - 1.00 j
	-0.0046 + 1.00 j

Table A-6, One set of parameters that cause equations 9.1 and 9.2 to exhibit decaying oscillations

Blade Number	Natural Frequency Cycles/Sec.
1	1.15
2	1.185
3	1.10
4	1.08
5	1.11
6	1.14
7	1.19
8	1.20
9	1.18
10	1.12
11	1.13
12	1.175
13	1.165
14	1.10
15	1.175
16	1.14
17	1.195
18	1.085
19	1.09
20	1.155
21	1.145
22	1.17
23	1.115
24	1.165

Table A-7, The natural frequencies of the blades in figure 10-1

Bibliography of the Author

	Bahman Azizi
Date of Birth	July, 26, 1955
Place of Birth	Tehran, Iran
Father's name	Yahooda
Mother's name	Molouk
Institutions attended	Lehigh University, Bethlehem, Pa Rutgers University, New Brunswick, NJ
Degrees obtained	Master of Science, Mechanical Engineering, June 1983, Lehigh University Bachelor of Science in Mechanical Engineering, June 1978, Rutgers University
Academic Honors	Member of National Engineer's Honor Fraternity, Tau, Beta, Pi Member Mechanical Engineer's Honor Fraternity
Teaching and Reseach Experience	
Sep. '78 to June '79 Jan. '80 to June '80	Teaching Assistant in Mechanical Drawing, Heat Transfer Lab and Mechanics of Solids
June '79 to Jan '80	Reseach Assistant for the NASA project which led to this thesis